Università degli Studi di Napoli Federico II
Facoltà di Ingegneria

Comunità Europea
Fondo Sociale Europeo

Dottorato di Ricerca
in Ingegneria delle Costruzioni

XVIII ciclo

Doctoral Thesis

Experimental and Theoretical Analysis of the Structural Behaviour of Ancient Timber Structures

Costantino Giubileo

November 2005

Il Coordinatore
Prof. Ing. Federico M. Mazzolani

Acknowledgements

At the end of these three years I would like to thank all the people which have driven me during this PhD. First of all, thank you to my tutor Prof. Federico M. Mazzolani for his constant incitement during all the experimental activity; his lessons have been extremely important for my personal and scientific growth.

Particular thanks also to Proff. Bruno Calderoni and Gianfranco De Matteis, which have always helped me during my (sometimes) tortuous scientific approach.

Many thanks to all my friends, which know that their names don't remain in this page but in my memory.

Finally, I would like to remember my parents and their idea of the life (your education has made me a free man).

CONTENTS

CHAPTER 4

EXPERIMENTAL CAMPAIGN ON ANCIENT TIMBER ELEMENTS

CHAPTER 5

EXPERIMENTAL ANALYSIS ON DEFECT-FREE SMALL SPECIMENS

CHAPTER 6

EXPERIMENTAL ANALYSIS ON TIMBER ELEMENTS IN ACTUAL DIMENSION

CHAPTER 7

EXPERIMENTAL ANALYSIS ON ANCIENT TIMBER ELEMENTS CONNECTED BY MEANS OF METAL FASTENERS

CHAPTER 8

NON-DESTRUCTIVE TESTS ON ANCIENT CHESTNUT ELEMENTS

INTRODUCTION

The refurbishment of structures, intended as restoration of deteriorated elements or, more generally, as static and functional rehabilitation of buildings, has always held an important role in the history of construction, especially in Italy, where the protection of the building heritage appears as a fundamental exigency. Furthermore, during the last decades, it has been registered a consistent growth of the number of refurbishment interventions on existing structures. This is due to various reasons, such as: natural ageing of the material; increasing environmental aggression, due to the multiplication of the polluting agents; lack of adequate maintenance; designing and construction bad practices; need to provide to both the structural upgrading, because of the changed boundary conditions, and the post-earthquake repairing.

This problem is particularly relevant in the case of timber structures. Wood, in fact, is prevalently constituted by organic substances, it suffers a deterioration due to biological causes, in addition to mechanical, physical and chemical attacks. Such a biological degradation is closely connected to the external environmental conditions,

which, therefore, has a strong influence on the structure durability. Furthermore, natural wood presents always a number of defects (i.e. knots, shakes, shrinkage, shape imperfections, fibre deviations, etc.) and structural anomalies (i.e. cracking, deformations induced by long duration loads, connection degradation, etc.). In addition, the intervention procedures on complex structures is always difficult, due to a series of successive alterations and modifications occurred during their life (Bertolini, 1992).

In the end, it appears to be extremely important the evaluation of the efficiency of the ancient timber structures.

1. EVALUATION OF THE STRUCTURAL BEHAVIOUR OF ANCIENT TIMBER STRUCTURES

the current practice is affected by strong difficulty in evaluating the deterioration condition of the basic material and, consequently, in defining of the actual residual load bearing capacity and efficiency degree of the structural elements. This leads to frequently irrational and harmful interventions, mainly characterised by the substitution of wood with other structural materials, causing an irreversible alteration of the original structures (Tampone, 1996).

In order to correctly focus on such a wide problem, it is necessary to remark some consequential considerations. First of all, both at national and international level, a considerable progress in the intervention technologies and in the deterioration diagnostics must be recognised. With reference to the technology development, large numbers of researches on composite structures, which are constituted by structural materials working together in virtue of techniques based on the use of nowadays available glues, have strongly boosted the intervention possibilities. Actually, a

number of effective techniques are available, based principally on the integration of the original structure with any additional elements (both internal and external ones, both adhesive and non adhesive ones) and on the use of resins for partial substitutions and for reinforcing impregnations. At the same time, the lack of technical solutions which respect to the traditional building techniques, must be denoted.

A great contribution in designing of the refurbishment interventions is provided by the modern non-destructive or semi-destructive diagnostics. They allow to determine the mechanical and physical properties of the wooden members, their preservation condition and decay pathologies. Different non-destructive techniques exist. They are based on the use of ultrasounds, radiographic techniques or penetration equipment (such as resistographic analyses). Nonetheless, the difficulty and the uncertainty in the determination of these structural data is unquestionable, due to the intrinsic heterogeneity of basic materials, the mechanical damaging phenomena undergone by the structure and the natural obsolescence of materials themselves. Furthermore, local investigations carried out in the original context of the building does not allow an analytical correlation between these data and a reliable determination of the overall structural response. All the mentioned problems are particularly aggravated in the case of ancient timber structures, subjected to degradation phenomena and complex time-dependent behaviour.

At the European level, the recent efforts in the scientific research have been devoted to the definition of the Eurocode 5, which refers principally to the evaluation of the structural response of new constructions, neglecting to dealt with ancient timber structures in detail. Therefore, the current methods for calculation, which are based on the evaluation of the bearing capacity of set up timber members, are usually based on simplified and obsolete approaches, proposed by different overcome national

Standards (i.e. UNI 8198, BS 4978, BS 5756, DIN 4074, SIA 4978, etc.). Only recently, in some Countries of the North Europe and of the North America more reliable calculation methodologies are going to be developed, based on the results of full-scale tests on typical elements and their correlation with the results of non-destructive investigations. However, nowadays, general and reliable calculation methodologies on wood species widespread in Italy are not yet available. In fact, the theoretical studies available in Italy are either related to mere structural qualitative conception or to specific and narrow practical application fields. On the contrary, it appears necessary to provide contributions to the research activities in two different directions: (1) further improving of the diagnostic methodologies, aiming at operational cost reduction and promoting the spreading of technical knowledge; (2) increase of the level of technical methodologies related to ancient timber structures, in relation to the relevant deterioration phenomena which undermine their bearing capacity. In both cases, for the wooden structural elements, which are already set up, it is necessary evaluating both the mechanical properties and the deterioration conditions, by means of specific procedures, methods and criteria (Bonamini *et al.*, 1991; Lanius *et al.*, 1981).

It appears necessary a synthetic determination of the stiffness and bearing capacity of structural members by means of destructive loading tests on typical elements, but it is also evident that such a way is not always pursuable, because of the impossibility of extracting sacrificial elements from the structural context. Thus, the best compromise appears to be the one based on the non-destructive diagnostics to be performed directly on the set up beams, aiming at determining some physical properties that are directly related to the material rupture strength. Then, it should be possible to correlate these results to the ones promptly deducible from the full-scale tests, by means of correlation curves opportunely calibrated for the wood species under

investigation. Therefore, based on validation by means of the experimental evidence on prototypes, it could be possible to adopt procedures universally and formally accepted. These procedure can actually allow the correct evaluation of the structural reliability on the basis of the in situ acquisition of the main geometrical and mechanical features (by means of geometrical survey, visual inspection of defects and deteriorations, non-destructive tests on wood, etc.) as well as of the examination of connections and of their functionality degree.

2. PRINCIPAL AIMS OF THE THESIS

The present thesis refers to the evaluation of the structural behaviour of ancient timber elements subjected to bending and axial forces, such as the bearing structure of floor and trust structures of buildings of the Italian and Mediterranean historical centres. More particularly, this study is focused on the typical timber floors of the buildings realized until the first years of the twentieth century. Such timber structures are often constituted by natural beams of chestnut, larch, fir or spruce having circular or square cross-sections. In particular, in the case of simple floor typologies, the only beam frame was directly leaned on perimeter walls, with a 4-5 m span length at a distance on center of 50-80cm, with a superposed secondary wood elements and filler materials. With the composite floor typologies, thanks to the double frame of principal floor beams, it was possible to cover longer spans-length. Anyway, generally, beams were set up without providing any special treatment. Therefore, they present remarkable shape defects and a considerable cross-section variation between the end-beams. It is worth noting that these structural members present the major calculation uncertainties on theoretical bases, due to the strong influence of the behavioural response exercised by knots and structural defects.

A wide experimental campaign based on a series of ancient chestnut beams in actual dimension have been carried out. First of all, a preliminary visual inspection have

been executed on the timber elements, in order to have an exhaustive relief of the actual geometry of the beams, the quality of wood and the deterioration state conditions.

Later the main physical and mechanical properties of the base material has been determined. In particular, the moisture content and the density have been determined together with the elastic and post-elastic structural behaviour of wood. Compressive (in longitudinal and transversal direction), bending and shear tests on defect-free small specimens extracted from the members have been carried out in order to obtain the compressive strength, the longitudinal elastic modulus, the tensile resistance and the shear strength. These properties have been successively compared with the one obtained by means of full-scale tests on timber elements in actual dimension.

Next phase of the research program concerns the evaluation of the structural behaviour of ancient timber elements subjected to full-scale static tests. Such type of elements present many calculation uncertainties due to the presence of not negligible degradation phenomena which can produce a strong reduction of the load bearing capacity. This experimental activity is based on a series of compressive and bending tests. In particular, compressive tests were carried out on three timber elements previously subjected to Non-destructive Resistographic analyses, while bending tests have been performed on four beams of about 4 m span length. They have been tested according to two different loading condition (three and four-point bending tests) as indicated in international regulations. Some interesting considerations have been made on their partially unexpected failure mechanism.

Later, an experimental campaign on samples jointed by means of metal fasteners has been discussed. First, embedding tests in longitudinal and transversal direction have

been carried out on ancient chestnut samples, in order to determine the embedment strength of the material. In addition, a series of bending tests on connected timber beams in small dimension have been performed. Tests were executed according to the same loading conditions used for bending tests on small and actual whole beams. Several differences in the cross-section dimensions and in the number of the metal connectors have been analysed.

Next phase refers to Non-Destructive experimental Tests (NDT) on chestnut members. In particular, Resistographic analyses have been carried out on the samples successively used for full-scale compressive tests. A large number of local drilling measures have been executed on such elements both in longitudinal and transversal direction, in order to have in-depth information. Several considerations have been made on the correlation between longitudinal and transversal measures, which are the ones commonly operable in the in situ investigations. In addition, comparison between longitudinal analyses and the corresponding compressive strength have been investigated. In order to guarantee a more reliable correlation between destructive and nondestructive tests, Resistographic analyses and compressive tests have been carried out also on spruce defect-free small specimens, obtained from classified spruce beams usually available in commerce. By means of these analyses a correlation curve has been determined, which allow to deduce the mechanical properties of wood exclusively by means of Resistographic analyses.

CHAPTER 1:

Structure of wood and main physical and mechanical properties

Wood as building material appears to be strongly influenced by its organic nature. Therefore, a correct use of this material needs the acquaintance of the main physical and mechanical features. In this Chapter, a brief summary of these properties has been presented. First, the structure of wood and its specific parts have been discussed, together with the principal features necessary to identify different wood species. Later, the main physical properties of wood has been described. In particular, attention has been focused on the weight, density and moisture content. Furthermore, some information has been done on the mechanical properties of wood, which is characterised by an orthotropic structural behaviour. Three different principal direction (parallel to grain, radial and tangential to the annual growth rings) are usually considered in technical literature. For each direction, elastic and shear modulus and main strength properties have been considered. The last paragraph is devoted to biodeterioration of wood. Main decay, due to fungi and insect attacks, has been briefly investigated.

1. STRUCTURE OF WOOD

The structural behaviour of wood is strongly influenced by his fibrous nature. Wood is primarily composed of hollow, elongate, spindle-shaped cells that are arranged parallel to each other along the trunk of a tree. The characteristics of these fibrous cells and their arrangement affect such properties as strength and shrinkage as well as the grain pattern of the wood.

In Figure 1 is shown a cross section of a tree defining the following features: bark, which may be divided into an outer corky dead part (A), whose thickness varies greatly with species and age of trees, and an inner thin living part (B), which carries food from the leaves to growing parts of the tree; wood, which in merchantable trees of most species is clearly differentiated into sapwood (D) and heartwood (E); and pith (F), a small core of tissue located at the center of tree stems, branches, and twigs about which initial wood growth takes place. Sapwood contains both living and dead tissue and carries sap from the roots to the leaves. Heartwood is formed by a gradual change in the sapwood and is inactive. The wood rays (G), horizontally oriented tissue through the radial plane of the tree, vary in size from one cell wide and a few cells high to more than 15 cells wide and several centimeters high. The rays connect various layers from pith to bark for storage and transfer of food. The cambium layer (C), which is inside the inner bark and forms wood and bark cells, can be seen only with a microscope.

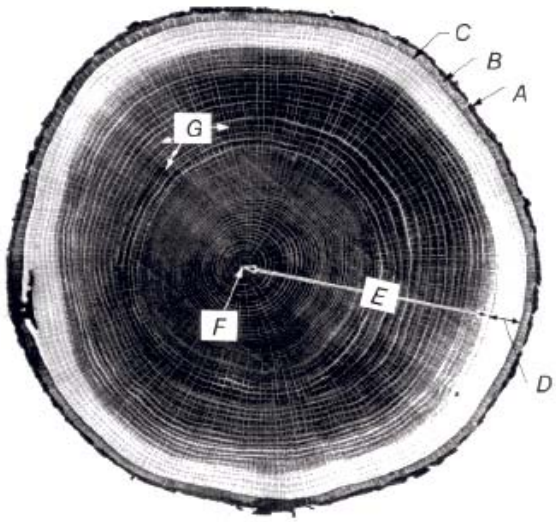

Figure 1. Cross section of a tree trunk

As the tree grows in height, branching begins by lateral bud development. The lateral branches are intergrown with the wood of the trunk as long as they are alive. After a branch dies, the trunk continues to increase in diameter and surrounds that portion of the branch projecting from the trunk when the branch died. If the dead branches drop from the tree, the dead stubs become overgrown and clear wood is formed. Most growth in thickness of bark and wood is caused by cell division in the cambium. No growth in diameter takes place in wood outside the cambial zone; new growth is purely the addition and growth of new cells, not the further development of old ones. New wood cells are formed on the inside of the cambium and new bark cells on the outside. Thus, new wood is laid down to the outside of old wood and the diameter of the woody trunk increases. In most species, the existing bark is pushed outward by the formation of new bark, and the outer bark layers become stretched, cracked, and ridged and are finally sloughed off. Sapwood contains both living and dead cells and functions primarily in the storage of food; in the outer layers near the cambium,

sapwood handles the transport of water or sap. It may vary in thickness and number of growth rings, but commonly ranges from 4 to 6 cm in radial thickness. As a rule, the more vigorously growing trees have wider sapwood. Heartwood consists of inactive cells that do not function in either water conduction or food storage. The transition from sapwood to heartwood is accompanied by an increase in extractive content. Frequently, these extractives darken the heartwood and give species their characteristic color. All darkcolored heartwood is not resistant to decay, and some nearly colorless heartwood is decay resistant. However, none of the sapwood of any species is resistant to decay. Heartwood extractives may also affect wood by reducing permeability, making the heartwood slower to dry and more difficult to impregnate with chemical preservatives, increasing stability in changing moisture conditions, increasing weight. However, as sapwood changes to heartwood, no cells are added or taken away, nor do any cells change shape. The basic strength of the wood is essentially not affected by the transition from sapwood cells to heartwood cells.

The age of a tree at any cross section of the trunk may be determined by counting well-marked annual growth rings (Fig. 2).

Figure 2. Cross section showing growth rings

However, if the growth in diameter is interrupted, by drought or defoliation by insects for example, more than one ring may be formed in the same season. In such an event, the inner rings usually do not have sharply defined boundaries and are termed false rings. Trees that have only very small crowns or that have accidentally lost most of their foliage may form an incomplete growth layer, sometimes called a discontinuous ring. The inner part of the growth ring formed first in the growing season is called earlywood and the outer part formed later in the growing season, latewood. Actual time of formation of these two parts of a ring may vary with environmental and weather conditions. Earlywood is characterized by cells with relatively large cavities and thin walls. Latewood cells have smaller cavities and thicker walls. The transition from earlywood to latewood may be gradual or abrupt, depending on the kind of wood and the growing conditions at the time it was formed. When growth rings are prominent, as in most softwoods and ring-porous hardwoods, earlywood differs markedly from latewood in physical properties. Earlywood is

lighter in weight, softer, and weaker than latewood. Because of the greater density of latewood, the proportion of latewood is sometimes used to judge the strength of the wood.

Wood cells represent the structural elements of wood tissue. They are of various sizes and shapes and are quite firmly cemented together. Dry wood cells may be empty or partly filled with deposits, such as gums and resins, or with tyloses. The majority of wood cells are considerably elongated and pointed at the ends; these cells are customarily called fibers or tracheids. The length of wood fibers is highly variable within a tree and among species. Hardwood fibers average about 1 mm in length; softwood fibers range from 3 to 8 mm in length. In addition to fibers, hardwoods have cells of relatively large diameter known as vessels or pores. These cells form the main conduits in the movement of sap. Softwoods do no contain vessels for conducting sap longitudinally in the tree. Both hardwoods and softwoods have cells (usually grouped into structures or tissues) that are oriented horizontally in the direction from pith toward bark. These groups of cells conduct sap radially across the grain and are called rays or wood rays. The rays are most easily seen on edgegrained or quartersawn surfaces, and they vary greatly in size in different species. Rays also represent planes of weakness along which seasoning checks readily develop.

Dry wood is primarily composed of cellulose, lignin, hemicelluloses, and minor amounts (5% to 10%) of extraneous materials. Cellulose, the major component, constitutes approximately 50% of wood substance by weight. During growth of the tree, the cellulose molecules are arranged into ordered strands called fibrils, which in turn are organized into the larger structural elements that make up the cell wall of wood fibers. Lignin constitutes 23% to 33% of the wood substance in softwoods and

16% to 25% in hardwoods. Although lignin occurs in wood throughout the cell wall, it is concentrated toward the outside of the cells and between cells. Lignin is often called the cementing agent that binds individual cells together.

2. MAIN PHYSICAL PROPERTIES

Many species of wood have unique physical, mechanical, or chemical properties. Efficient utilization dictates that species should be matched to end-use requirements through an understanding of their properties. This requires identification of the species in wood form, independent of bark, foliage, and other characteristics of the tree. General wood identification can often be made quickly on the basis of readily visible characteristics such as color, odor, density, presence of pitch, or grain pattern. Where more positive identification is required, a laboratory investigation must be made of the microscopic anatomy of the wood.

2.1 Appearance

The terms grain and texture are commonly used rather loosely in connection with wood. Grain is often used in technical literature to indicate annual growth rings, as in fine grain and coarse grain, but it is also used to indicate the direction of fibers, as in straight grain, spiral grain, and curly grain. Earlywood and latewood within a growth increment usually consist of different kinds and sizes of wood cells. The difference in cells imply difference in appearance of the growth rings, and the resulting texture of the wood. “Even” texture generally means uniformity in cell dimensions. Fine-textured woods have small, even-textured cells.

Timber can be cut from a log in two distinct ways: (a) tangential to the annual rings, producing flatsawn or plainsawn timber in hardwoods and flatsawn or slash-grained lumber in softwoods, and (b) radially from the pith or parallel to the rays, producing

quartersawn lumber in hardwoods and edgegrained or vertical-grained timber in softwoods (Fig. 3).

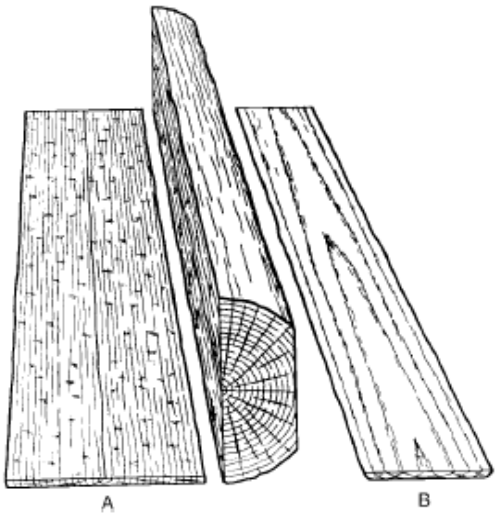

Figure 3. Quartersawn (A) and Plainsawn (B)

Quartersawn timber is not usually cut strictly parallel with the rays. In plainsawn boards, the surfaces next to the edges are often far from tangential to the rings. In commercial practice, timber with rings at angles of 45° to 90° to the wide surface is called quartersawn, and timber with rings at angles of 0° to 45° to the wide surface is called plainsawn. Hardwood timber in which annual rings form angles of 30° to 60° to the wide faces is sometimes called bastard sawn. On quartersawn surfaces, these rings form stripes, which are not especially ornamental unless they are irregular in width and direction.

2.2 Moisture content

Wood exchanges moisture with air; the amount and direction of the exchange (gain or loss) depend on the relative humidity and temperature of the air and the current amount of water in the wood. This moisture relationship has an important influence on wood properties and performance. Moisture content of wood is defined as the weight of water in wood expressed as a fraction, usually a percentage, of the weight of ovendry wood. Weight, shrinkage, strength, and other properties depend upon the moisture content of wood. In trees, moisture content can range from about 30% to more than 200% of the weight of wood substance. In softwoods, the moisture content of sapwood is usually greater than that of heartwood, while in hardwoods, the difference in moisture content between heartwood and sapwood depends on the species. Moisture can exist in wood as liquid water (free water) or water vapour in cell lumens and cavities and as water held chemically (bound water) within cell walls. Green wood is often defined as freshly sawn wood in which the cell walls are completely saturated with water; however, green wood usually contains additional water in the lumens. The moisture content at which both the cell lumens and cell walls are completely saturated with water is the maximum possible moisture content. Specific gravity is the major determinant of maximum moisture content. Lumen volume decreases as specific gravity increases, so maximum moisture content also decreases as specific gravity increases because there is less room available for free water. Wood in service is exposed to both long-term (seasonal) and short-term (daily) changes in relative humidity and temperature of the surrounding air. Thus, wood is always undergoing at least slight changes in moisture content. These changes usually are gradual, and short-term fluctuations tend to influence only the wood surface.

2.3 Shrinkage

Wood is dimensionally stable when the moisture content is greater than the fiber saturation point. Wood changes dimension as it gains or loses moisture below that point. It shrinks when losing moisture from the cell walls and swells when gaining moisture in the cell walls. Threrefore, wood is an anisotropic material in terms of shrinkage characteristics. It shrinks most in the direction of the annual growth rings (tangentially), about half as much across the rings (radially), and only slightly along the grain (longitudinally). The combined effects of radial and tangential shrinkage can distort the shape of wood pieces because of the difference in shrinkage and the curvature of annual rings. The major types of distortion as a result of these effects are illustrated in Figure 4.

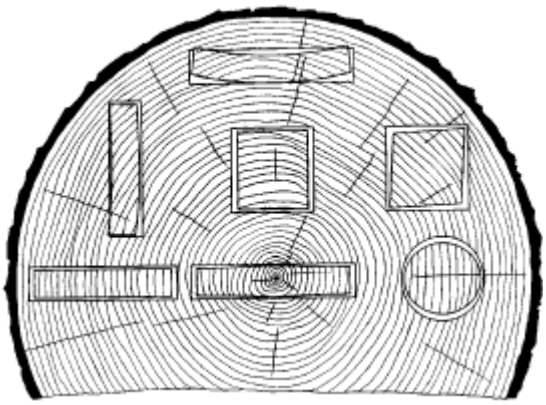

Figure 4. Characteristic shrinkage and distortion of flat, square, and round pieces.

The shrinkage of wood is affected by a number of variables. In general, greater shrinkage is associated with greater density. The size and shape of a piece of wood can affect shrinkage, and the rate of drying for some species can affect shrinkage.

Transverse and volumetric shrinkage variability can be expressed by a coefficient of variation of approximately 15%. Longitudinal shrinkage of wood (shrinkage parallel to the grain) is generally quite small. Average values for shrinkage from green to ovendry are between 0.1% and 0.2% for most species of wood. However, certain types of wood exhibit excessive longitudinal shrinkage, and these should be avoided in uses where longitudinal stability is important. Reaction wood, whether compression wood in softwoods or tension wood in hardwoods, tends to shrink excessively parallel to the grain. Wood from near the center of trees (juvenile wood) of some species also shrinks excessively lengthwise. Reaction wood and juvenile wood can shrink 2% from green to ovendry. Wood with cross grain exhibits increased shrinkage along the longitudinal axis of the piece. Reaction wood exhibiting excessive longitudinal shrinkage can occur in the same board with normal wood. The presence of this type of wood, as well as cross grain, can cause serious warping, such as bow, crook, or twist, and cross breaks can develop in the zones of high shrinkage.

2.4 Weight, density, and specific gravity

Two primary factors affect the weight of wood products: density of the basic wood structure and moisture content. The density of wood, exclusive of water, varies greatly both within and between species. Although the density of most species falls between about 320 and 720 kg/m^3, the range of density actually extends from about 160 kg/m3 for balsa to more than 1,040 kg/m^3 for some other imported woods. A coefficient of variation of about 10% is considered suitable for describing the variability of density within common domestic species. Wood is used in a wide range of conditions and has a wide range of moisture content values in use. Moisture makes up part of the weight of each product in use; therefore, the density must reflect this fact. The calculated density of wood, including the water contained in the wood, is usually based on average species characteristics.

3. **MECHANICAL PROPERTIES OF WOOD**

Wood may be described as an orthotropic material. Therefore, it presents unique and independent mechanical properties in the directions of three mutually perpendicular axes: longitudinal, radial, and tangential (Fig. 5). The longitudinal axis (D_1) is parallel to the fiber (grain); the radial axis (D_2) is normal to the growth rings (perpendicular to the grain in the radial direction); and the tangential axis (D_3) is perpendicular to the grain but tangent to the growth rings.

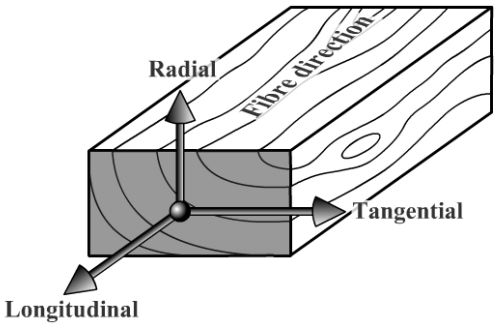

Figure 5. Three principal axes of wood with respect to grain direction and growth rings

Twelve constants are necessary to describe the elastic behaviour of wood: three moduli of elasticity in i-direction E_i, three shear moduli in ij-plane G_{ij}, and six Poisson's ratios μ. In particular, the moduli of elasticity and Poisson's ratios are related by expressions of the form:

$$\frac{\mu_{ij}}{E_i} = \frac{\mu_{ji}}{E_j},$$

with: $i \neq j$, being $i, j = D_1, D_2, D_3$

3.1 Modulus of Elasticity

Elasticity implies that deformations produced by low stress are completely recoverable after loads are removed. When loaded to higher stress levels, plastic deformation or failure occurs. The three moduli of elasticity, which are denoted by E_1, E_2, and E_3, respectively, are the elastic moduli along the longitudinal, radial, and tangential axes of wood. These moduli are usually obtained from compression tests; however, data for E_2 and E_3 are not extensive. The elastic ratios, as well as the elastic constants themselves, vary within and between species and with moisture content and specific gravity. The modulus of elasticity determined from bending, E_3, rather than from an axial test, may be the only modulus of elasticity available for a species. E_3 includes an effect of shear deflection; E_3 from bending can be increased by 10% to remove this effect approximately.

3.2 Poisson's Ratio

When a member is loaded axially, the deformation perpendicular to the direction of the load is proportional to the deformation parallel to the direction of the load. The ratio of the transverse to axial strain is called Poisson's ratio. The Poisson's ratios are denoted by μ_{12}, μ_{21}, μ_{13}, μ_{31}, μ_{23}, and μ_{32}. The first letter of the subscript refers to direction of applied stress and the second letter to direction of lateral deformation. For example, μ_{12} is the Poisson's ratio for deformation along the radial axis caused by stress along the longitudinal axis. Values for μ_{21} and μ_{31} are less precisely determined than are those for the other Poisson's ratios. Poisson's ratios vary within and between species and are affected by moisture content and specific gravity.

3.3 Shear modulus

The shear modulus indicates the resistance to deflection of a member caused by shear stresses. The three shear moduli denoted by G_{12}, G_{13} and G_{23} are the elastic constants in the 12, 13, and 23 planes, respectively. As with moduli of elasticity, the

shear moduli vary within and between species and with moisture content and specific gravity.

3.4 Strength Properties

In the following a brief summary of the main strength properties of wood, as usually reported in technical literature, has been considered.

Modulus of rupture. It reflects the maximum load carrying capacity of a member in bending. It is proportional to maximum moment reached by the specimen. Modulus of rupture is an accepted criterion of strength, although it is not a true stress because the formula by which it is computed is valid only to the elastic limit range.

Work to maximum load in bending. It is the ability in absorbing shock with some permanent deformation and more or less damages to a specimen. Work to maximum load is a measure of the combined strength and load bearing capacity of wood under bending stresses.

Compressive strength parallel to grain. It is the maximum stress sustained by a compression parallel-to-the-grain specimen having a ratio of length to least cross-section dimension of less than 11.

Compressive stress perpendicular to grain. It is commonly considered as the stress reached at the proportional limit. In fact, for this property it is impossible to clearly define the ultimate stress.

Shear strength parallel to grain. It represents the ability to resist internal slipping of one part upon another along the grain. Usually, in technical literature the presented values represent the average strength in radial and tangential shear planes.

Impact bending. In the impact bending test, a hammer of given weight is dropped upon a beam from successively increased heights until rupture occurs or the beam deflects 152 mm or more. The height of the maximum drop, or the drop that causes failure, is a comparative value that represents the ability of wood to absorb shocks that cause stresses beyond the proportional limit.

Tensile strength perpendicular to grain. It is the resistance of wood to forces acting across the grain that tend to split a member. The values commonly present in technical literature are the average of radial and tangential observations.

Hardness. It is generally defined as the resistance to indentation using a modified Janka hardness test, measured by the load required to embed a 11.28-mm ball to one-half its diameter. As in the previous properties, values presented in technical literature refer to the average of radial and tangential penetrations.

Tensile strength parallel to grain. It represents the maximum tensile stress sustained in direction parallel-to-the-grain. Relatively few data are available on the tensile strength of various species of clear wood parallel-to-the-grain. In the absence of sufficient tension test data, modulus of rupture values are sometimes substituted for tensile strength of small, clear, straightgrained pieces of wood.

3.5 Natural Characteristics Affecting Mechanical Properties

Clear straight-grained wood is used for determining fundamental mechanical properties; however, because of natural growth characteristics of trees, wood

products vary in specific gravity, may contain cross grain, or may have knots and localized slope of grain. Natural defects such as pitch pockets may occur as a result of biological or climatic elements influencing the living tree. These wood characteristics must be taken into account in assessing actual properties or estimating the actual performance of wood products.

The substance of which wood is composed is actually heavier than water; its specific gravity is about 1.5 regardless of wood species. In spite of this, the dry wood of most species floats in water, and it is thus evident that part of the volume of a piece of wood is occupied by cell cavities and pores. Variations in the size of these openings and in the thickness of the cell walls cause some species to have more wood substance per unit volume than other species and therefore higher specific gravity.

A knot is that portion of a branch that has become incorporated in the bole of a tree. The influence of a knot on the mechanical properties of a wood member is due to the interruption of continuity and change in the direction of wood fibers associated with the knot. The influence of knots depends on their size, location, shape, and soundness; attendant local slope of grain; and type of stress to which the wood member is subjected. Most mechanical properties are lower in sections containing knots than in clear straight-grained wood because (a) the clear wood is displaced by the knot, (b) the fibers around the knot are distorted, resulting in cross grain, (c) the discontinuity of wood fiber leads to stress concentrations, and (d) checking often occurs around the knots during drying. Knots have a much greater effect on strength in axial tension than in axial short column compression, and the effects on bending are somewhat less than those in axial tension. In long columns, knots are important because they affect stiffness. In short or intermediate columns, the reduction in

strength caused by knots is approximately proportional to their size; however, large knots have a somewhat greater relative effect than do small knots.

In some wood product applications, the directions of important stresses may not coincide with the natural axes of fiber orientation in the wood. This may occur by choice in design, from the way the wood was removed from the log, or because of grain irregularities that occurred while the tree was growing.

Elastic properties in directions other than along the natural axes can be obtained from elastic theory. Strength properties in directions ranging from parallel to perpendicular to the fibers can be approximated using a Hankinson-type formula
(Bodig and Jayne 1982):

$$N = \frac{PQ}{P\sin^n\theta + Q\cos^n\theta}$$

where: N is strength at angle θ from fiber direction, Q strength perpendicular to grain, *P* strength parallel to grain, and *n* an empirically determined constant.

The term slope of grain relates the fiber direction to the edges of a piece. Slope of grain is usually expressed by the ratio between 25 mm of the grain from the edge or long axis of the piece and the distance in millimeters within which this deviation occurs (tan θ). The term cross grain indicates the condition measured by slope of grain. Diagonal grain is cross grain caused by growth rings that are not parallel to one or both surfaces of the sawn piece. Diagonal grain is produced by sawing a log with pronounced taper parallel to the axis (pith) of the tree. Diagonal grain also occurs in lumber sawn from crooked logs or logs with butt swell. Cross grain can be quite localized as a result of the disturbance of a growth pattern by a branch. Any form of cross grain can have a deleterious effect on mechanical properties or machining characteristics.

Stresses perpendicular to the fiber (grain) direction may be at any angle from 0° (D_3) to 90° (D_2) to the growth rings. Perpendicular-to-grain properties depend somewhat upon orientation of annual rings with respect to the direction of stress. The effects of intermediate annual ring orientations have been studied in a limited way. Modulus of elasticity, compressive perpendicular-to-grain stress at the proportional limit, and tensile strength perpendicular to the grain tend to be about the same at 45° and 0°, but for some species these values are 40% to 60% lower at the 45° orientation.

Abnormal woody tissue is frequently associated with leaning boles and crooked limbs of both conifers and hardwoods. It is generally believed that such wood is formed as a natural response of the tree to return its limbs or bole to a more normal position, hence the term reaction wood. In softwoods, the abnormal tissue is called compression wood; in hardwoods, the abnormal tissue is known as tension wood.

Many of the anatomical, chemical, physical, and mechanical properties of reaction wood differ distinctly from those of normal wood. Perhaps most evident is the increase in density compared with that of normal wood. The specific gravity of compression wood is commonly 30% to 40% greater than that of normal wood; the specific gravity of tension wood commonly ranges between 5% and 10% greater than that of normal wood, but it may be as much as 30% greater. Reaction wood may be stronger than normal wood. However, compared with normal wood with similar specific gravity, reaction wood is definitely weaker. Compression and tension wood undergo extensive longitudinal shrinkage when subjected to moisture loss below the fiber saturation point. Longitudinal shrinkage in compression wood may be up to 10 times that in normal wood and in tension wood, perhaps up to 5 times that in normal wood.

Juvenile wood is the wood produced near the pith of the tree; for softwoods, it is usually defined as the material 5 to 20 rings from the pith depending on species. Juvenile wood has a high fibril angle (angle between longitudinal axis of wood cell and cellulose fibrils), which causes longitudinal shrinkage that may be more than 10 times that of mature wood. Compression wood and spiral grain are also more prevalent in juvenile wood than in mature wood and contribute to longitudinal shrinkage. In structural lumber, the ratio of modulus of rupture, ultimate tensile stress, and modulus of elasticity for juvenile to mature wood ranges from 0.5 to 0.9, 0.5 to 0.95, and 0.45 to 0.75, respectively. The juvenile wood to mature wood ratio is lower for higher grades of lumber than for lower grades, which indicates that juvenile wood has greater influence in reducing the mechanical properties of high-grade structural lumber.

Excessive compressive stresses along the grain that produce minute compression failures can be caused by excessive bending of standing trees from wind or snow; felling of trees across boulders, logs, or irregularities in the ground; or rough handling of logs or lumber. Products containing visible compression failures have low strength properties, especially in tensile strength and shock resistance. The tensile strength of wood containing compression failures may be as low as one-third the strength of matched clear wood.

4. BIODETERIORATION OF WOOD

Decay-producing fungi may, under conditions that favour their growth, attack either heartwood or sapwood in most wood species. The result is a condition designated as decay, rot, dote, or doze. Fresh surface growths of decay fungi may appear as fanshaped patches, strands, or root-like structures, usually white or brown. Sometimes fruiting bodies are produced that take the form of mushrooms, brackets,

or crusts. The fungus, in the form of microscopic, threadlike strands, permeates the wood and uses parts of it as food. Some fungi live largely on the cellulose; others use the lignin as well as the cellulose. Certain decay fungi colonize the heartwood (causing heart rot) and rarely the sapwood of living trees, whereas others confine their activities to logs or manufactured products, such as sawn lumber, structural timbers, poles, and ties. Although heartwood is more susceptible to decay than is sapwood in living trees, for many species the sapwood of wood products is more susceptible to decay than is the heartwood.

Two kinds of major decay fungi are recognized: brown rot and white rot. With brown-rot fungi, only the cellulose is extensively removed, the wood takes on a browner color, and it can crack across the grain, shrink, collapse, and be crushed into powder. With white-rot fungi, both lignin and cellulose usually are removed, the wood may lose color and appear “whiter” than normal, it does not crack across the grain, and until severely degraded, it retains its outward dimensions, does not shrink or collapse, and often feels spongy. Brown-rot fungi commonly colonize softwoods, and white-rot fungi commonly occur on hardwoods, but both brown- and white-rot fungi occasionally colonize both types of wood. A third and generally less important kind of decay is known as soft rot. Soft rot typically is relatively shallow; the affected wood is greatly degraded and often soft when wet, but immediately beneath the zone of rot, the wood may be firm.

CHAPTER 2:

In-situ evaluation of ancient timber structures

The refurbishment of ancient timber structures requires the acquaintance of the actual physical and mechanical properties of the members, in order to determine its load-bearing capacity and a consequent reliable design of the repairing interventions. An universal accepted method is based on a first visual inspection of the whole structure and its singular elements (first level inspection), followed by an instrumental inspection (second level inspection), which provided a deepen check up. In the following paragraphs either inspection levels have been discussed.

1. FIRST LEVEL INSPECTION

Principal purpose of the first level inspection is the visual examination of the timber members. First of all an architectural relief of the whole structure must be realized. By means of this, it is possible to identify those components which are missing, broken or in an advanced deterioration state. In fact, frequently, a not negligible

number of structural members have been removed or have fallen away during the last years, due to an extensive deterioration phenomena.

In this phase the survey of several properties of wood is required. A detection of past or current moisture problems in the critical points of the structures, as evidenced by moisture stains on the member surface. The points of insertion of the beams in their supports placed in the masonry walls and, more generally, the contact zone between the beams and a possible vector of humidity have been observed (Kasal *et al.*, 2004).

Further, visual inspection enables detection on the external surface of fungi or insect activity, so determining the presence of decay fruiting bodies, mycelial fans of fungal growth, insect bore-holes or wood substance removed by wood-destroying insects. Mycelial fans are the interconnected fibres of wood-destroying fungi (called hyphae). These fibres are the mechanism by which the fungus progresses through the wooden member. Visual inspection provides a rapid means of identifying areas that may need further investigation. In addition, it can be possible an internal decay, occulted by the lack of evidence on the surface of the wood. For advanced decay, deepen investigations allows for detection of potentially serious deterioration. They can be executed with a sharp pick. This technique is intrusive but it enables a rapid detection of voids in the wood not visible on the surface. Even for the early stage of decay, termed incipient decay, probing is beneficial. It can reveal areas of incipient decay. Wood without incipient decay tends to offer more resistance to probing, owing to the higher density and more intact internal wood structure.

The acquaintance of the timber structure includes the species identification. Species identification is accomplished by examining the anatomical features of the wood under a light microscope. For this purpose, small samples can be removed from the

timber elements. They need to have sufficient size to remove ultra-thin sections from various faces of the wood sample to examine its microscopic features. These features may include resin canals, common to many coniferous woods, such as pines, or tyloses, found in hardwoods, such as chestnut. Identification of particular features under the microscope is the most common means of reliably determining species of wood once it is cut from a defoliated tree. The physical appearance of wood may change with time, owing to weathering factors (moisture, temperature and ultraviolet light), however, the microscopic features generally remain unchanged. Knowing the species is important for estimating structural capacity, as different species can have quite different strength properties. Wood species may also be important for determining the historical significance of a particular timber within a structure (Bertolini *et al.*, 1998).

A deepen study of the history of the timber elements is also important. It allows to know if it must be considered as original in the structure or if it was subsequently substituted.

2. SECOND LEVEL INSPECTION

The instrumental inspection must be used for determining mechanical and physical properties of structural timber elements and for obtaining more reliable information on the deterioration condition of their masked part. Avoiding the alteration of the general condition of such elements, various Non-Destructive Tests (NDT) can be used for the in-situ diagnosis.

Historically, the wood products community has developed and used NDT techniques almost exclusively for sorting or grading structural products (Ross *et al.*, 1994). Two excellent examples are machine stress rating (MSR) of lumber and ultrasonic grading of veneer. As currently practiced in North America, MSR couples visual sorting

criteria with NDT measurements of the stiffness of a piece of lumber to assign it to an established grade. Similarly, laminated veneer manufacturing facilities use stress wave techniques to sort incoming veneer into strength classes prior to processing into finished products. However, a need also exists for NDT techniques to be used in the in situ evaluation of structures.

NDTs for wood differ greatly from the ones for homogeneous, isotropic materials. In fact, in such materials, whose mechanical properties are known and tightly controlled by manufacturing processes, NDT techniques are used only to detect the presence of discontinuities, voids, or inclusions. On the contrary, in wood these irregularities occur naturally, induced both by their organic nature and by degradative agents in the environment. This led researchers to examine several NDT techniques for grading structural timber elements. All the NDT techniques for wood are based on a fundamental hypothesis initiated by Jayne (Jayne *et al.*, 1959). He proposed that the energy storage and dissipation properties of wood materials, which can be measured by using a number of NDT techniques, are controlled by the same mechanisms that determine the static behaviour of such material. As a consequence, useful mathematical relationships between these properties and static elastic and strength behaviour should be attainable through statistical regression analysis. This methods can be used to establish mathematical relationships between NDT parameters and performance characteristics. Based on what previously said, in Chapters 8 and 9 a series of correlations coefficient between NDT data and mechanical properties of wood has been investigated.

In the following a briefly description of several type of NDT techniques has been reported.

2.1. Stress wave and ultrasound methods

Stress wave and ultrasound methods for the wood investigation are based on propagation of sound waves through the element. Stress wave methods are generally low frequency (in the audible range) while ultrasonic frequencies are above the audible range.

Although stress wave and ultrasonic methods are affected by numerous factors, including moisture content, wood species and growth ring orientation, they are useful means of detecting the condition of wood in structures. Several techniques that utilize stress wave propagation have been researched (U.S.D.A. (a)). To illustrate these techniques, consider application of one-dimensional wave theory to the homogeneous viscoelastic bar. After an impact hits the end of the bar, a wave is generated. This wave immediately begins moving down the bar as particles at the leading edge of the wave become excited, while particles at the trailing edge of the wave come to rest. The wave moves along the bar at a constant speed, but its individual particles have only small longitudinal movements as a result of the wave passing over them. After travelling the length of the bar, this forward-moving wave impinges on the free end of the bar, is reflected, and begins traveling back down the bar. Energy is dissipated as the wave travels through the bar; therefore, although the speed of the wave remains constant, movement of particles diminishes with each successive passing of the wave. Eventually all particles of the bar come to rest. Monitoring the movement of a cross section near the end of such a bar in response to a propagating stress wave results in waveforms that consist of a series of equally spaced pulses whose magnitude decreases exponentially with time (Ross *et al.*, 1994).

Note that wood is neither homogeneous nor isotropic; therefore, the usefulness of one-dimensional wave theory for describing stress wave behaviour in wood could be

considered dubious. However, several researchers have explored application of the theory by examining actual waveforms resulting from propagating waves in wood and wood products and have found that one-dimensional wave theory is adequate for describing wave behaviour. For example, Bertholf (Bertholf, 1965) found that the theory could be used to accurately predict dynamic strain patterns in small wood specimens. He verified predicted stress wave behaviour with actual strain wave measurements and also verified dependence of propagation velocity on the modulus of elasticity of clear wood.

As their results show, energy loss characteristics as measured by stress wave techniques provide useful information pertaining to the performance of woodbased materials. Longer propagation times are generally indicative of deteriorated wood, or wood with lower stiffness or density. Density is an important variable that must be measured if one wants to utilize stress wave analysis to estimate dynamic modulus of elasticity. Density measurements cannot be effectively taken nondestructively, so tabulated values for various species are used in combination with stress wave time to predict modulus of elasticity.

Stress wave measurements used to predict modulus of elasticity are useful when stiffness or buckling is a concern. Estimates of material strength, based on predictions of modulus of elasticity, can be subject to considerable sources of variation, including the factors noted above for stress wave measurements, as well as errors in the correlation between modulus of elasticity and strength properties. This is one reason why other methods are being developed, including the penetration technique described in follow in this chapter. Similarly, quantification of deterioration due to decay or insect damage is difficult with stress wave measurements. Techniques such as resistance drilling, provide a more reliable means

of quantifying deterioration in timber in situ. Nonetheless, stress wave methods offer the ability to rapidly screen large volumes of timbers for deterioration. Employing stress wave measurements in conjunction with other more definitive measurements is often effective for investigating the condition and integrity of structural timbers.

2.2. The Pilodyn method

The Pilodyn method uses a steel pin of a fixed diameter driven into the material by a dynamic force. The depth of penetration is correlated with material density. A relationships between the depth of penetration of a standard pin and the density of the wood exist. The correlation coefficient varied from 0.74 to 0.92, and depended on number of measurements and species. The empirical relationships are affected by moisture content. Thus, one should adjust the Pilodyn measurements to a common wood moisture content, such as 12%. Nail withdrawal tests have been used to estimate the densities in standing trees and the method is potentially suitable in historic structures. However, the method suffers from relatively low correlation between the wood density and applied force (0.3–0.85). This correlation seems to be affected by species, therefore, species-based calibrations are required (Kasal *et al.*, 2004).

2.3. Digital radioscopy

Traditional X-ray technology, using film and high-energy X-ray sources, has been used to examine structures for several years. However, owing to safety concerns and the high costs involved, use has been quite limited in structural timber evaluation. Use of digital real-time X-ray technology is quite recent and shows considerable promise for timber structures. Digital radioscopy offers significant advantages for assessment of structures over traditional X-ray techniques.

X-rays emitted from traditional high-energy electromagnetic radiation sources are capable of penetrating most materials used for building construction. Depending on the properties of the object being inspected, a photographic image is produced which reflects the density, thickness, energy absorption and chemical properties of the material.

Real-time radiography, or radioscopy, originated in the late 1800s. Termed fluoroscopy, it provided a two-dimensional image of an object of interest immediately on a screen. Because of its portable nature and ability to produce 'real-time' images, radioscopy, unlike film X-ray techniques, allows for easy manipulation of the test material during inspection, thereby allowing for better examination. Fluoroscopy had two primary disadvantages, which has limited its use: although somewhat portable there were safety concerns with the X-ray source and there was no means to store the image for later processing. Digital radioscopy does not have these disadvantages as technological advances make it safer to operate and images can be stored. Perhaps, though, the most useful feature is the ability to post-process the X-ray image by zooming in on particular details and changing contrast, brightness or position.

2.4. Resistographic analysis

A deepen investigation of the timber elements allows more exhaustive information on its mechanical and physical properties and degradation condition. Defects and biological decay are usually in the inner part of the members. Therefore, neither a mere visual inspection nor instrumental analysis based on measuring overall quantity on timber elements, such as their response in the stress wave or ultrasound analysis, can provide local information, which are particularly important in operating on ancient timber structures. An NDT technique which investigate on local features of

members is the penetration analysis. Several type of instruments are usually present in commerce. They are based on the common principle of measuring the resistance of the timber to the advancement of a small-diameter needle-like drill. This technique was firstly introduced by Rinn in 1988. In particular, NDT investigations carried out in our experimental campaign refers to the “Resistograph”. It is a commercial device which use a small 1.4 mm diameter of drill bit. The Resistograph is illustrated in Figure 1. The drill is advanced at a constant speed through the timber and the recorded resistance provides a measure of the density of the material through the sample. The particular conformation of the drilling device allows that the resistance is principally influenced by its bit. Also, a not linear path is avoided during the test.

The "Resistograph" produces a real-time graph of the relative magnitude of the torque required by the drill to keep the bit moving at a constant speed, against the depth of penetration. This graph is also stored in the onboard computer. Later it is possible to process the electronic data to highlight the deteriorated regions and provide comments on the assessment of the test. A typical processed drill report is shown in Figure 2. The "Resistograph" provides significant advantages over traditional drilling methods. The 1.4 mm drill bit is smaller than the standard 12 mm drill bit using in semi-destructive standard techniques, having a negligible effect on the overall structural system. The drill is advanced at a constant speed through the timber and the density of the material is determined from the recorded resistance and therefore does not rely on the operators experience or judgement. Initial tests conducted using the "Resistograph" identified problems with the drill bits breaking, however there have been no such problems with the more recent testing. Testing conducted in the laboratory on members with significant cracking defects, identified the importance of ensuring that the drill is not positioned directly on a crack or within 20 mm of the crack to reduce the likelihood of the "Resistograph" following the path of least resistance, along the crack. This also highlighted the importance of

conducting a visual inspection of the beam at the drill location and recording this information for use in conjunction with the "Resistograph" results, to ensure that cracks are correctly identified and not misinterpreted as rot defects within the member (Bale *et al.*, 2004).

Figure 1. the Resistograph during the NDT campaign.

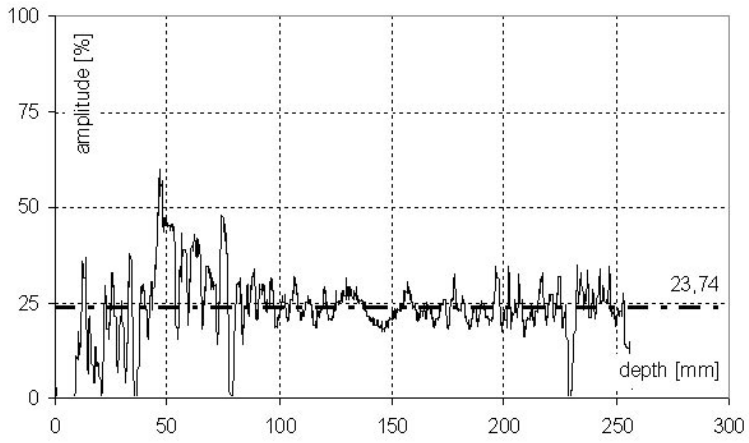

Figure 2. A typical processed drill report: the dashed line represents the main value of the relative amplitude measured during the whole penetration.

CHAPTER 3:

The study case: ancient timber floors and principal wood species

Ancient timber structures were commonly used in the historic buildings of Italy and the Mediterranean area until the first decades of the twentieth century. They represented the bearing structures of floors and roof trusts. These structures were realized by using timber beams of chestnut, larch, fir and spruce. In particular, in the South of Italy, chestnut wood was the most used species in the past, while nowadays timber beams are made of spruce wood. According to which previously said, this chapter concerns a general description of the ancient timber floor, whose refurbishment interventions are the most frequently case occurred in the current practice. In addition, some general information on chestnut and spruce wood have been reported, together with physical and mechanical properties of wood usually expected in technical literature. These properties will be recalled in the following chapters concerning the experimental campaign on ancient timber beams in actual dimension and on defect-free small specimens extracted from the beams. In particular, compressive and shear strength in direction parallel-to-the-grain and

longitudinal elastic modulus have been referred to the analogous ones obtained by testing old wood. They were used in evaluating the differences in terms of strength and stiffness between new and old wood, usually characterised by different defects patterns.

1. ANCIENT TIMBER FLOORS

1.1. General information

In this paragraph several typologies of ancient timber floor generally used in the past in different part of the Country and the Mediterranean area have been presented. Also, the structural interaction between these elements and the other part of the building have been investigated.

Ancient timber floors are elements of high vulnerability in the buildings located in seismic zone. This is principally due to the nature of the base material, and the consequent degradation state occurred during the life, and to the adopted techniques of realization of the timber structures, which often caused structural anomalies (i.e. splitting, shakes, cracking, etc.) in the members. Also, in case of earthquakes, their inertia, which is different in comparison with the one of the masonry elements, produces vibrations with different periods.

Several information can be deduced by consulting the available treatises (Bertolini *et al.*, 2001). The main information on the structural systems which are present in these sources is principally based on the arrangement of the timber elements, such as geometrical dimensions and laying out. In the following some recommendations of different authors of treatises will be examined.

In the historic treatises, the timber floor structures are defined as floor having span length equal to the width of the room to be covered. Also, they are classified as: simple floor, whose bearing structures was made of timber beams placed along the width of the room at a low distance on centres and with a superposed deck; compound floor, made of a main bearing structures realized by timber beams placed along the short side of the room and an superposed secondary bearing structures of beams placed orthogonally with respect to the main disposition.

Some indications on the design of dimensioning for simple timber floor beams, can be obtained by Scamozzi (1615). He provided a proportional ratios in function of the span length of beams: depths must be equal to about 1/24 - 1/30 of the span length, width must be of about 1/4 - 1/3 of the depths.

During the end of nineteen century, the current practice of using a simple floor for span lengths of about 3 – 4 m and a compound floor for span length ranging 3 - 6 m appears to be well established. Also, some indications were gave about the realization of beam supports on the masonry. In particular, indications by Alberti (1485) and Milizia (1785) contemplate several connections to be realized between timber beams and walls by means of cramps, copper clasps or iron cramps and metal fibulae. Also, some treatises indicate a distance of the beams in the wall. They were equal to the half of the thickness of wall, if it was large, and to the whole thickness in case of thin walls. In general, a depth of about 30 cm is considered. A more refined solution indicate the realization an external timber support which is opportunely infixed in the wall and connected to the beam by means of brackets.

Furthermore, the historical treatises proposed different solutions to avoid the decay processes at the end-beams infixed in the masonry. The main solutions were obtained

by preparing an air space of about 4 – 5 cm around the end-beam (Alberti, Emy) or by inserting hardwood or brick pieces under the end-beam in the wall (Emy).

1.2. Ancient timber floor in the South of Italy

In the South of Italy, ancient timber floor was generally constituted of a bearing structure, realized with chestnut, larch or white spruce beams having a span-length of about 5 meters. As the beams were used without any working, by simply disbarking the wooden trunks, their cross-sections were not constant along the whole length. Also, on the lateral surface they presented several shape irregularities. The secondary structure was realized with wood planks, the so-called "panconcelli", on which a mortar infill layer was placed (Fig. 1).

The wooden beams were placed directly in the masonry walls with a distance on center of about 50 – 70 cm and in alternate positions, in order to remedy to the natural difference of the transversal dimensions (Fig. 2a). Usually, their supports were constituted by the space between the stones of the wall or by a layer realised with bricks, which have higher compressive resistance. Sometimes, supports were realised with offsets in the walls (Fig. 2b). In this case, the presence of the wooden beams improves the global stability of the structure. In fact, the global reaction force at the base of the wall without offsets has a load eccentricity at the external side. Such type of eccentricity, if higher than the limit values for which the base cross-section of the walls can be considered wholly resistant in compression, induces its overturning. On the other side, the loads transferred by the beams, reduce the external eccentricity.

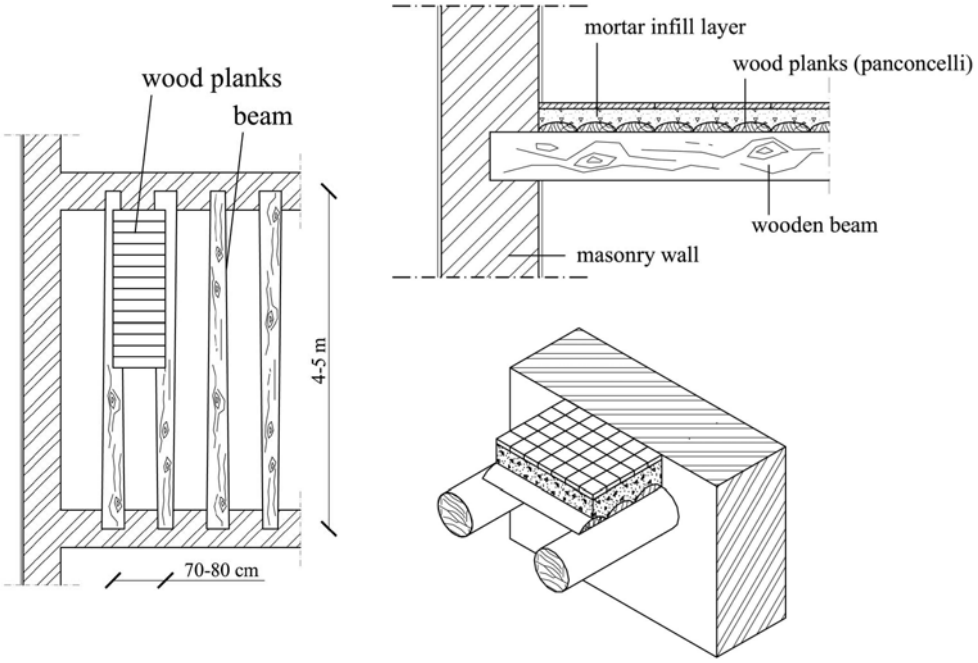

Figure 1. The structure of an ordinary ancient timber floor.

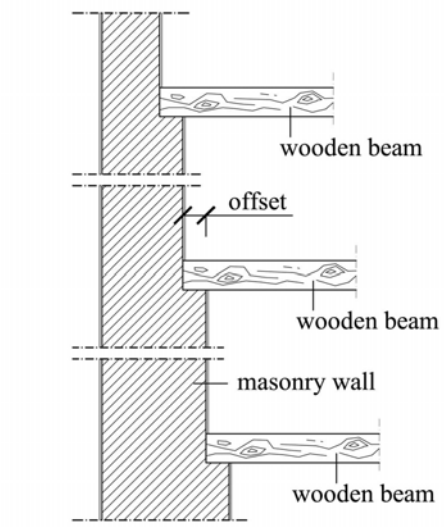

Figure 2. The supports of the wooden beams in the masonry walls.

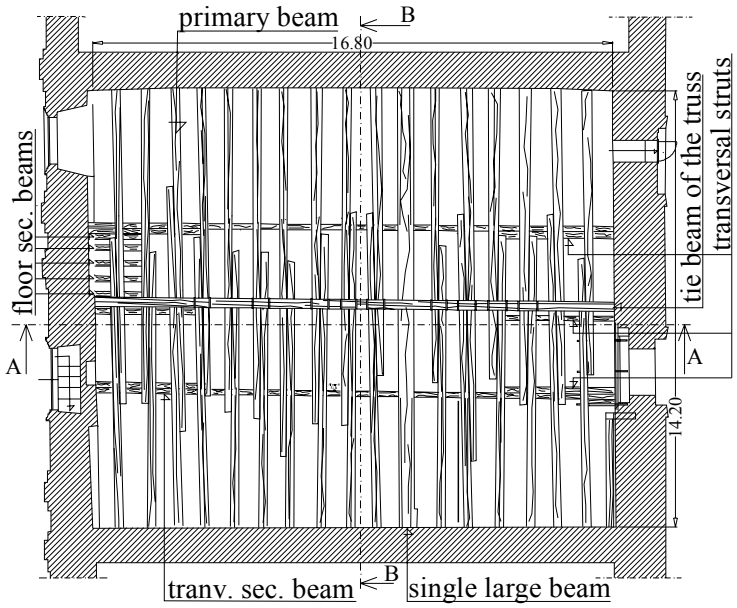

Figure 3. The principal bearing structures of the timber floor having span length higher than the ordinary one.

When the timber structures was realized for floor having span length higher than 5 – 6 meters, a different typologies had to be used. This structures were constituted by a double order of the bearing structures: the ordinary one, which is similar to the one used for simple floor structures was supported by the principal one. In this case, for the principal bearing structure higher wooden members were used, joined together by means of metal fasteners (usually iron nails) having square cross-section with maximum dimension of about 1.5 - 2 cm. They were placed along a large overlapping zone. In the Figure 3, the floor structures of a room of the Royal Palace of Naples is represented in plant. In this case the principal bearing structures have a span length of about 14 m. It was obtained by connecting two chestnut beams of

about 9 m, with an overlapping zone of about 1/3 of the whole length. The distance on center of the principal beams is of about 1.5 m.

2. WOOD SPECIES USED IN THE EXPERIMENTAL CAMPAIGN

2.1. Chesnut wood (Castanea vesca)

Until the first part of the twenty century this species was commonly used for building scopes, particularly for bearing structures of timber floors. Chestnut is an hardwood largely diffused in the hill and mountain of Italy and the south of Europe and in part of the North of Africa. Its principal botanic characteristic are the grey bark in the young tree, while it becomes brown/red in the adult tree. Also, due to its longevity, chestnut wood can reach high dimension, both in transversal and in longitudinal. On the average, for a tree of about 100 years, chestnut presents a diameter of about 80 cm and height of about 25 m. Leaf are green and about 10 – 15 cm long; they have a lance shape with deep teeth.

Wood is yellowish in the young tree, while it grows dark during its life. the annual growth rings are clearly identifiable, due to the presence of the vessels with high diameter (about 300 – 500 micron) in the earlywood and with low diameter in the latewood. Its grain is strictly dependent of the ambient conditions and the presence of branches, which determine an helicoidal fiber deviation.

Chestnut wood shows a good formability, but it produces an high corrosion when used with metals in humidity condition. Chestnut wood seasoning is slow, but the final seasoned products are very stable. Also, it is not much affected by parasite attacks.

The density of chestnut wood at the normal ambient condition (humidity of 12%) is equal to about 580 Kg/m^3, while the longitudinal, radial and tangential shrinkages are equal to 0.3 %, 4.3 % and 6.6 %, respectively.

Typical defects of chestnut wood are principally present in the grafted tree. They show not negligible deformations at the graft branch, such as differences of diameters and fibre deviation. Also, large knots and inner degraded zones due to the presence of parasite attacks are present. Therefore, grafted tree are rarely used for building scopes. On the side, wild tree has usually an erect stem and it is commonly used to extracted beams from the duramen.

In technical literature physical and mechanical properties are reportd. In particular, compression strength in parallel-to-grain direction is equal to about 35 – 55 Mpa, while the compression strengths in transversal direction are equal to about 5 – 10 MPa. If considered as an elastic linear material, chestnut wood has a longitudinal elastic flexural strength equal to 60 – 90 MPa and a longitudinal elastic modulus in tension and in compression of about 11500 MPa. Shear strength along the grain is about 7.5 MPa. All the mechanical properties are directly dependent on density and inversely on humidity (Giordano, 1989).

2.2. Spruce wood

Like in the case of chestnut wood, spruce wood is commonly used for building scopes. Spruce is a softwood largely diffused in the Middle and North of Europe. With the term “spruce” two different species of wood is indicated, Picea and Abies, which correspond to red spruce and white spruce, respectively. Differences between these two species are limited and their physical and mechanical properties are quite similar. They are noticeable in the macroscopic aspect, such as the colour of the bark

in young and old tree, the leaf and the fruits. Spruce wood has erect stems with length up to 35 m and diameter up to 60 cm. Also, it presents an undifferentiated duramen. In all the species the annual growth rings are clearly identified, but in the case of white spruce a difference of colour between earlywood and latewood is more evident. Spruce wood is also characterised by a regular grain and a low shrinkage. The presence of knots is strictly related to the ambient condition and the density of the forest: it decreases together to a thick vegetation.

The density of spruce wood varies in a very large interval. At the normal ambient condition (humidity of 12%) wooden density ranges between 300 Kg/m^3 to 620 Kg/m^3, with a main value of about 450 Kg/m^3.

In technical literature physical and mechanical properties are reported in relation to the density of wood and the humidity. In particular, at the normal condition of humidity compression strength in direction parallel to the grain ranges from 25 MPa to 55 MPa, resulting lower than the corresponding value of the chestnut wood in the same condition. If considered as an elastic linear material, spruce wood presents a longitudinal elastic flexural strength ranging from 50 MPa to 90 MPa and a longitudinal elastic modulus, equal in tension and in compression, of about 14000 - 15000 MPa. Shear strength along the grain is of 5 Mpa and 6.5 MPa for white and red spruce, respectively.

Note that the mechanical properties usually considered in technical literature are obtained by means of tests on defect-free small specimens. If compared with the recommended design values, they present safety coefficient of about 5, absolutely cautious also for the usual codes. This is due to the low possibility of using timber elements without defects. Principal defects of spruce wood are related to the presence of knots and longitudinal cracking. Also, if the tree is without bark on the lateral

surface a series of shrinkage are present. By surveying the end-beam it is important to control the depth of the annual growth rings, which in the case of white spruce strongly varies during the life (Giordano, 1989).

CHAPTER 4:

Experimental campaign on ancient timber elements

The ancient timber structures exist in many buildings located in the historical centres of Italy and other Countries of Mediterranean area built until the end of the nineteenth century, where they constitute the bearing structures of floor and top slabs. These structures are elements of high vulnerability both for their intrinsic nature and for the consequent degradation state occurred during their life, and for the adopted techniques of erection, which often cause structural anomalies (i.e. splitting, shakes, cracking, etc.) in the elements. Therefore, it is very common the need of appropriate structural reinforcing interventions. In order to guarantee an efficient design of such interventions, a preventive acquaintance of the physical and mechanical properties of the wooden elements, the evaluation of their elastic (for stiffness determination) and post-elastic (for determining the actual static reserves) behaviour and the different failure mechanisms are necessary.

In this thesis a wide experimental campaign, devoted to evaluating the structural behaviour of ancient timber elements, has been carried out. In addition, an extensive campaign of non-destructive tests has been performed on such elements. In such a way it has been possible to provide a valid correlation between destructive and non-destructive tests, which evaluate the wood features without altering the set-up ancient structures.

1. GENERAL INFORMATIONS ON TESTED TIMBER ELEMENTS

The experimental program is based on a series of ancient chestnut beams in actual dimension. They have been recently extracted from a floor of an intermediate storey of a typical multi-storey ancient masonry building located in the historical centre of Naples, built up at the beginning of the 19^{th} century. They were used as bearing structures of the wooden floor, having a span-length of about 4.5 m.

Therefore, the period of usage of the beams was about 200 years. During all this period, the beams were located in a residential environment of a Mediterranean area, they being subjected to temperature and relative humidity varying approximately in the range 17-27 °C and 55-70%, respectively.

During the first visual inspection the age of the timber structural elements was measured by counting the annual growth rings on each end-beam cross-section. It resulted of about 35 years.

The tested beams are about 4 meters long with a quite circular cross-section with diameter ranging from 20 to 25 cm. As the wooden beams are obtained by directly disbarking the tree trunks, their cross-sections are irregular and not constant throughout the length of the member.

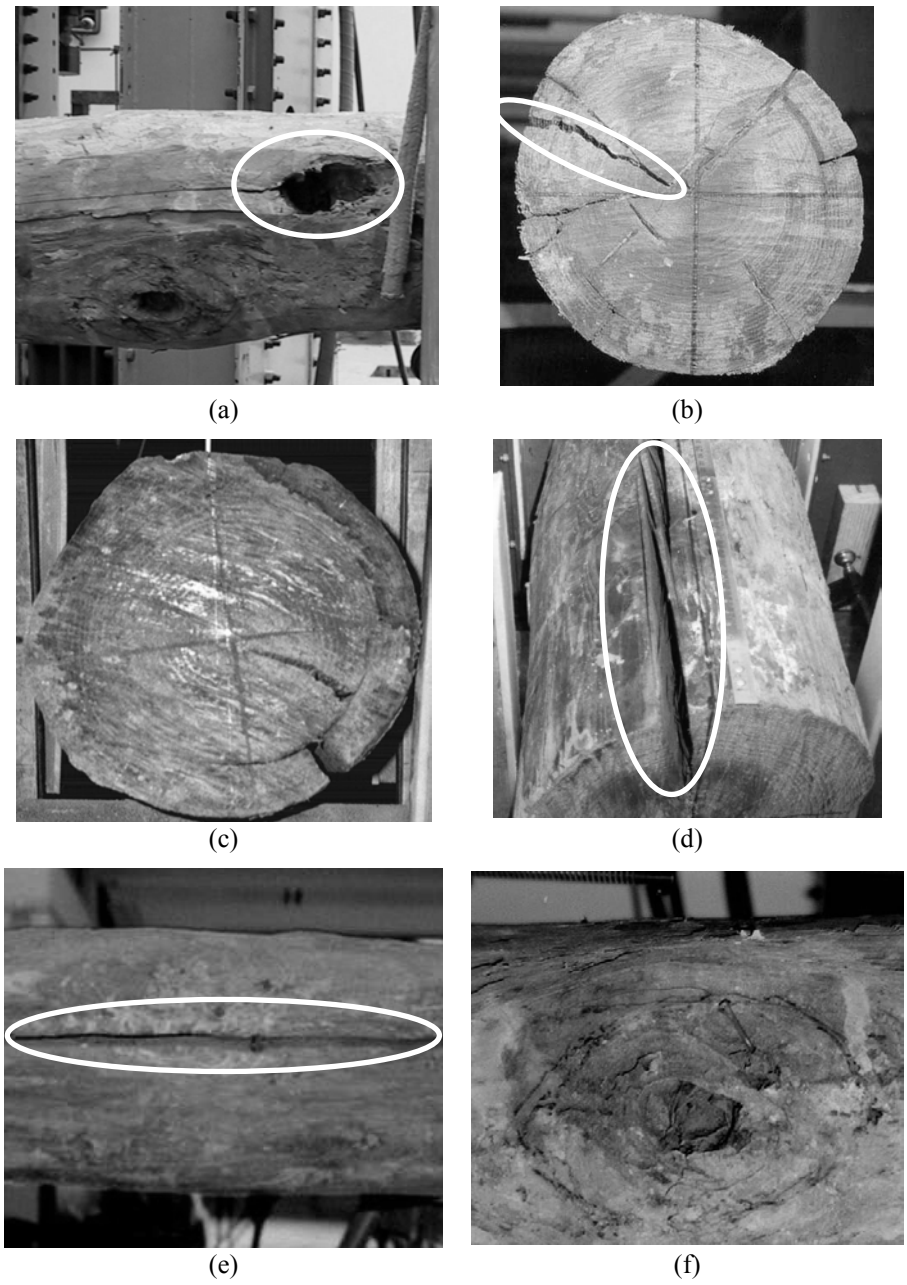

Figure 1. Typical defects of tested specimens: degraded zones and holes (a,f), transversal cracking (b, c), longitudinal splitting starting from end-beam (d, e).

Along the external surface, the beams present several shape irregularities and an extensive degradation state of the base material, mainly consisting of longitudinal splitting, cracking, shakes, degraded zones and holes, due to nails and insect attacks (Fig. 1).

After their replace, the wooden elements were stored in a closed internal location, having temperature and humidity similar to the ones existing inside common houses. Therefore the moisture content of timber resulted, before testing, of about 12%.

The mean value of density (ρ_{mean}) was measured on several specimens in the same ambient condition and resulted equal to 622 kg/m^3, while the characteristic value ($\rho_{0,05}$) was slightly lower (596 kg/m^3), due to a low value of the standard deviation equal to 16 kg/m^3.

2. THE EXPERIMENTAL PROGRAM

The research program was constituted by a multi-phase organization, divided into 6 steps, as reported in the following. Every step has been specifically described in a chapter of the thesis. This experimental campaign was completed during 3 years of the PhD course. All the tests have been performed at the Laboratory of the Department of Structural Analysis and Design (D.A.P.S.) of the University of Naples "Federico II".

1) First level inspection of the structural elements (visual inspection and survey) (Chapter 5);
2) Mechanical characterisation of the ancient chestnut wood by means of experimental tests on defect-free small specimens extracted from the beams (Chapter 5);

3) Full-scale static tests of beams (bending and compressive tests) (Chapter 6);
4) Experimental test on ancient wooden elements extracted from the beams, jointed by means of steel connectors (Chapter 7);
5) Second level inspection on wooden elements by means of Non Destructive Tests (resistographic analysis) (Chapters 8 and 9);
6) Correlation between the results of the experimental tests and the results of the "resistographic" analyses and set-up of simplified calculation methods and structural models (chapters 8 and 9).

2.1. First level inspection of the structural elements (visual inspection and survey)

As preliminary step for the execution of experimental tests and numerical simulations, it is absolutely necessary to perform an accurate geometrical survey of beams (first level inspection). Generally, the visual inspection is carried out in-situ, by directly observing the structural elements. First of all, the ambient conditions (such as temperature and humidity) were surveyed, in order to identify the biological risk class, according to the UNI EN 335. Later, a detailed relief is carried out. It has the scopes of evaluating the original quality of wood, the deterioration state, the actual geometry of the structural system and the dimensions of the elements. All these operations were necessary for surveying the beam geometry and for precautionary identifying the topical zones of beams (attacked or deteriorated), on which the second level inspection have been carried out after the full scale experimental tests.

2.2. Mechanical characterisation of the ancient chestnut wood by means of experimental tests on defect-free small specimens extracted from the beams

A wide experimental campaign has been performed on defect-free specimens in small dimension extracted from the ancient beams, in order to study the mechanical properties of the base material. In fact, generally, the behavioural heterogeneity of

wood determines a natural variation of the local properties as respect to the global ones of the structural elements in actual dimension. Also, it can be noted that, in the case of ancient timber elements, the presence of widespread degradation states can produce a strong reduction of the bearing capacity of the structural elements. For this reason, it makes extremely important the comparison between local and global properties.

Various types of tests have been carried out (compression tests in parallel, radial and tangential direction, bending and shear tests) in order to determine the ultimate compressive stress of the material, the elastic modulus (E) and tensile resistance in the grain (longitudinal) direction, and the ultimate tangential stress.

2.3. Full-scale static beam tests (bending and compressive tests)

This step of the research concerns the evaluation of the local and overall structural behaviour of the ancient wooden beams in actual dimension. These elements were representative of the typical situations which can be met during the professional activity. In particular, static bending and compression tests were carried out. The investigation aims at determining the global response of the system under progressively increasing external loads. Such analyses have been allowed the successive calibrations of the simplified methods for analytical calculations.

The determination of the load-displacement curve (specially the elastic stiffness modulus and the collapse load) and of the relevant failure mechanism was the main purpose. In the case of bending tests, the latter was the most important aspect. In fact, the structural damage level, which characterised the examined beams, helped the activation of sliding phenomena induced by the shear stress during the test. They were particularly felt in the case of a contemporary presence of large cracks in the

longitudinal direction and a low span length/cross-section diameter ratio of beams. Such circumstances have a high scientific interest, because the usual static calculations are based on the prediction of the collapse load in bending, as it generally occurs in current practice, providing possible unsafe results, by misleading the actual resistant mechanism of the system.

In the case of compression tests on trunks having actual transversal dimension, collapse loads have allowed to obtain mean values of the compressive strength, which have been associated with the ones obtained by resistographic analyses, previously carried out on the same elements.

2.4. Experimental test on ancient timber elements extracted from the beams, jointed by means of steel connectors

This step was devoted to the analysis of structural behaviour of ancient wooden elements jointed by means of steel nails. The adopted typology of tested connection was the one commonly used in ancient floor slabs where the span was longer than the ordinary ones. In such a case, load bearing beams, mainly subjected to static flexure, were jointed by means of iron nails placed along a quite large overlap zone.

Therefore, embedding tests in direction both parallel and perpendicular to the grain were carried out, in order to determine the ultimate embedment strength and to compare it with to the values reported in technical literature for clear wood. Also, bending tests on specimens arranged similarly to ones used on defect-free beams (see step 2) and full-scale tests on beams in actual dimension (see step 3) were also performed for evaluating stiffness, ductility and bearing capacity of the investigated connection systems. Several different configurations of the specimens were analysed, varying the number, the distance and the dimension of steel connectors in addition to the width of the cross-section of the connected elements.

2.5. Second level inspection on timber elements by means of Non Destructive Tests (resistographic analysis)

In this step diagnostic local investigations by means of mechanical equipment were carried out. Usually, such kind of inspections are used for integrating the results deduced by the first level inspection, providing an in-depth knowledge of deterioration and identifying the effective section of degraded structural elements and estimating the actual stiffness and mechanical strength parameters of wood, to be used for the application of methods for static calculation. Generally, they allowed to determine the deformability and resistance properties of the in-situ elements, without the execution of local or overall destructive tests, which should lead the loss of structural capacity of the whole structure. Since they do not significantly affect the mechanical resistance of wood and, at the same time, do not require a high economic effort, they are very suitable for the characterization of the average behaviour of the structural element on the base of detailed evaluations of local conditions of the zones more degraded and then more significant for the static behaviour.

In particular, the so-called "Resistographic" tests were performed. The results in terms of the penetrometric resistance, were correlated to the actual ultimate stress of material, which have been already directly determined from the results of tests on defect-free specimens (see step 2) and the full-scale tests on beams in actual dimension (see step 3). Such a correlation is clearly dependent on the effective degradation conditions of the elements. The results of the "Resistographic" tests, performed in longitudinal direction on samples extracted from the tested beams, allowed the determination of the ratio between the resistance in the longitudinal direction (which mainly influences the static behaviour of the beam) and the one in the radial direction (which can be more simply obtainable from in-situ tests).

2.6. Correlation between the results of the experimental tests and the "Resistographic" analyses and set-up of simplified calculation methods

On the base of the experimental analyses developed in the previous steps and the comparison of their relevant results, during this step the quantitative influence of different types of imperfections on the global response of structural elements (initial stiffness, collapse load, failure mechanism) was determined. By means of the comparison of results deduced by experimental and theoretical models, it was possible to correlate the actual degradation conditions of the system (such as the position, the amount and the quality of cracks existing on the study beam) to the ratio between the ultimate strength of the actual material and the one of an equivalent ideal material. In this way, the effect of the degradation condition, the structural defects and the shape anomalies of wood beams can be implicitly accounted for a lower value of the resistance. The efficiency of the simplified method of calculation, based on models of calculation with perfect material and geometry and strength reduction coefficients, was guaranteed by setting strength correlation graphics to be assumed for perfect material and for deteriorated material of imperfect structural elements, on the base of diagnostic investigations of first and second levels.

CHAPTER 5:

Experimental analysis on defect-free small specimens

A series of defect-free wooden specimens in small dimension have been tested under different testing configurations and loading conditions, in order to obtain the mechanical properties and define the stress-strain relationship of the base material.

The tested specimens were extracted from ancient timber elements in actual dimension. These structural elements exhibited defects usually observable in such kind of structures, as a consequence of both the natural origin of wood and the degradation due to aging and biological attack, which produces a non homogenous pattern strongly influencing the structural behaviour. On the contrary, the mechanical description of structural "new" wood is usually done by testing small specimens only, where imperfections are not present. Therefore, the corresponding results are not directly applicable for the structural analysis of ancient elements (Madsen, 1991). In addition, codes specifically dealing with design values for ancient wooden structures are not yet available.

Due to the lack of direct tools, the global influence of the typical defect pattern on the behaviour of old timber beams can be evaluated by comparing the overall behaviour of such beams with the one of the small specimens. Therefore, in parallel with the analysis of the structural behaviour of wooden beams in actual dimension, a wide experimental campaign has been done on small specimens, whose results are given in details in this chapter.

1. THE EXPERIMENTAL ACTIVITY

As it is well known, the cellular structure and the physical organization of the cellulose chain within the cell-wall make the physical and mechanical properties of wood dependent on the direction of loading. In particular, wood may be defined as an orthotropic material, which has different mechanical properties dependent on the selected direction. Usually the directions of three mutually orthogonal axes (Fig. 1) are considered in the applications: the longitudinal direction parallel to the wood fibre (D_1), the radial direction perpendicular to the annual growth rings (D_2) and the tangential direction perpendicular to the grain but tangent to the annual growth rings (D_3). The mechanical properties of wood along longitudinal direction are higher than the ones along radial and tangential directions, because the grain direction is coincident with the orientation of primary bonds of the major chemical components of the wood cell-wall. For these reasons, a comprehensive study of the mechanical behaviour of the base material requires to perform tests along all the 3 fundamental directions (U.S.D.A. (a)).

Note that, due to the difficult in the determination of the elastic properties in the transversal directions, the following simplified assumptions are currently adopted in the technical literature:

$E_2 = E_3 = E_1/10$;

$G_{12} = G_{13} = G$;

$G_{23} = G/4$,

where: E_i is the elastic modulus in i-direction and G_{ij} is the tangential modulus in the ij-plane.

Consequently, the total number of elastic constant to be directly determined by tests is reduced to longitudinal elastic modulus E_1 and tangential modulus G.

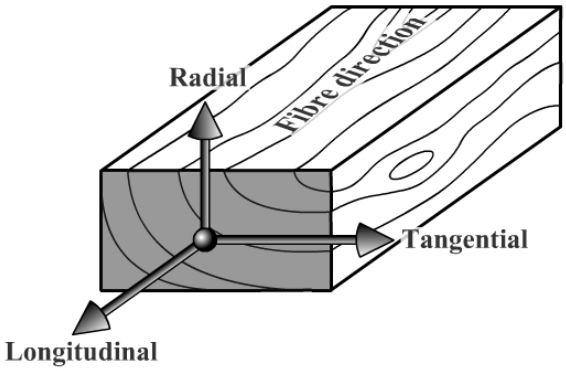

Figure 1. Principal axes of wood with respect to longitudinal direction (D_1), radial direction (D_2) and direction tangential (D_3) to the growth rings.

The experimental activity has been performed on a series of defect-free specimens of small dimension, extracted from ancient wooden beams (Mazzolani *et al.*, 2004(a)). Different typologies of testing have been carried out, as shown in Table 1, where the number of tested specimens is also indicated.

Table 1. Test typologies and number of specimens for each test.

Test typology	*Num. of specimens*
1. Compression test along longitudinal direction	23
2. Compression test along radial direction	10
3. Compression test along tangential direction	11
4. Bending test	3
5. shear test	4

Compression tests have been carried out to determine the ultimate compressive stress of the material, while bending tests are used for the indirect evaluation of elastic modulus (E_l), tangential modulus (G) and tensile resistance in grain (longitudinal) direction, which cannot be simply obtained in a direct way, as well as to characterise the bending behaviour of specimens beyond the elastic range. Furthermore, shear tests are used to evaluate the ultimate tangential stress.

All performed tests have been carried out according to the Italian UNI-ISO codes, by using a testing equipment which loads the specimen in displacement control (Fig. 2). Each specimen was placed between two steel plates having dimensions higher than the geometrical dimension of the samples. In particular the bottom one presents a particular conformation which prevents the horizontal displacements during the loading phase. The load was applied by means of a steel thread bar, restrained by a rigid steel reaction frame: the rotation of the bar for a given angle causes a corresponding increasing of the displacement on the sample in perpendicular direction. The torsional effects due to the particular testing equipment was avoided using a cylindrical hinge placed under the steel thread bar. Also, according to the UNI ISO regulations a spherical hinge was used in order to guarantee an uniform

distribution of the applied loads. In each test, the displacement increasing rate has been chosen very slow, in order to provide a quasi-static load application.

The imposed displacement has been progressively increased up to reach the sample collapse. It has been measured by electric transducers (LVDT) with accuracy of 1×10^{-3} mm. The corresponding reaction force, given by the specimen, has been measured by means of a load cell. Both transducers and load cell have been connected to an electronic device and to a PC, in order to allow data acquisition and recording.

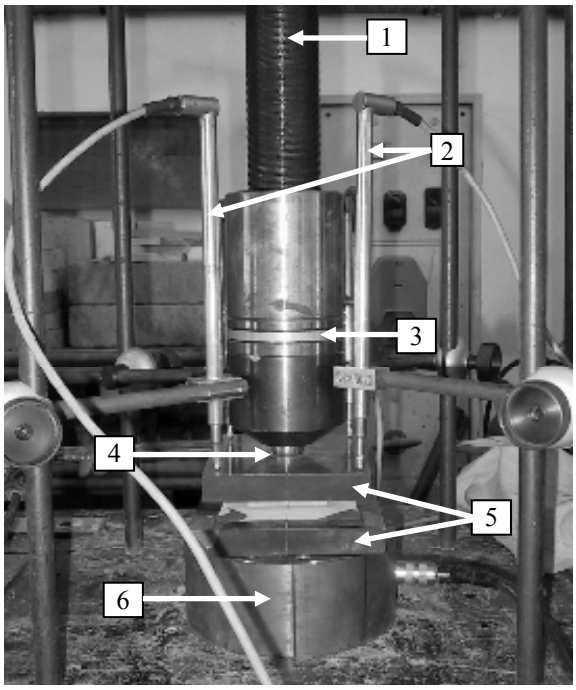

Figure 2. Testing equipment: 1) steel thread bar; 2) LVDT; 3) cylindrical hinge; 4) spherical hinge; 5) steel plates; 6) load cell.

2. COMPRESSION TESTS IN LONGITUDINAL AND TRANSVERSAL DIRECTION

Compression tests along grain direction (longitudinal – D1) have been carried out on 23 specimens having dimension (square cross-section and length) in accordance with Italian regulations UNI-ISO 3787. 15 specimens (group A) had a 2 cm x 2 cm cross-section and 4 cm length, while other 8 specimens (group B) had a 3 cm x 3 cm cross section and a length of 9 cm, respectively. The samples have been loaded by means of a top rigid steel plate spherically hinged for ensuring an uniform load distribution.

(a) (b) (c)

Figure 3. Compression test in direction parallel to the grain (D1): specimen shape and testing equipment (a), specimens before and after testing (b, c).

The applied displacements have been measured by means of four LVDTs, located at the steel plate corners. The mean value of the corresponding measures has been considered as representative of the top displacement of the sample. In Figure 3b, as an example, one specimen is represented before and after the attainment of the collapse mode.

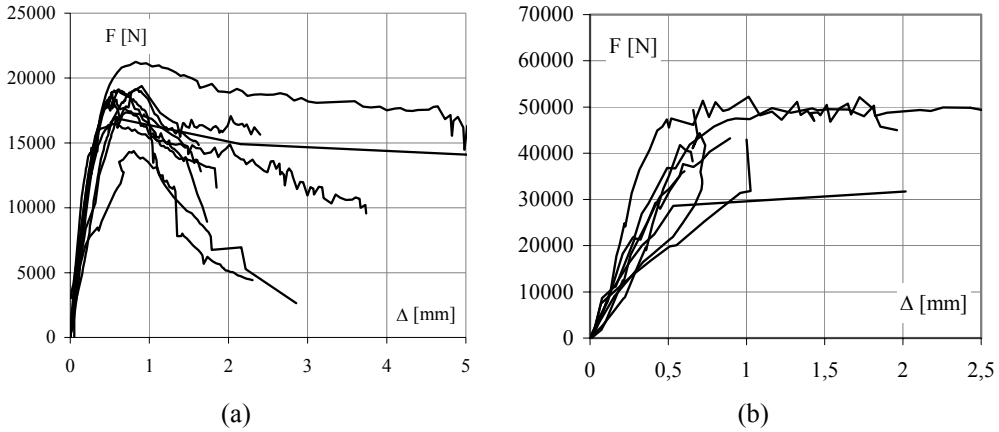

Figure 4. Compression test in direction parallel to the grain (D1): F–Δ curves for specimens of group A (a) and group B (b).

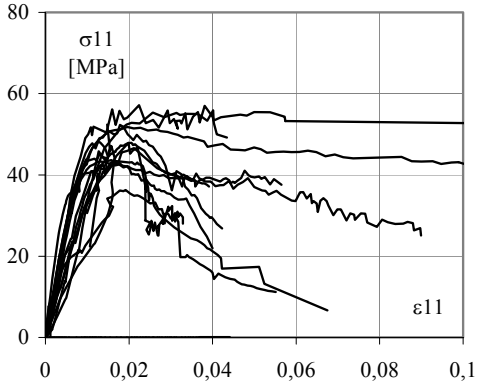

Figure 5. Compression test in direction parallel to the grain (D1): σ_{11} –ε_{11} curves for all specimens.

The obtained F-Δ curves are shown in Figures 4a and 4b for the two group of specimens, respectively. In Figure 5 all the σ–ε curves of tested specimens are plotted. The longitudinal compressive stress ($\sigma_{c,11}$) has been calculated with reference to the applied force and to the whole cross-section area, while the corresponding longitudinal strain (ε_{c11}) has been evaluated on the total length of the sample.

The peak compressive stress ($\sigma_{c11,max}$) exhibited by the different specimens is quite constant, with an average of about 48 MPa, this value being in a good accordance with those reported in literature for new chestnut wood (Feio *et al.*, 2004; Giordano, 1989). It can be noted that all experimental curves are quite similar in the elastic (pre-peak) field, while they largely differ in the post-peak field.

In fact, during compression tests, the attainment of the peak compressive strength occurs by means of different mechanism, which modify the collapse behaviour. Principally, collapse mechanism is due to a micro-buckling of the fibres, which can be associated with a contemporary breakaway for the attainment of the limit tensile stress in the transversal direction. Also, collapse can occur with a fracture cleavage having an inclination on the horizontal plane higher than 30°. This is visible in the stress-strain curves which present a short plastic range, corresponding to the attainment of the cleavage fracture, before the complete collapse of the sample. When the collapse mechanism occurs with the formation of the longitudinal cracks, stress-strain curves show a noticeable sub-horizontal plastic branch, highlighting a ductile behaviour of the material.

Note that the differences in the post-elastic behaviour were partially due to the testing apparatus. In fact, as the displacement transducers are fixed to the steel plate at the top of the sample, when first plastic deformation occurs at the plate to specimen interface, the plate can be interested by unforeseen rotations, which modify the original configuration, so reducing the physical meaning of measured displacements.

Compression tests in the direction perpendicular to the annual growth ring (D2) have been carried out on 11 specimens, according to the Italian regulation UNI-ISO 3132.

In particular, 7 specimens (group C) with a 2 cm x 6 cm rectangular cross-section and 2 cm length, and other 4 specimens (group D) with a 3 cm x 9 cm cross-section and 3 cm length have been considered.

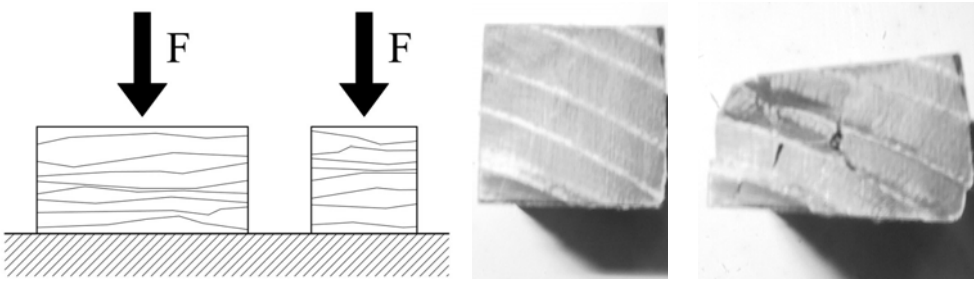

(a) (b) (c)

Figure 6. Compression test in direction perpendicular to the rings (D2): specimen shape and testing equipment (a), specimens before and after testing (b, c).

In Figure 6b two cross-section views of a specimen tested in D2 direction are shown: the first before testing and the second after testing. This latter highlights the significant transversal deformation due to tensile force developed along the annual growth rings.

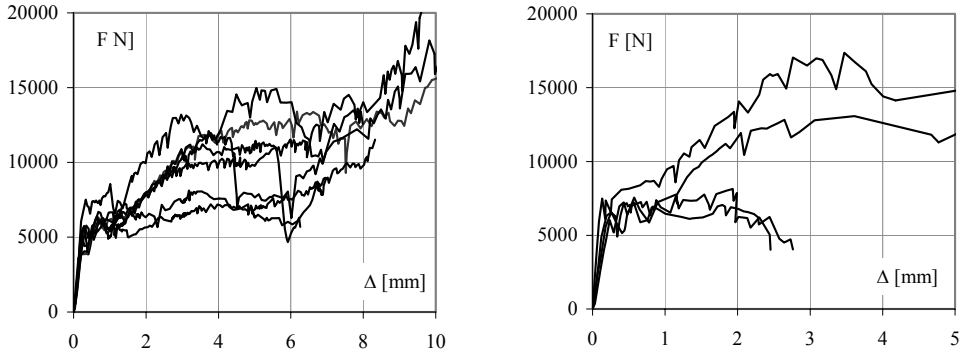

(a) (b)

Figure 7. Compression test in direction perpendicular to the rings (D2): F–Δ curves for specimens of group C (a) and group D (b).

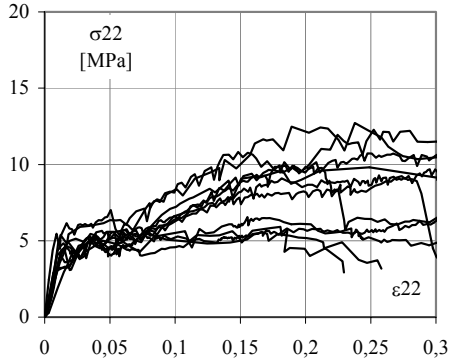

Figure 8. Compression test in direction perpendicular to the rings (D2): σ_{22} −ε_{22} curves for all specimens.

In Figures 7a and 7b the experimental F-Δ curves are depicted separately for the two groups of specimens. Figure 8 shows the σ_{c22}–ε_{c22} curves for all tested specimens. It is worthy to note that in this case, due to a viscous behaviour of material, which causes a significant hardening of wood, a peak compressive stress is not identified. For this reason a conventional yield compressive stress ($\sigma_{c22,y}$) has been defined as the stress corresponding to the occurrence of the first significant horizontal branch after the elastic field.

As shown in the Figure 8, the behaviour of all tested specimens was quite uniform both before and after yielding. The mean value of $\sigma_{c22,y}$ resulted equal to about 5 MPa. As expected, this value is about 1/10 of the compression resistance exhibited in the longitudinal direction (Giordano, 1989).

Compression tests in the direction tangential to the annual growth rings (D3) have been carried out on 10 specimens, according to the Italian regulation UNI-ISO 3132. The sample size and the testing arrangement were the same of the above tests related

to the direction D2. In this case, 6 specimens (group E) and 4 specimens (group F) with different dimensions have been considered.

Figure 9b shows two views of a specimen tested in D3 direction, before (a) and after (b) testing: it can be noted the separation in many layers of the growth rings at the occurrence of failure, due to transversal deformation.

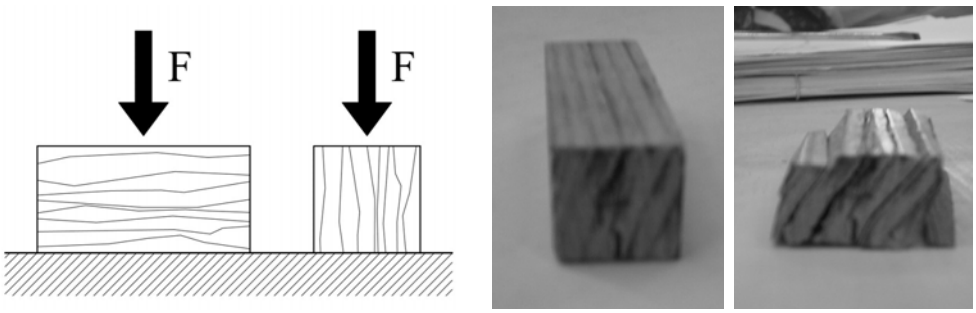

(a) (b) (c)

Figure 9. Compression test in direction tangential to the growth rings (D3): specimen shape and testing equipment (a), specimens before and after testing (b, c).

The experimental F-Δ and σ_{c33}–ε_{c33} curves are depicted in Figures 10a, 10b and 10c, respectively. It can be observed that, in this case, the post-elastic behaviour after the linear elastic field does not show a hardening branch, which does not occur due to the particular failure mechanism characterized by separation of wood in layers. Nevertheless, the maximum resistance level, which again can be defined as a "yield" stress of the material ($\sigma_{c33,y}$), is clearly evident from test.

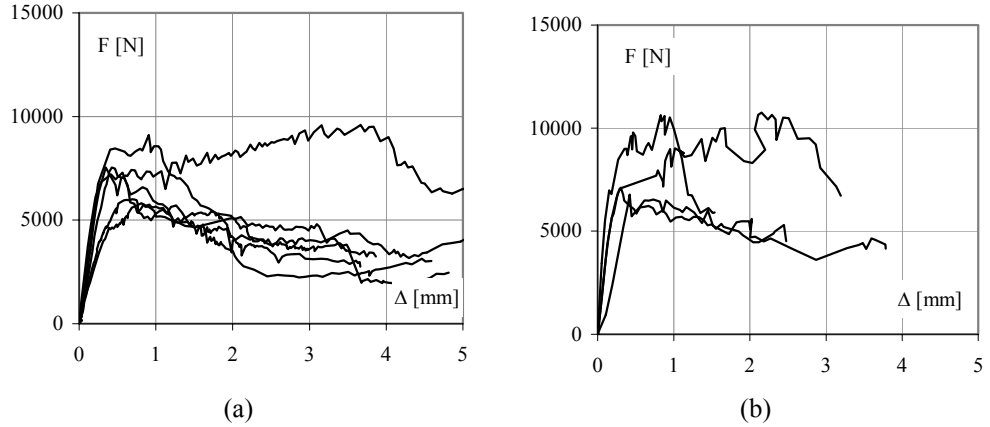

Figure 10. Compression test in direction tangential to the growth rings (D3): F–Δ curves for specimens of group E (a) and group F (b).

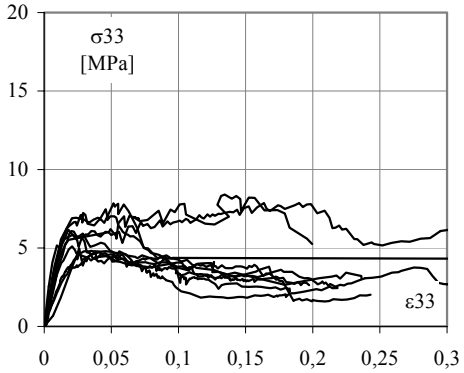

Figure 11. Compression test in direction tangential to the growth rings (D3): σ_{33} –ε_{33} curves for all specimens.

The behaviour of the specimens in these tests was quite uniform particularly before yielding. The mean value of $\sigma_{c33,y}$ is equal to about 5.7 MPa, very similar to the one obtained in the D2 direction, despite the different observed failure mode.

3. BENDING TESTS

Bending tests have been carried out according to UNI ISO-3133 [13] and UNI-ISO 3349 [14] on specimens working in the grain direction. Three small beams with different dimensions have been tested under two different loading conditions, both acting on simply supported static scheme. In particular, the sample Be1 has been loaded by two symmetric concentrated forces (four-points bending test), while samples Be2 and Be3 have been subjected to a single mid-span concentrated force (three-points bending test), as shown in Figures 12 and 13. The geometrical characteristics of specimens are given in Table 2.

Table 2. Main dimensions of tested specimens (bending tests).

Specimen	*span*	*cross section*		*loading scheme*
	L [mm]	*width b [mm]*	*depth h [mm]*	
Be1	360	30.8	28.8	a
Be2	300	30.0	31.0	b
Be3	300	24.8	25.0	b

Tests have been carried out by using the already described loading equipment. The imposed force has been transferred to the specimen by appropriate steel devices, different for the load schemes (a) and (b) (Figg. 12 and 13). The external supports are made of two steel half-cylinders. Mid-span deflection has been measured by means of LVDTs, located both on the loading device and on the beam. During the test, deflection has been progressively increased up to the collapse of the specimen, by means of a quasi-static procedure.

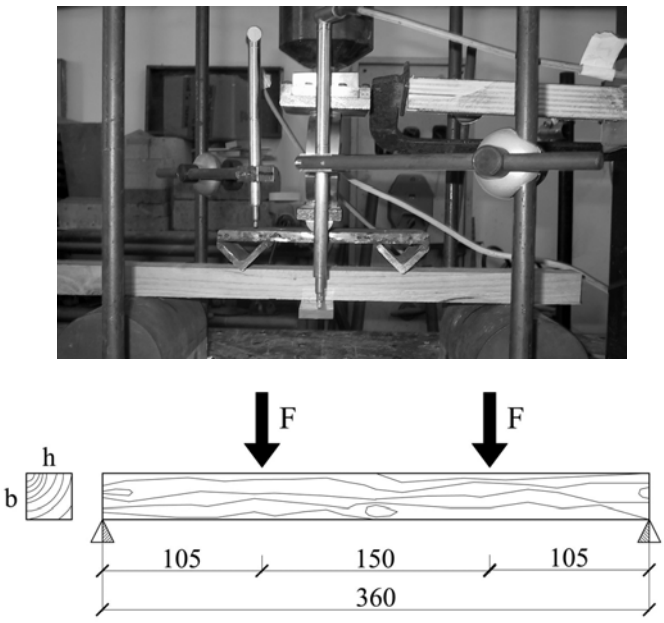

Figure 12. Testing arrangement for scheme (a).

The typical collapse mode of the tested beams is shown in Figure 14. Note that in all cases the failure occurred at the bottom of the central section due to excess of tensile stress. In addition, a partial compression failure was observed for specimen Be2.

The reaction force vs. mid-span deflection (F-Δ) curves are given in Figures 15a, 15b and 15c for each tested beam. The square dots indicate the maximum reaction force exhibited during the test, while the crosses represent the deflection when the device used for measuring displacement, originally fixed to the specimen, fell off.

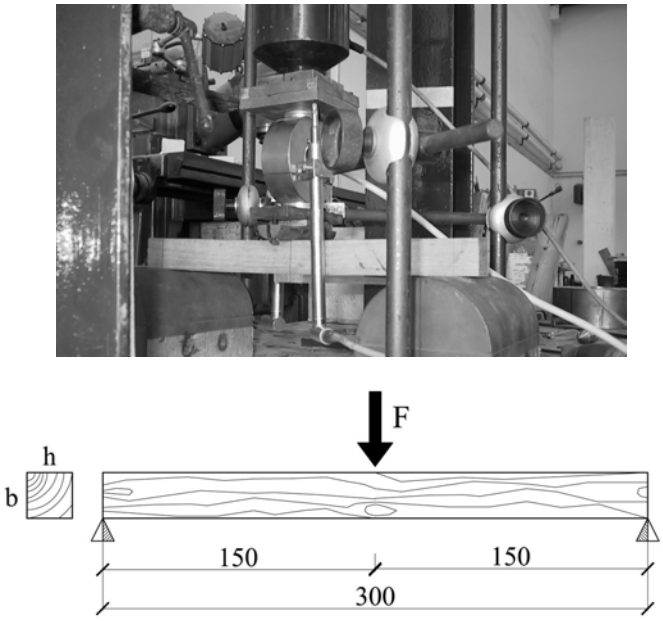

Figure 13. Testing arrangement for scheme (b).

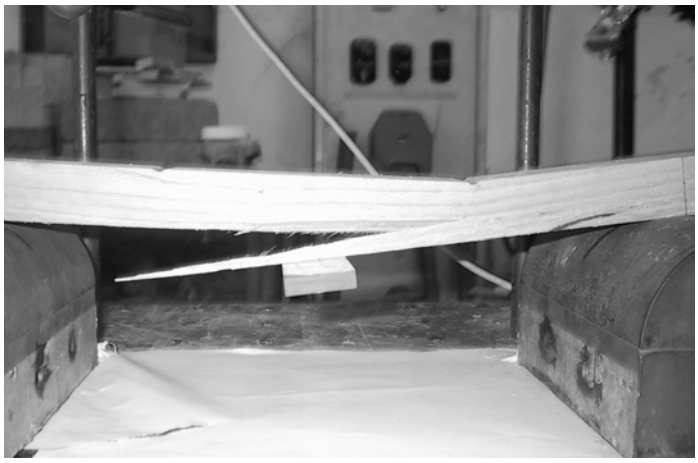

Figure 14. Flexural collapse mechanism for samples tested according to scheme (a).

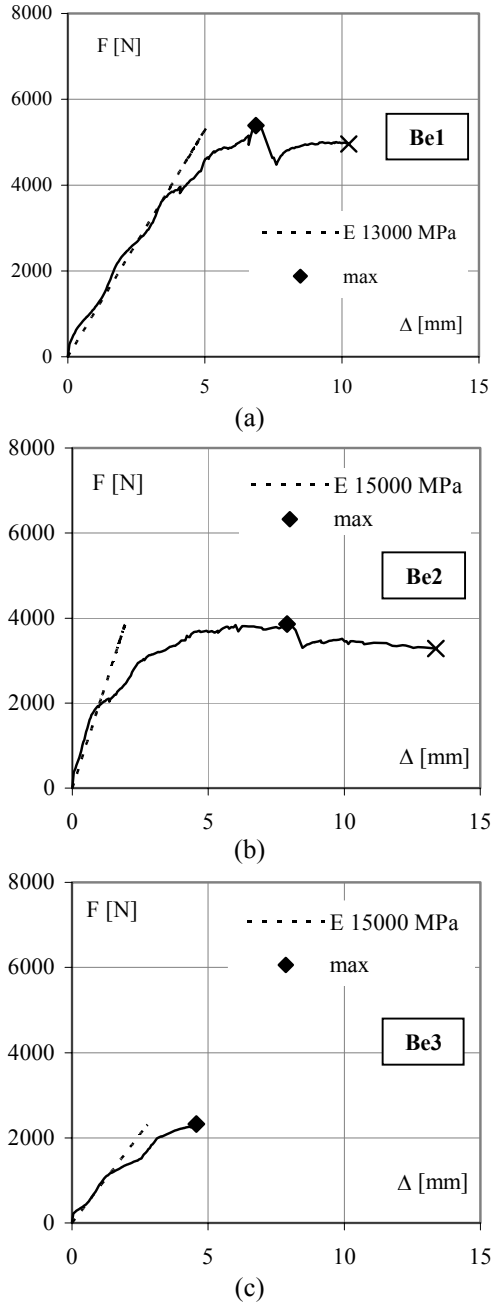

Figure 15. F-Δ curves for sample Be1 (b), Be2 (c) and Be3 (d).

It is important to remember that bending tests have been performed in order to obtain tensile resistance and longitudinal elastic modulus E_1 (in the following E_{long}) of wood, these mechanical properties being very difficult to obtain in direct way by means of tensile and/or compression tests. In this perspective, some considerations should be drawn. In fact, when the force is acting along the grain direction, the material response is different in tension and in compression. In the first case wood exhibits an elastic-brittle behaviour, while in the second case it presents an elastic-plastic behaviour with limited ductility. Furthermore, the ultimate tensile stress is about twice the compression one, while the longitudinal elastic modulus E_{long} in tension and compression is practically the same (ranging between 10000 - 15000 MPa for chestnut species) (Giordano, 1989). For these reasons and also for the unavoidable imperfections mainly existing in ancient wood but also in new beams, a brittle collapse can occur before the material has completely exhausted its plastic resource in compression. Then, for practical application, both technical literature and codes suggest to fix a conventional flexural strength, to be used for flexural checks, equal for tension and compression, obtained by considering an equivalent linear elastic behaviour of the whole section up to collapse.

Starting from the above experimental results, the longitudinal elastic modulus, the conventional ultimate flexural strength, the actual ultimate tensile stress and the maximum strain experienced in compression are evaluated in the following in case being.

For determining the conventional flexural strength ($\sigma_{fl,el,max}$) and the elastic longitudinal modulus E_{long} the beam behaviour is initially considered as completely linear-elastic. In this case the (elastic) curvature of each section is derived directly from the acting bending moment, according to the well known relationship:

$$\chi(z) = \frac{1}{r} = -\frac{M(z)}{E_{long} I} \tag{5.1}$$

where: I = moment of inertia of cross section along flexural axis, M(z) = bending moment in the z section of the beam.

The curvature can be also expressed as a function of mid-span beam deflection (δ) obtained from test. Then, with reference to mid-span cross-section, it results:

- loading scheme (a) $$\chi = \frac{24 \cdot \delta}{L^2 \cdot (3 - 4a^2/L^2)} \tag{5.2}$$

- loading scheme (b) $$\chi = \frac{12 \cdot \delta}{L^2} \tag{5.3}$$

where: L = span of specimen, a = distance between load point and external supports of the specimen.

By equating equation (5.1) with (5.2) or (5.3), with reference to mid-span section and to values of bending moment in the same section giving rise to compression stress surely lower than the (elastic) ultimate one, the elastic longitudinal modulus E_{long} is obtained. In our specific case, E_{long} resulted equal to 13000 MPa for sample Be1 and to 15000 MPa for samples Be2 and Be3, as reported in Table 3. The dashed lines depicted in Figures 15 represent the theoretical elastic stiffness of the tested specimens evaluated by adopting the above values of E_{long}. As expected, the slope of these lines is practically coincident with that of the elastic initial branch of the corresponding experimental curves.

According to the same hypotheses, the flexural limit elastic stress ($\sigma_{fl,el,lim}$) in the cross-section can be obtained by the Navier formula:

$$\sigma_{fl,el,lim} = \frac{M_{el}}{I_{el}} \cdot r_m \tag{5.4}$$

where M_{el} is the measured maximum bending moment in the elastic field, while r_m is either the radius of an equivalent circular cross-section or, in the case of rectangular cross-section, h/2 (where h is the depth of the beams).

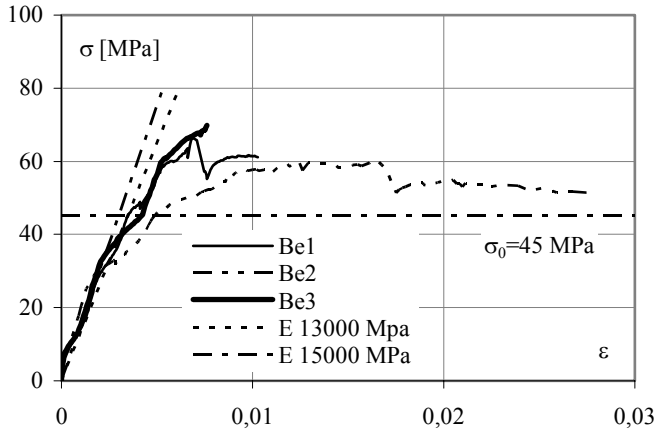

Figure 16. Stress-strain relationships from bending tests on small specimens.

In Figure 16 the results of all bending tests have been shown in terms of stress-strain diagram of the most stressed fibre (top or bottom) of the mid-span cross-section. Note that the stress has been derived from equation (5.4), while the strain has been obtained from the curvature evaluated by applying equation (5.2) or (5.3).

It can be observed that the behaviour of all tested specimens is practically elastic up to the value of $\sigma_{fl,el,lim}$, ranging from 38 to 45 MPa, which is quite in line with the main value of peak elastic compressive stress obtained from longitudinal compression tests. Then, the curves show a non linear behaviour, and stresses and strains cannot be evaluated in linear elastic hypothesis. In fact, the compressive stress

in the section cannot be higher than its peak value (σ_0), determined from direct test and assumed equal to 45 MPa. Such a value is represented in the figure by an horizontal dashed line. Also, the non-linear branch of the curves is useful to define the conventional flexural stress ($\sigma_{fl,el,max}$) to be used to determine the flexural resistance of beam for practical applications. This conventional stress is the peak value of the curves, which represents the stress to be considered for evaluating the bending moment resistance of the section in the hypothesis of a linear elastic behaviour up to the collapse load. In such a way the bending resistance is assumed to be equal to the actual ultimate resistance of the specimen obtained by testing, which is higher than the peak compressive stress but lower than the ultimate tensile one ($\sigma_{t,ult}$), which ranges from 60 to 70 MPa.

As the different behaviour in tension and in compression influences the bending behaviour, a more accurate analysis should be done. In particular, when compression stress reaches the maximum value σ_o, the behaviour of the section becomes non-linear: as far as the external action increases, the compressive stress keeps constant, while both strain and curvature increase (due to ductile behaviour in compression) as well as the maximum tensile stress. Moreover, the curvature cannot be derived directly from the experimental value of the mid-span deflection (equations (5.2) or (5.3)). On the other hand, it would be essential to evaluate the maximum strain reached in compression, and then the ductility exhibited by the cross-section. Furthermore, the ultimate tensile stress, corresponding to the maximum strength experienced by the beam in the test, can be obtained by the equilibrium of the cross-section and considering a simplified material σ–ε relationship, i.e. indefinitely elastic in tension and elastic perfectly plastic in compression with a limit value of stress equal to σ_0. The solution of the corresponding three equations (two equations of equilibrium - translation along longitudinal axis and rotation around any horizontal

transversal axis - and one of compatibility - i.e. the linearity of strains along the section), obtained by an iterative procedure, gives the ultimate tensile stress ($\sigma_{t,ult}$), the position of neutral axis (x_c) and the extension of the compressed zone in plastic range (a_c), as shown in Figure 17b.

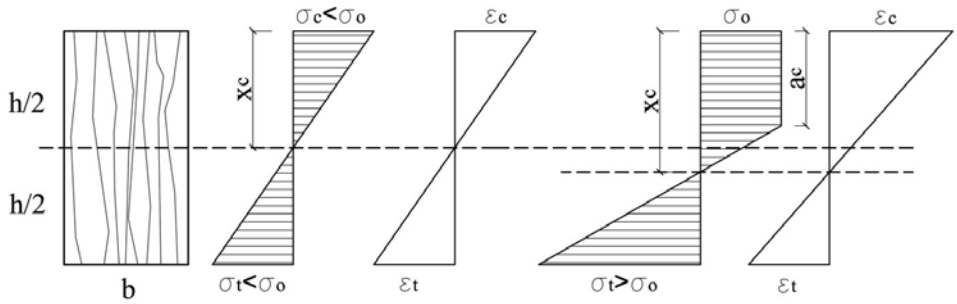

Figure 17. Stress-strain distribution on the cross-section in the elastic field ($\sigma_c < \sigma_o$) (a) and in the post elastic field ($\sigma_c = \sigma_o$) (b).

Based on the above procedure, the ultimate tensile stress ($\sigma_{t,ult}$), experienced by the tested specimens at the attainment of maximum bending moment, have been computed and provided in Table 3.

Table 3. Main values of stress and strain in the mid-span cross section (bending tests).

Specimen	M_{max} *[N*m]*	E_{long} *[MPa]*	$\sigma_{fl,el,max}$ *[MPa]*	$\sigma_{t,ult}$ *[MPa]*	$\varepsilon_{t,ult}$ *[%]*	$\varepsilon_{c,ult}$ *[%]*
Be1	283.0	13000	66.45	73.20	0.56	0.63
Be2	289.5	15000	60.20	63.40	0.42	0.45
Be3	174.5	15000	69.80	79.20	0.56	0.62

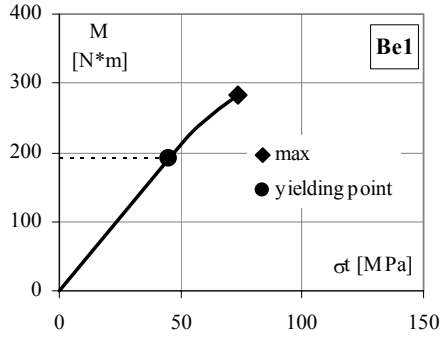

(a)

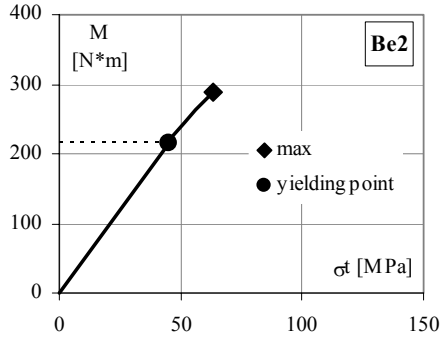

(b)

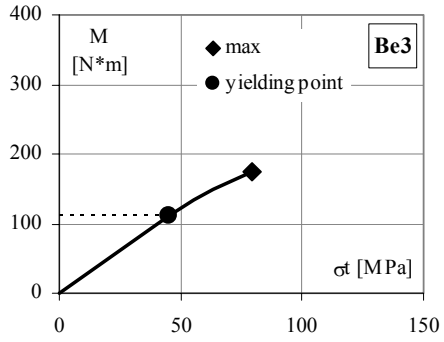

(c)

Figure 18. M vs. σ_t for sample Be1 (a), Be2 (b) and Be3 (c).

By using the same procedure, the theoretical relationship between bending moment and ultimate tensile stress in the mid-span cross-section for each of the three tested specimens, has been obtained and depicted in Figure 18a, 18b and 18c. The non linearity of these curves is evident. Obviously such curves are effective only up to the collapse of the beam, which is indicated by the square dot. In the same figure the horizontal dashed line indicates the value of the bending moment (M_y) corresponding to the attainment of the value of compressive strength σ_0, which is the beginning of the non-linear behaviour.

Due to the fact that all specimens have rectangular (or square) transversal cross-section, by normalizing the bending moment M by means of M_y, a normalized theoretical curve, which is independent of the dimensions of the transversal section of the beam, can be draw (Fig. 19). On such curve the limit values of M obtained in the tests for each specimen are also indicated. It can be noted that the increase of strength beyond the elastic limit in compression ($M/M_y = 1$) is not negligible, ranging from 1.4 to 1.6. Such an increasing strength factor can be considered as a generalized cross sectional shape factor.

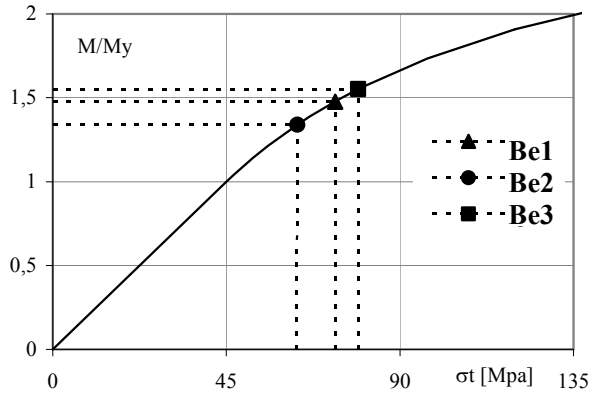

Figure 19. Normalised M/My vs. σ_t curve for each tested specimens.

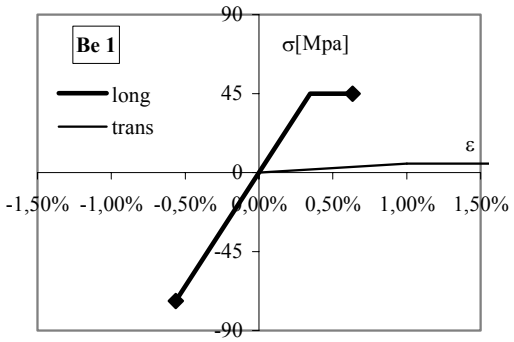

(a)

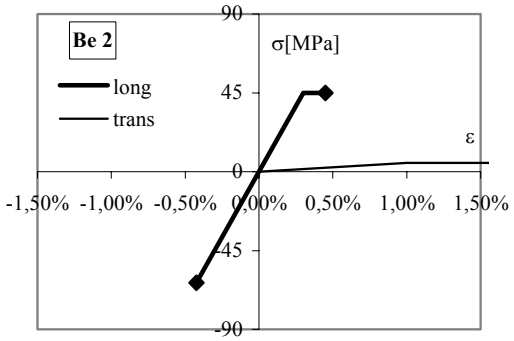

(b)

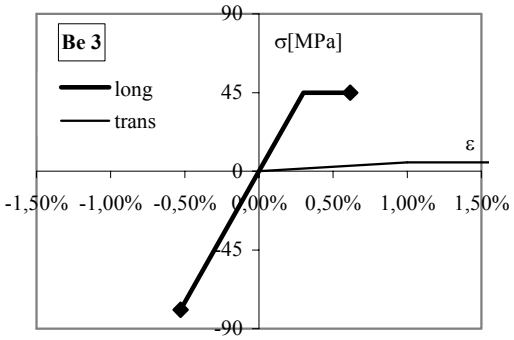

(c)

Figure 20. σ–ε curves for specimen Be1 (b), Be2 (b) and Be3 (c).

Since the elastic longitudinal modulus E_{long} has been previously evaluated with reference to the elastic behaviour of the beams, starting from the value of ultimate tensile stress and the depth of neutral axis, it is also possible to obtain the cross-section curvature. Finally, the maximum strain in compression is immediately derived from this curvature. The so calculated maximum experienced strain values are given in Table 3, together with the maximum strain reached in tension.

As it can be seen, the maximum strain in compression results equal to about 0.65%, which is about twice the one corresponding to σ_0 (dependent of the different values of E_{long} and equal to 0.30 – 0.35%), so confirming the capacity of wood to sustain a not negligible plastic deformation in the compressed zone. The corresponding maximum strain values in tension do not provide any additional information since the tensile behaviour is practically linear without appreciable ductility.

The complete stress-strain relationships for each tested specimens, obtained as above explained, are shown in Figure 20a, 20b and 20c. The dots indicate the maximum values of stress and strain in tension and compression exhibited by the material.

According to the UNI EN 408, the tangential modulus G can be determined from bending tests, using two different longitudinal elastic modulus, which are the ones obtained by four-points (E_f) and three-points (E_{app}) bending tests. In particular, in the case of three-point bending tests, due to the presence of the shear force along the whole beam, the influence of the shear deformation are not negligible and the mid-span deflection is obtained by the following equation:

$$\Delta w = \Delta w_f + \Delta w_v \tag{5.5}$$

where: $\Delta w = \frac{\Delta F \cdot l^3}{48 E_{app} I}$ is the mid-span deflection, while $\Delta w_f = \frac{\Delta F \cdot l^3}{48 E_f I}$ and $\Delta w_v = \frac{\chi V l}{G A}$ are the aliquots due to the bending moment and shear force, respectively, and χ is the shear factor (equal to 1.2 for rectangular cross-section) .

On the contrary, in the case of four-points bending test having a low distance between the loading-point and the corresponding end-beam, it is possible to omit the shear deformations. Therefore, the mid-span deflection and the corresponding longitudinal elastic modulus E_f can be determined considering the only flexural aliquot:

$$\Delta w = \Delta w_f \tag{5.6}$$

By substituting value of E_f obtained from equation (5.5) in the equation (5.6), G can be directly calculated by means of the following equation:

$$G = \frac{\chi h^2}{l^2 \left(\frac{1}{E_{m,app}} - \frac{1}{E_m} \right)} \tag{5.7}$$

Therefore, the tangential modulus G results equal to 1100 MPa and 950 MPa for samples Be2 and Be3, respectively, in good agreement with the values usually expected in technical literature. According to the simplified assumptions on the transversal elastic properties of wood explained in paragraph 1, G_{23} is equal to 275 MPa and 240 MPa for samples Be2 and Be3, respectively.

4. SHEAR TESTS

Shear tests have been carried out by means of a four-point bending scheme, where the two forces were placed very close to the support locations (Fig. 21). Consequently, the bending moment was practically absent and the shear force was constant near the supports, so to obtain a collapse in shear characterized by slipping at the beam ends.

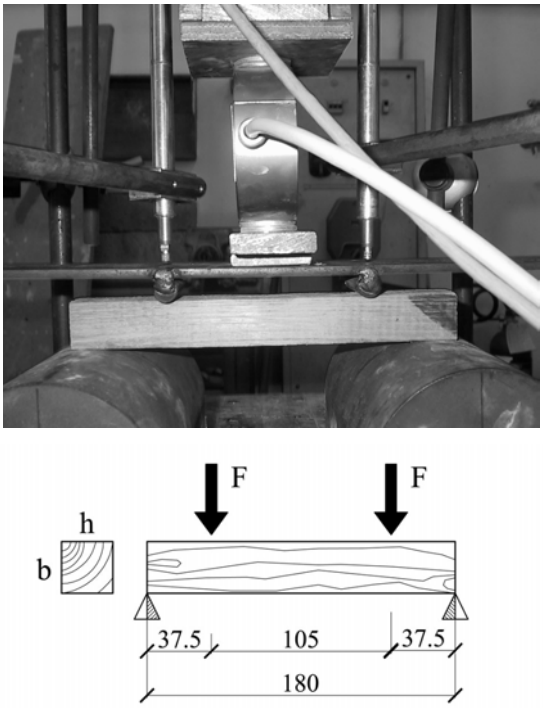

Figure 21. Loading scheme for shear test.

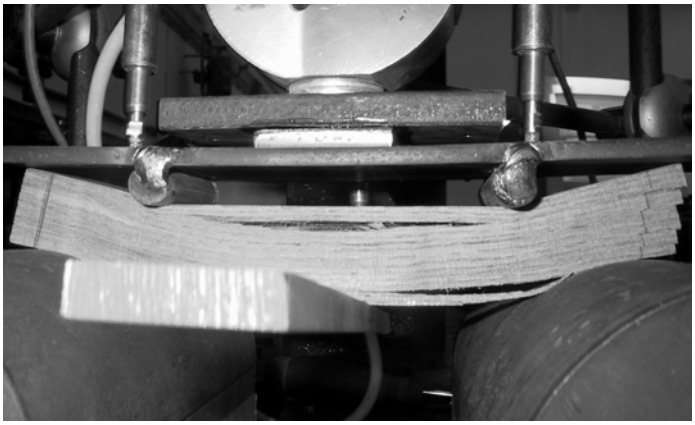

Figure 22. Typical shear type collapse mode.

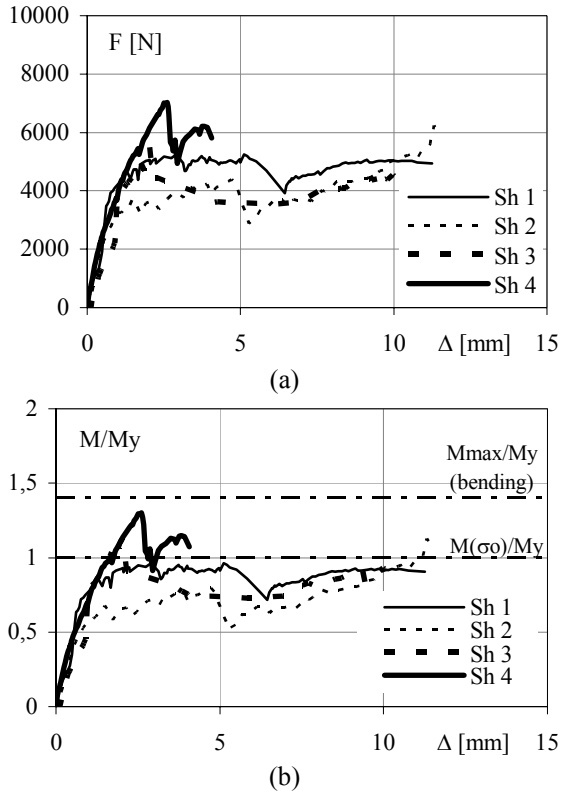

Figure 23. F-Δ curves (a) and M/My-δ curves (b) obtained from shear tests.

The tests have been performed on 4 specimens, having equal length and different cross-section, as specified in Table 4, by using the already described test equipment. The typical failure occurred during testing is shown in Figure 22. The slipping among the wood layers, defined by growth rings, is particularly evident.

Table 4. Main dimensions of tested specimens (shear tests).

Specimen	*span L [mm]*	*cross section*	
		width b [mm]	*depth h [mm]*
Sh1	180	23.7	24.0
Sh2	180	24.0	24.0
Sh3	180	23.8	24.0
Sh4	180	23.0	24.0

Test results are given in Figure 23a, in terms of force (F) vs. mid-span deflection (Δ) curves, and in Figure 23b, in terms of normalized maximum bending moment (M/M_y, M_y being evaluated according to $\sigma_0 = 45$ MPa) vs. mid-span deflection (Δ) curves. In these diagrams the two horizontal dashed lines refer to the values of M_y and the maximum bending moment from bending tests ($M_{Be,max}$), respectively. As confirmed by tests, it can be observed that the maximum flexural resistance was not reached in any tested specimen, this exhibiting a typical shear failure mode.

The maximum tangential stress in the beam, corresponding to the maximum value of shear force reached in each test, can be calculated by adopting the classic Jourawski's formulation:

$$\tau = \frac{V \cdot S}{I \cdot b} \tag{5.8}$$

where b is the cross-section width.

Note that, for specimen Sh4, where M_y has been over-passed before the attainment of shear failure, the maximum tangential stress has been conventionally evaluated using the same formulation, but with reference to the position of neutral axis determined according to the procedure provided in paragraph 3.

In Table 5 the maximum tangential stress ($\tau_{sh,max}$) for each tested samples is given. It can be noted a not negligible scatter in the values, probably due to the uncertainties in both experimental procedure and theoretical hypothesis. Nevertheless, the obtained values are in good agreement with the limit tangential stress ($\tau_{0,th}$), equal to about 7.5 MPa, given by technical literature for new chestnut wood (Giordano, 1989).

Table 5. Maximum shear force and corresponding maximum tangential stress in the cross-section (shear tests).

Specimen	V_{max} *[kN]*	$\tau_{Sh,max}$ *[MPa]*
Sh1	2.63	6.90
Sh2	2.20	5.70
Sh3	2.74	7.80
Sh4	3.52	9.35
	average value of $\tau_{sh,max}$	7.44

5. CONCLUSIONS

The results of the experimental activity on defect-free ancient wooden specimens in small dimension have provided complete information on mechanical properties of chestnut wood.

In particular, ultimate compressive resistance has been obtained from the compression tests, carried out throughout three different directions. An average resistance of 48 MPa has been exhibited in the direction parallel to the grain, while 1/10 of this resistance has been reached in the transversal directions.

Bending tests on small beams have confirmed that the wood behaviour is characterized by value of tensile ultimate stress higher than the compressive one and by a sort of ductility only in compression. Theoretical considerations applied to the experimental results allowed the quantitative definition of the $\sigma-\varepsilon$ curve, with the evaluation of a minimum ductile capacity and the measure of the longitudinal elastic modulus: the value of longitudinal elastic modulus E_{long} ranges from 13000 MPa and 15000 MPa, while the ultimate tensile stress is of about 70 MPa. Also, from bending tests on samples Be2 and Be3, tangential modulus G and G_{23} resulted equal to about 1000 MPa and 250 MPa, respectively.

From shear tests the ultimate shear resistance have been obtained in term of tangential stress, resulting of about 7.4 MPa.

CHAPTER 6:

Experimental analysis on timber elements in actual dimension

In this chapter, the results of an experimental campaign mainly based on the evaluation of structural behaviour of ancient chestnut elements in actual dimension are provided. Such members are the ones constituting the bearing structures of common timber floor of buildings located in many Mediterranean historical towns. This activity has been undertaken at the University of Naples Federico II.

These type of elements present many calculation uncertainties, due to the strong influence of natural (i.e. knots, shakes, shrinkage, shape imperfections and fibre deviations) and structural defects in the behavioural response. Therefore, the mechanical characterisation of wood obtained exclusively by means of tests on defect-free specimens in small dimension, as described in Chapter 5, is inadequate to have a valid and complete information on the structural behaviour of actual members and structures. Nowadays, the attention of the international research has to be moved towards the experimental investigation of the structural response of wood elements

having the same dimension of the actually used members. By means of these tests, it is possible to evaluate the differences between structural members and clear small specimens.

1. THE EXPERIMENTAL ACTIVITY

1.1. General information

The experimental activity described in this Chapter is based on the study of the structural behaviour of ancient timber elements in actual dimensions, subjected to stress-strain states usually present in-situ on such type of elements. Two different test typologies have been carried out on several number of specimens, as reported in Table 1. In particular, compressive tests along the grain direction and bending tests on chestnut beams have been performed, aiming at the evaluation of stiffness, load bearing capacity, post-elastic behaviour and collapse mechanism. In such a way, the global influence of the typical defect pattern on the behaviour of the tested samples have been evaluated by comparing the so-determined properties with the ones obtained by using the mechanical properties of defect-free specimens (see Chapter 5) (Tampone, 2001; Lanius et al., 1981).

Table 1. Test typologies and number of specimens for each test

Test typology	*Num. of specimens*
1. Compressive test along grain direction	3
2. Bending test	4

All the tested elements presented several shape irregularities and an extensive degradation state. They mainly consist of longitudinal splitting, cracking, shakes, degraded zones and holes, due to nails and insect attacks.

Full-scale tests have been carried out according to the Italian UNI-ISO codes, by using two different testing equipment which load the specimen in displacement control. The imposed displacement has been progressively increased up to reach the sample collapse.

Compression tests have been carried out by means of a testing frame, having a fixed base support and an upper moveable beam, on which an hydraulic actuator was placed (Fig. 1a). The actuator have a loading capacity of 3000 kN in compression. Also, the testing equipment was constituted of an incorporated displacement transducer with a maximum stroke of 75 mm and a load cell which measures the reaction force. According to the UNI ISO regulations, in order to guarantee an uniform distribution of the applied loads, a spherical hinge was placed between the load actuator and the top-end of the samples (Fig. 2a).

In each test, the displacement increasing rate has been chosen equal to 0.005 mm/sec up to a displacement of 5 mm (about twice the one corresponding to the attainment of the peak load value) and equal to 0.02 mm/sec up to the end of the test. Furthermore, electric displacement transducers (LVDT) with an accuracy of 1×10^{-3} mm were placed along the wooden elements (Fig. 2b). Both transducers and load cell have been connected to an electronic device and to a PC, in order to allow data acquisition and recording.

Full-scale bending tests have been performed by means of a testing frame having an hydraulic actuator with a loading capacity of 500 kN, able to apply reversible loads (Fig. 1b). Where necessary (i.e. in the case of loading scheme A, see paragraph 3.1), the concentrated forces were applied by interposing a rigid steel profile between the actuator and the tested beam, using purposely arranged wooden collars, as shown in

Figures 3a and 3b. The beams have been supported by means of steel semi-cylindrical hinges, located on heavy reinforced concrete blocks, which prevent any kind of displacement of the supports. Furthermore in order to avoid any transversal movements of the beam during testing, lateral steel devices have been fixed on the blocks on both sides of the specimen (Fig. 3c).

For all tests, a quasi-static loading procedure has been applied, using a constant value of the displacement velocity equal to 0.10 mm/sec. The applied displacement was progressively increased up to reaching the member collapse. For Beams 1 and 2, a constantly increasing load was applied, while in the case of tests on Beams 3 and 4, also some partial unloading and reloading cycles were applied (Fig. 4). Anyway, test parameters were basically the same for all the experimental program, in order to obtain comparable results. The procedure was realized by increasing displacement steps equal to 10 mm. Each step was followed by an hold step ranging from 10 to 30 sec. Also, the measurement of the deflections of the beam in the elastic range has been obtained by LVDT displacement transducers, having an accuracy of 1×10^{-3} mm (Fig. 3d), while the corresponding reaction force, given by the specimen, has been measured by means of a load cell. Both transducers and load cell have been connected to an electronic device and to a PC, in order to allow data acquisition and recording.

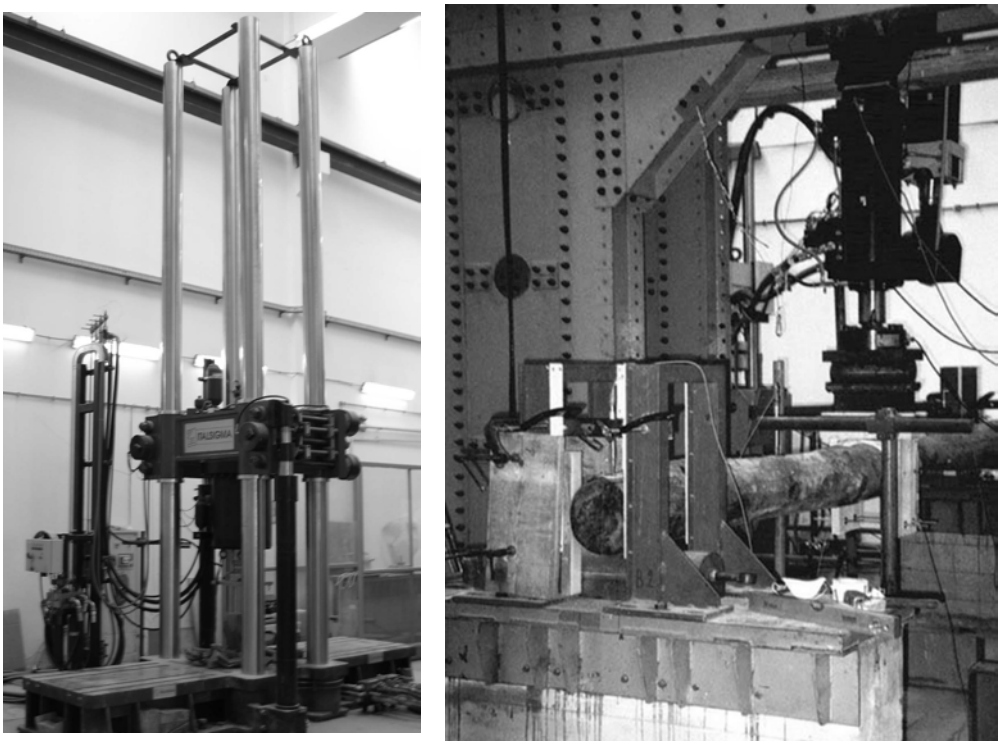

(a) (b)

Figure 1. Testing equipments used for compression tests (a) and bending tests (b).

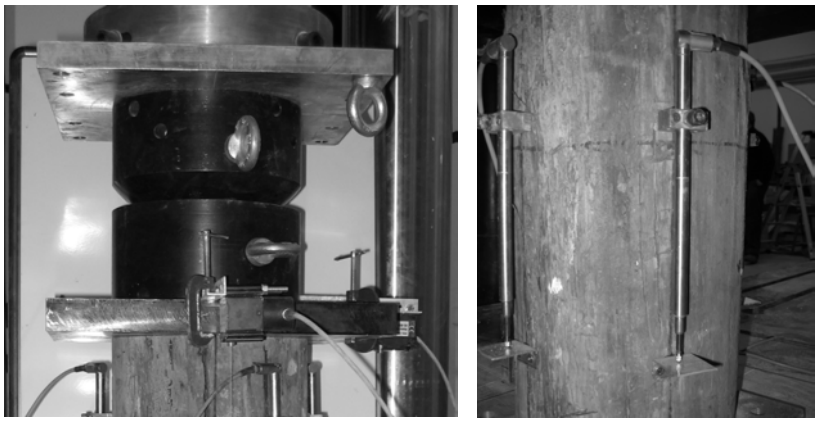

(a) (b)

Figure 2. Testing equipments used for compression tests: (a) spherical hinge at the top-end of the specimen; (b) LVDT transducer placed on the sample.

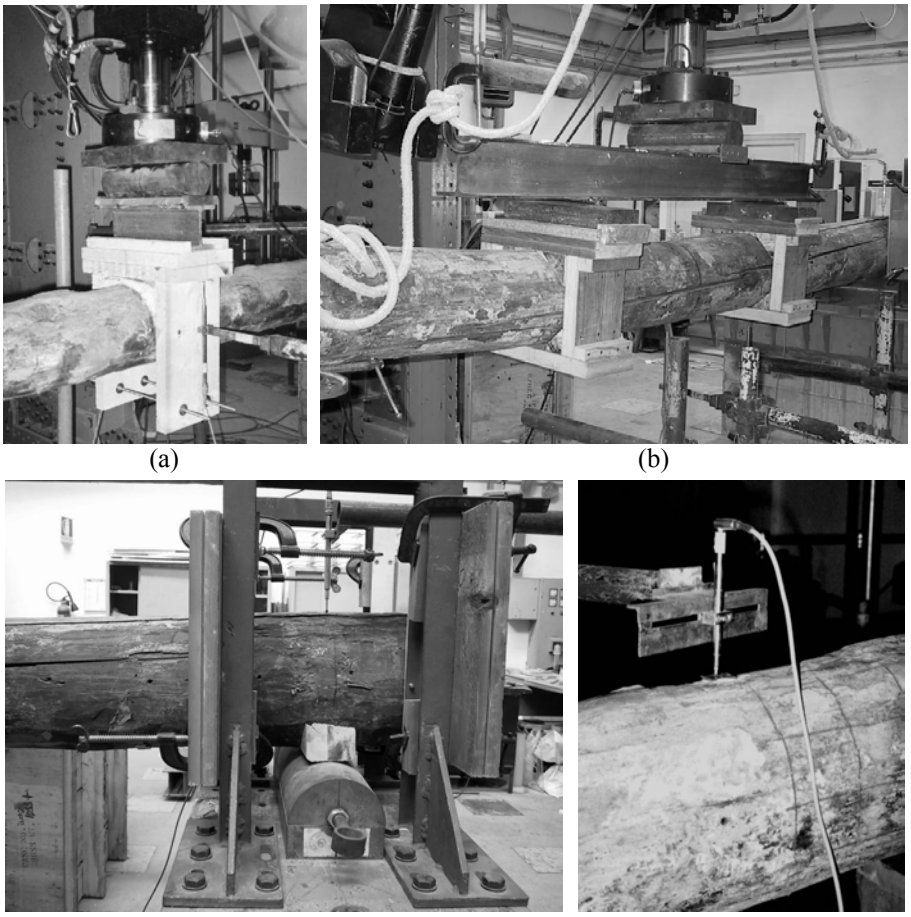

(a) (b)

(c) (d)

Figure 3. Testing equipment used for bending tests: load device used for scheme A (a); mid-span load for scheme B (b); one of the external hinged support (c); a LVDT transducer placed on the beam (d).

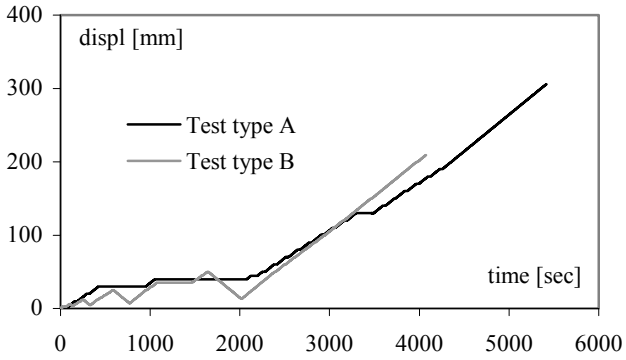

Figure 4. Adopted testing procedures (b).

1.2. Visual Inspection

An accurate geometrical survey of the beams were executed before testing. Usually, for such kind of structures the visual inspection is carried out in-situ, by directly observing the structural elements and determining the ambient conditions (such as temperature and humidity), in order to identify the biological risk class (UNI EN 335). Later, a detailed relief of the structure and its members is carried out. In this case, the timber elements were placed in the Laboratory. Therefore, a more exhaustive survey has been undertaken.

In particular, the geometric survey were carried out on parts of beams of about 65 cm. On each part the variability of three cross-section dimension and the corresponding deflection of beam were relieved. Furthermore, defects, such as knots, hole and longitudinal and transversal cracking, and degradative state were relieved.

The acquaintance of both the cross-sections dimension and the defect pattern was indispensable to elaborate a numerical model used for valuating the longitudinal elastic modulus. Furthermore, the relief of the end-beams cross-sections has been used for obtaining the tangential stress state along the section.

As an example, In Figure 5 the general relief is reported for a part of Beam 3, while in Figures 6, 7, 8 and 9 typical defects present in Beam 1, 2, 3 and 4, respectively, is depicted.

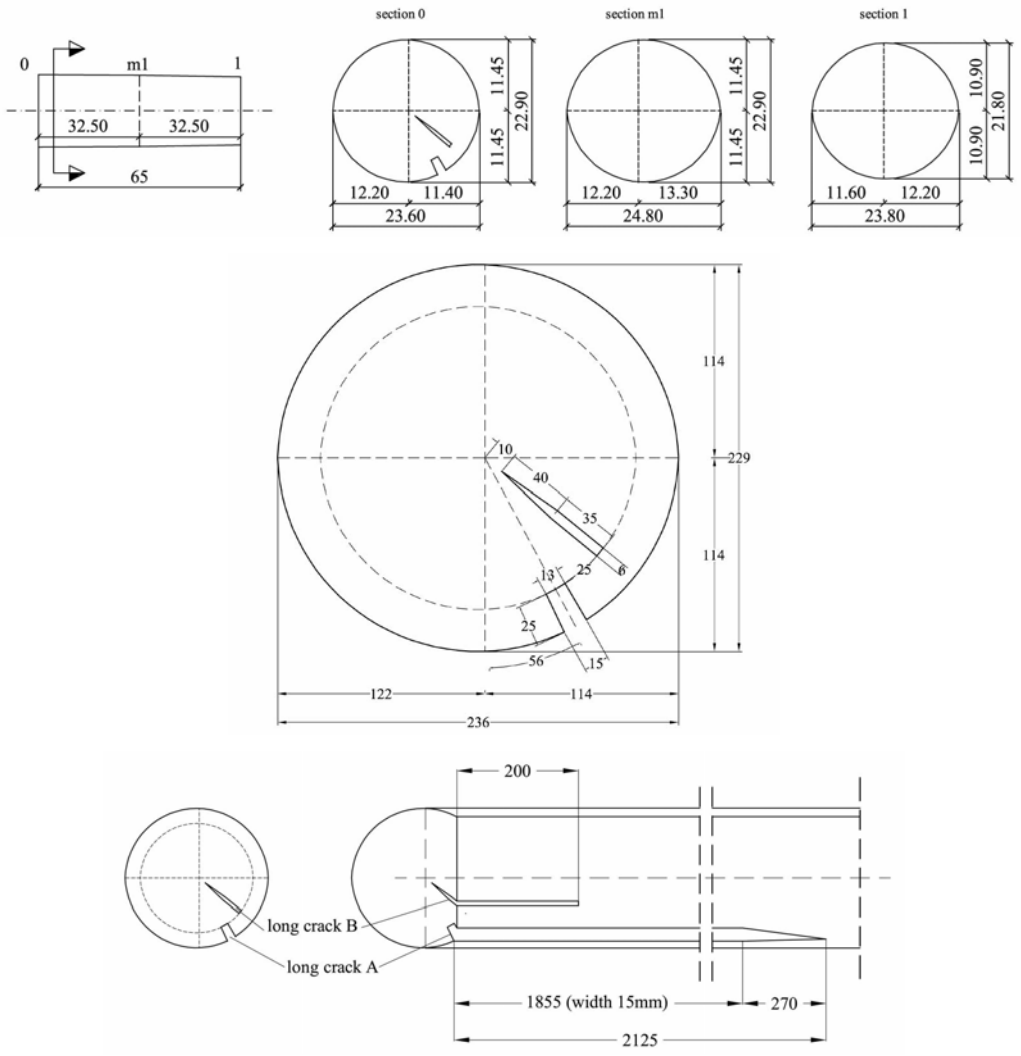

Figure 5. Relief of maximum end-beam cross-section of Beam 3.

Figure 6. Defect pattern of Beam 1.

Figure 7. Defect pattern of Beam 2.

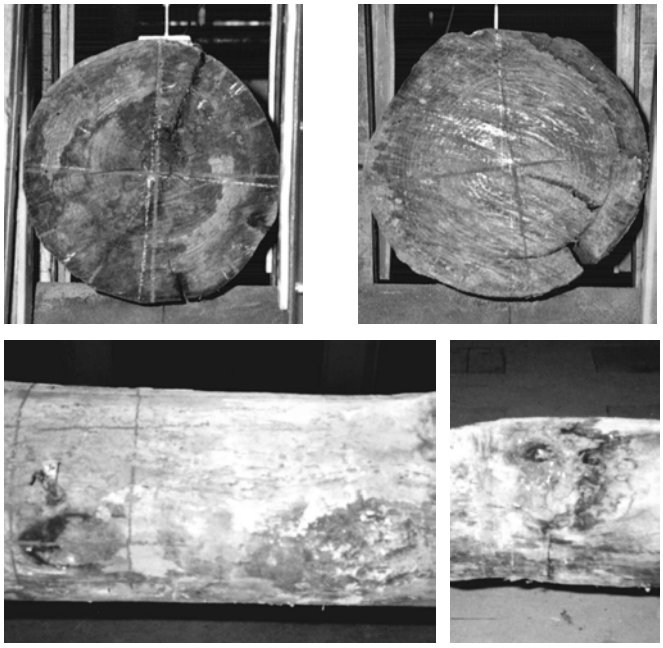

Figure 8. Defect pattern of Beam 3.

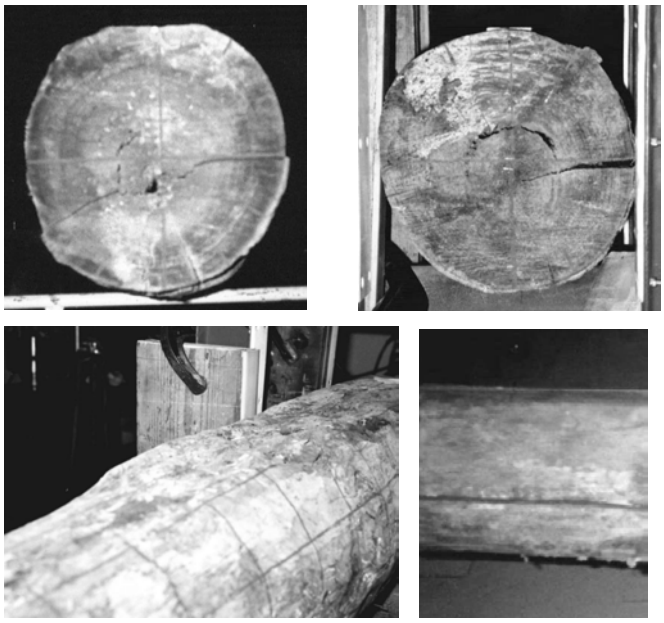

Figure 9. Defect pattern of Beam 4.

2. COMPRESSION TESTS

2.1. Testing set-up

Full-scale compression tests along grain direction have been carried out on 3 specimens extracted from an ancient chestnut beams. These chestnut trunks had a quite circular cross-section with diameter of about 200 – 250 mm and a length of about 450 mm. Since the samples were obtained by disbarking natural elements, their cross-sections are not constant and their lateral surface present several types of defects and shape irregularities. In Table 2 and Figure 10 the principal dimensions of the samples are reported.

Table 2. Geometry of tested samples.

Samples	*Length [mm]*	*Max end-beam diameters [mm]*	*Min. end-beam diameters [mm]*
1	435	255 - 260	242 – 256
2	455	247 – 255	245 – 250
3	440	250 – 255	255 – 247

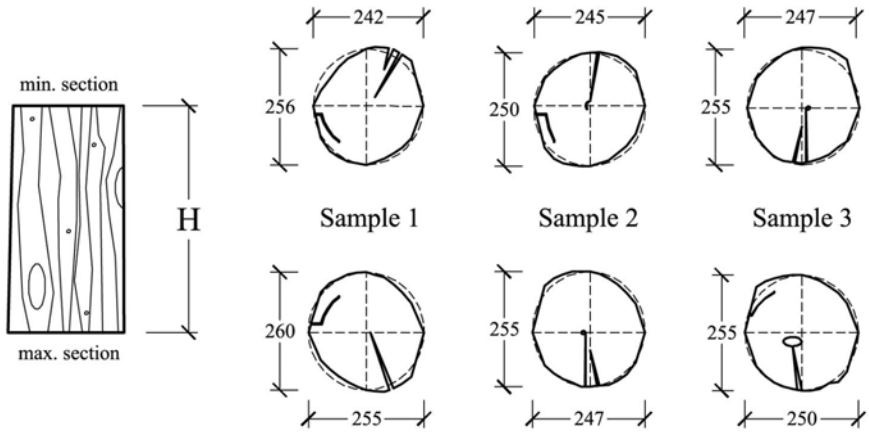

Figure 10. Principal dimensions of the samples.

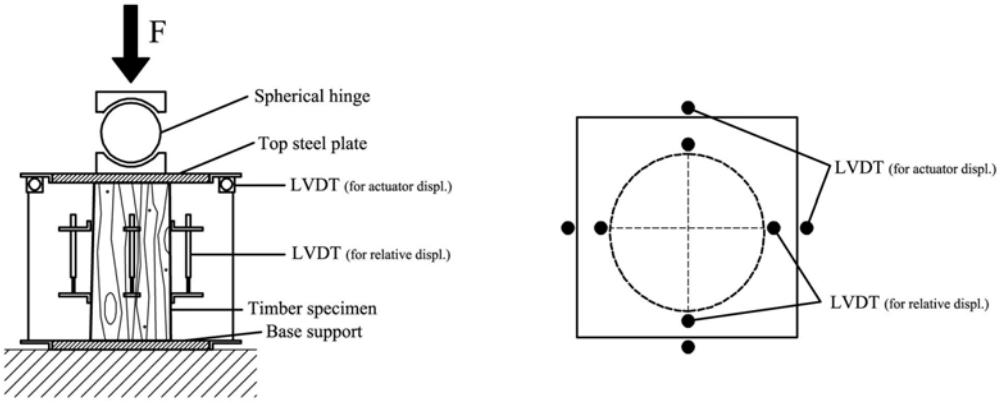

Figure 11. The disposition of the transducers during the test.

The applied displacements have been measured by means of an internal transducer of the loading equipment. Also, during the tests 4 LVDTs have been located at the opposite sides of the hinge device, until the attainment of a displacement of about 5 mm, in the post-peak field. The mean value of the 4 corresponding measures has been considered as representative of the top displacement of the sample. Furthermore, in order to measure the relative displacements Δl at the middle of the samples in the elastic range, 4 LVDTs have been placed on the wooden trunks. In Figure 11 the disposition of all the transducers is shown.

2.2. Experimental results

The experimental results are shown in Figures 12a, 12b and 12c in terms of the applied actuator load (F) versus actuator displacement (Δ) for samples 1, 2 and 3, respectively. The so-obtained F - Δ curves allow to highlight the global behaviour of the samples up to the collapse, which appears similar for all tests. After an initial phase characterised by a very low rigidity, due to the accommodation of the loading equipment to the top-end of the samples, the curve shows a linear elastic branch up to

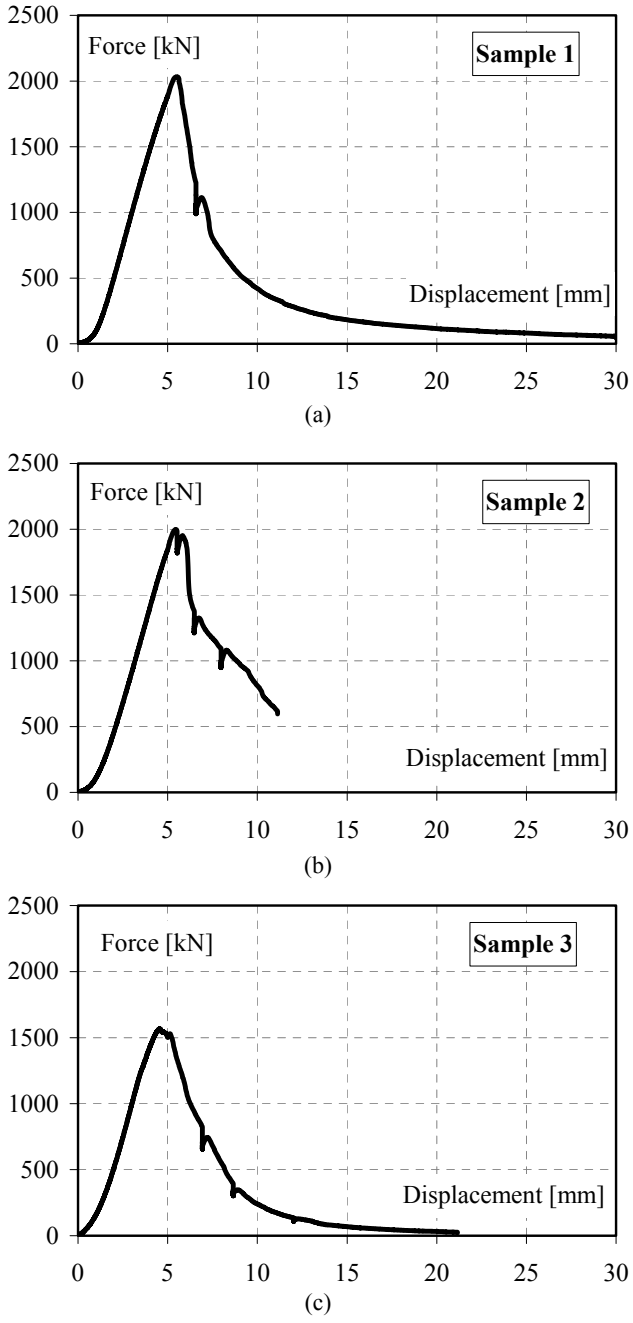

Figure 12. F – Δ curve for Sample 1 (a), 2 (b) and 3 (c).

(a) (b) (c)

Figure 13. A specimens before the test (a), at the attainment of the collapse mechanism (b) and after the end of the test (c).

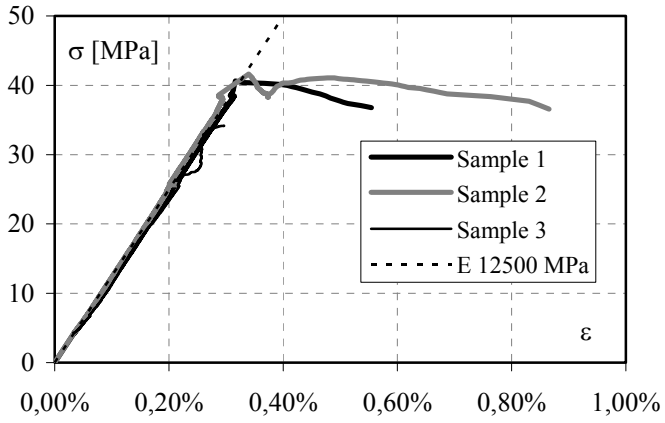

Figure 14. σ_c–ε_c curves for all tested specimens.

the peak load reached during the test, corresponding to the actual collapse of the sample. The post-peak field of the curve presents a significant load-bearing reduction which have an initial strength decrease more pronounced.

All the tested samples have shown a similar collapse mechanisms, due to the attainment of the cleavages quite parallel to the fibre and a consequent buckling of the separated parts. In Figure 13, as an example, one specimen is represented before and after the attainment of the collapse mechanism.

In Figure 14 the σ_c–ε_c curves of each tested specimens are plotted together. The longitudinal compressive stress σ_c has been calculated with reference to the applied force and to the actual cross-section area, while the corresponding longitudinal strain ε_c has been evaluated at the middle part of the samples on a distance of 200 mm.

The peak compressive stress $\sigma_{c,max}$ is practically coincident for all the samples, with an average value of about 41 MPa. Also in the case of the longitudinal elastic modulus E_{long}, evaluated in the elastic range at different values of the compressive stress, the obtained value is the same for all specimens and equal to about 12500 MPa. These values appear to be lightly lower than the ones obtained by compressive tests on defect-free specimens, in good accordance with those reported in literature for new chestnut wood (Giordano, 1989). In the case of the compressive tests, in fact, the difference in the loss of bearing capacity of the wooden member between actual and defect-free samples, is less influenced by the presence of the defect patterns.

3. BENDING TESTS

3.1. Testing set-up

Bending tests have been performed on a series of 4 ancient chestnut beams in actual dimension (Calderoni *et al.*, 2003; Mazzolani *et al.*, 2004 (b)). As specifically described in Chapter 4, this series of beams had a quite circular cross-section, whose diameter ranges from 200 to 250 mm, and a span length of about 4 m (Table 3). Also,

as occurred in the case of wooden samples used for full-scale compression tests, they present defects, degraded zones and shape irregularities. In particular, for the Beams 1, 2 and 4, a longitudinal splitting which is also deep in transversal direction, can be observed.

Table 3. Geometry of tested beams in actual dimension.

Beam	*Beam length [mm]*	*Span length [mm]*	*Max diameters [mm]*	*Min. diameters [mm]*
1	3930	3400	245 – 261	202 – 217
2	3930	3400	248 – 254	214 – 220
3	3900	3600	229 – 236	205 – 228
4	3880	3600	275 – 282	236 – 238

Full scale bending tests have been carried out on simply supported beams using two different loading schemes, as shown in Figures 15a and 15b. In particular, scheme A (four-points bending tests) with two symmetric concentrated forces was used for testing Beams 1 and 2, and scheme B (three-points bending test) with single mid-span concentrated force for Beams 3 and 4. Note that, the first static scheme is characterized by a constant bending moment zone and a maximum shear-to-bending moment ratio, while the second structural scheme presents an higher moment gradient, with maximum bending moment in the mid-span section, and a lower shear-to-bending moment ratio. In order to measure the deflections of the beam in the elastic range, displacement transducers (LVDT) with an accuracy of 1×10^{-3} mm were used. LVDTs were placed throughout the beam, at mid-span, at loading points and at beam ends (Fig. 16).

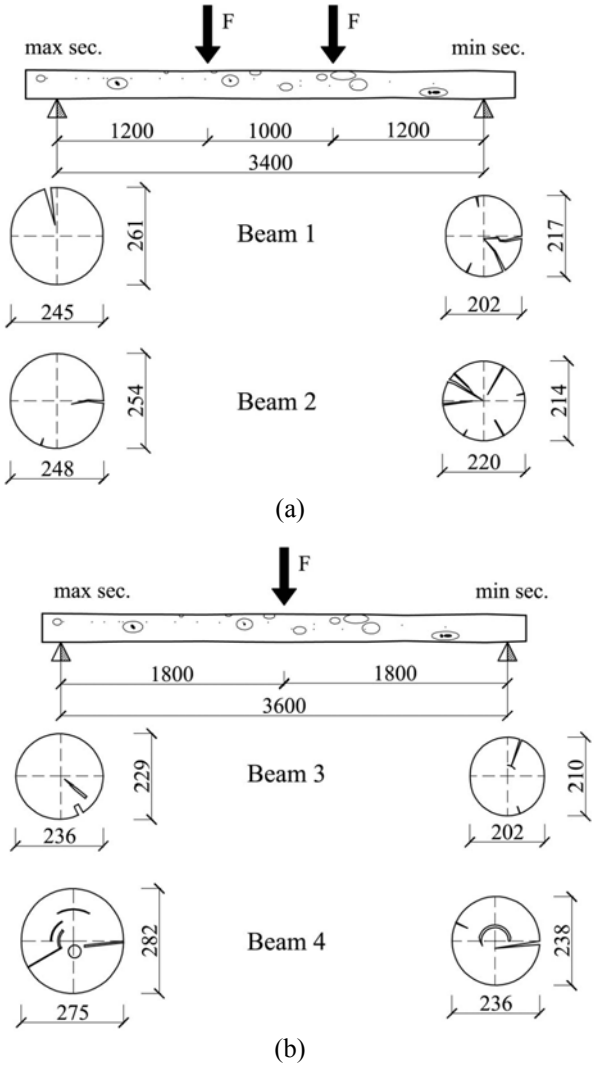

Figure 15. The loading scheme A (a) and B (b) used for beam testing.

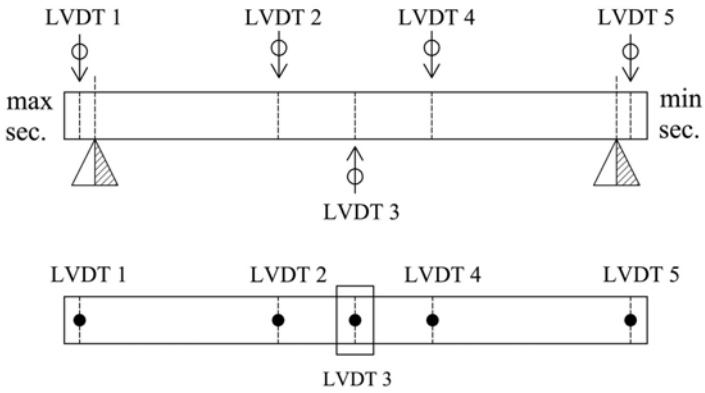

Figure 16. LVDT location: front view (upper) and top view (bottom).

3.2. Experimental results

Tested beams have shown different collapse mechanisms, even if the geometrical dimensions, degradation phenomena and mechanical properties of the base material were quite similar to each other. The experimental results are shown in Figures 17, 19, 21 and 23 for Beams 1, 2, 3 and 4, respectively, where the applied actuator load (F) (i.e. the global force applied on the beam) versus actuator displacement (Δ) relationship is provided. The obtained F-Δ curves allow the global behaviour of the systems during the whole test and up to the collapse to be detected.

For Beam 1, first cracks appeared in the bottom part of the beam, from mid-span to the end-beam, on the side with the smaller cross-section. The beam showed a quite linear behaviour up to the maximum load reached during the test, which is equal to 78 kN, for a displacement of 40 mm, when the first significant cracking occurred. Consequently, a first load-bearing reduction was noticed, corresponding to a shear-type slipping mechanism. Then, the system quickly resumed its bearing capacity up

to a load value F = 75 kN and a displacement Δ = 44 mm, where the behaviour showed a strength decrease more pronounced than the previous one. The longitudinal relative displacements among upper and lower part of the beam were very significant, as it can be observed from Figure 18. At the end of the test, a remarkable residual deformed shape of the beam was evident.

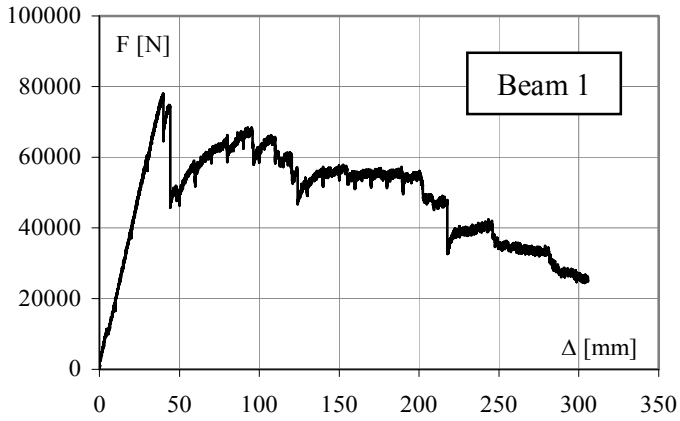

Figure 17. F – Δ curve for Beam 1.

(a) (b)

Figure 18. Slipping at the end section of Beam 1 (a); shear failure-type collapse mode of the tested beam (b).

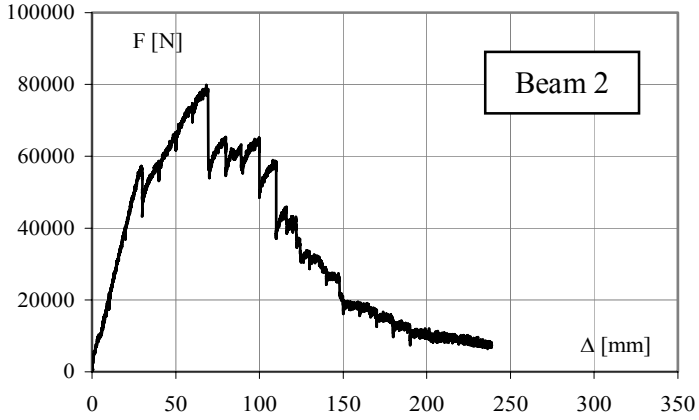

Figure 19. F – Δ curve for Beam 2.

(a) (b)

Figure 20. Slipping at the end-beam with small cross-section dimension of Beam 2 (a); failure-type collapse mode of Beam 2 (b).

For Beam 2, the obtained experimental curve shows an initial elastic linear behaviour up to peak load value of 57 kN and an actuator displacement of 29 mm. When this load value was reached, a moderate loss of bearing capacity followed, corresponding to first shear cracking developing in the beam. Subsequently, the beam showed a

flexural stiffness lower than the initial one. The applied force grew up to a maximum value of 80 kN, corresponding to an actuator displacement of 68 mm, where a more pronounced slipping of the smaller end-beam cross section appeared (Fig. 20). The stiffness and strength reduction was significant and the bearing capacity quickly dropped down. In this case, it is interesting to note that, even if the collapse mode was the same as occurred for Beam 1, the global response of the system was not linear up to the failure load.

Beam 3 showed a completely different collapse mode. The corresponding load vs. displacement curve exhibits an initial linear branch up to the peak load, equal to F = 55 kN for a displacement Δ = 76.50 mm (Fig. 21).

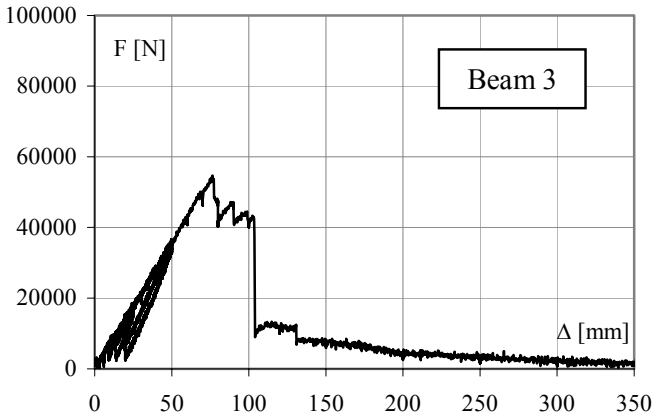

Figure 21. F – Δ curve for Beam 3.

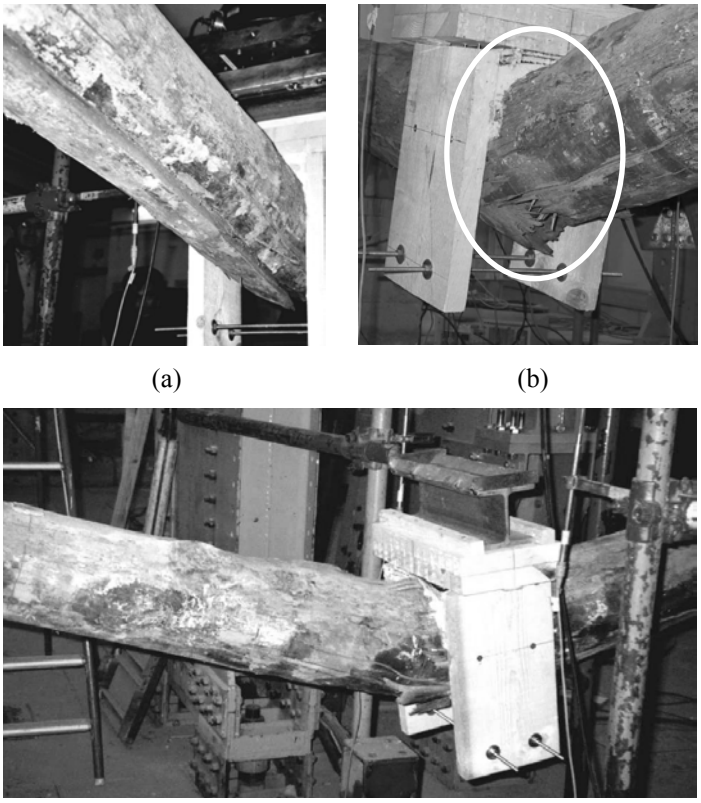

(a) (b)

(c)

Figure 22. Longitudinal splitting at the bottom part (a) and cracking in mid-span section (b, c) for Beam 3.

In this case, the first slipping occurred before the beam collapse for a load of about 25 kN and it was concentrated in the bottom part of the specimen starting from the mid-span section to the end-beam section having smaller diameter, even if without significant loss of bearing capacity. The applied load equal to 55 kN produced the failure mechanism of the beam, which started in the part of the member under tensile forces, very close to mid-span section (Fig. 22). Therefore, a flexural collapse mode occurred, with a consequent sudden loss of bearing capacity. Contrarily to the other

cases, where shear failure mechanism occurred, a very large strength reduction was evident.

Beam 4 showed a structural behaviour very similar to the one exhibited by Beam 1 (Fig. 23). The initial behaviour was almost linear up to a loading value of about 66 kN. Then, when displacement reached 60 mm, an evident shear slipping occurred at the side of beam having the smaller cross section, interesting the whole half length of the specimen, from the end side to the loading point. The load dropped down to about 48 kN and then again increased with a very low flexural stiffness. Further slipping developed as far as the displacement increased, until the collapse of the system occurred, due to flexural failure in both the two longitudinal parts in which the beam was split by the shear cracking (Fig. 24).

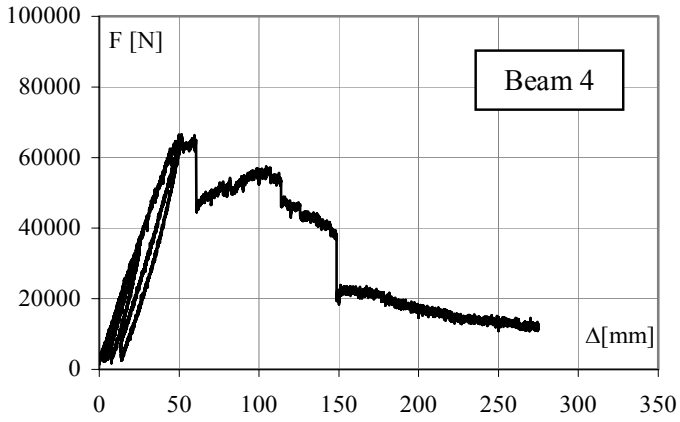

Figure 23. F – Δ curve for Beam 4.

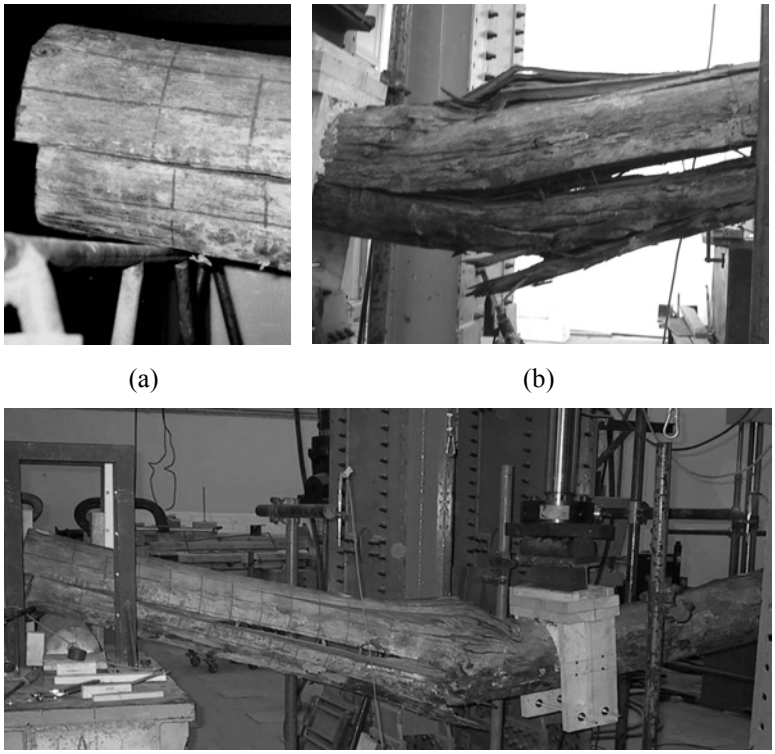

(a) (b)

(c)

Figure 24. Slipping at the beam end section and collapse mode for Beam 4.

3.3. Examination of bending behaviour

On the basis of the experimental results, it can be stated that Beam 3 has suffered a flexural failure, while the other beams have been characterized by a shear collapse mode, occurred with a significant longitudinal slip between upper and bottom part of the beam. It can be also observed that all tested beams have shown an almost linear behaviour up to the peak load, characterized by a sudden loss of the bearing capacity, which was more evident in the case of flexural collapse mode (Beam 3).

The analysis of the experimental results must necessarily start from the characterization of the mechanical properties of the base material. Therefore, before the examination of bending and shear behaviour some considerations have to be made. Tests on ancient wooden defect-free specimens in small dimension have been carried out on a number of appropriate samples. This experimental campaign, concerning compression, bending and shear tests as comprehensively described in Chapter 5. In particular, as wood is an orthotropic material, compression tests have been performed by applying the load in 3 different directions (one parallel to the grain and two orthogonal directions – radial and tangential to the annual growth rings). The stress-strain curve obtained for the direction parallel to the grain highlighted that the wood behaviour in compression is linear elastic with a limited ductility, while in tension it is linear elastic with brittle failure characterised by an ultimate tensile stress about twice the maximum compression stress (σ_0). The mean value of σ_0 resulted equal to about 45 MPa, in good agreement with values normally considered in technical literature for chestnut (Giordano, 1991; Tampone, 1996). Also, bending and shear tests have been carried out on simple supported small beams. From bending tests longitudinal elastic modulus (E_{long}) was obtained, ranging from 13000 to 15000 MPa. From shear tests the mean value at the ultimate tangential stress (τ_o) resulted about 7 MPa.

If we consider the basic material as homogenous, isotropic and elastic (the material properties throughout the longitudinal direction play the main role in the case being), the longitudinal maximum stress in the beam are given by:

$$\sigma_{fl,el} = \frac{M_{el}}{I_{el}} \cdot r_m \tag{6.1}$$

where M_{el} is the measured maximum bending moment in the elastic field, while r_m and I are the radius and the moment of inertia of an equivalent circular section, respectively.

Similarly, the equivalent longitudinal elastic modulus (E_{long}) may be gained by equating measured displacement with the one predicted by applying the simple linear elastic theory. For the tested beams, the obtained values of E_{long} are slightly lower than the ones given in the technical literature for new chestnut beams as well as those obtained by specimens in small dimension tested in bending. In particular, as shown in Table 4, E_{long} values obtained for Beams 2,3 and 4 are very close to each other (ranging from 7600 to 8000 MPa), while the elastic modulus for Beam 1 is significantly higher than the other ones. This can be explained by observing that during the test of Beam 1, out-of-plane vertical deformations developed, due to an asymmetric behaviour of tested beam and a subsequent loading eccentricity, affecting the measured deflections.

In Table 4, also the peak load (F_{max}) and the corresponding maximum value of shear force (V_{max}) and bending moment (M_{max}) reached in the tests are also provided.

Table 4. Maximum values of longitudinal elastic modulus and corresponding shear and bending moment for tested beams in actual dimension.

Beam	E_{long} *[MPa]*	F_{max} *[kN]*	M_{max} *[kNm]*	V_{max} *[kN]*
1	11600	78.04	46.90	39.02
2	8000	79.87	47.93	39.94
3	7600	54.75	49.28	27.38
4	7800	66.58	59.92	33.29

In addition, in Table 5 the radius of the equivalent circular cross-sections (r_m), the corresponding section elastic modulus (W), the longitudinal maximum stress

obtained by tests ($\sigma_{fl,max}$), the bending moment (M_y) and shear force (T_y) corresponding to the attainment of the stress σ_o = 45 MPa in the more stressed cross-section are provided. It can be noted that $\sigma_{fl,max}$ is always lower than σ_o.

In order to allow a direct comparison of obtained results, the previous curves have been presented in normalised format. In Figure 25 M/M_y versus Δ/Δ_{My} curves are presented, separately for the two groups of beams which have been subjected to the same loading scheme. Note that M is the maximum bending moment in the beam, Δ is the corresponding experimental deflection of mid-span section, while Δ_{My} is the theoretical deflection corresponding to M_y. In the diagrams, shown in Figure 25, the horizontal dashed lines indicate the theoretical M_y bending moment.

Table 5. Main values of flexural resistance for tested beams in actual dimension.

Beam	r_m *[mm]*	W *[mm^3]*	$\sigma_{fl,max}$ *[MPa]*	M_y *[kNm]*	V_y *[kN]*
1	118.0	1290x10^3	36.5	58.04	48.37
2	126.0	1570 x10^3	30.5	70.66	58.89
3	113.5	1148 x10^3	43.0	51.65	28.69
4	130.0	1725 x10^3	34.7	77.61	43.12

It can be observed that for Beam 3 the maximum stress attains approximately the σ_o value, while for Beams 1, 2 and 4 the value of the maximum normal stress is significantly lower (always less than 35 MPa), confirming the occurrence of shear collapse before flexural failure. For all the tested beams, the M_{max}/M_y ratio is always lower than the one obtained from bending tests performed on defect-free specimens in small dimensions (equal to about 1.40). This means that, even if flexural failure

has been experienced (as in Beam 3), the Beams in actual dimension are not able to profit of plastic resources of the material.

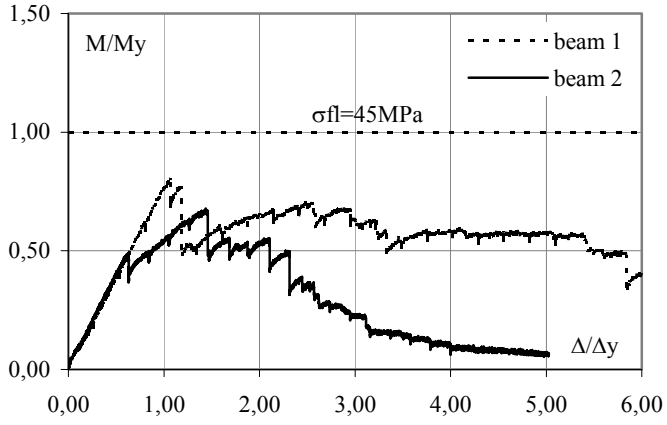

(a)

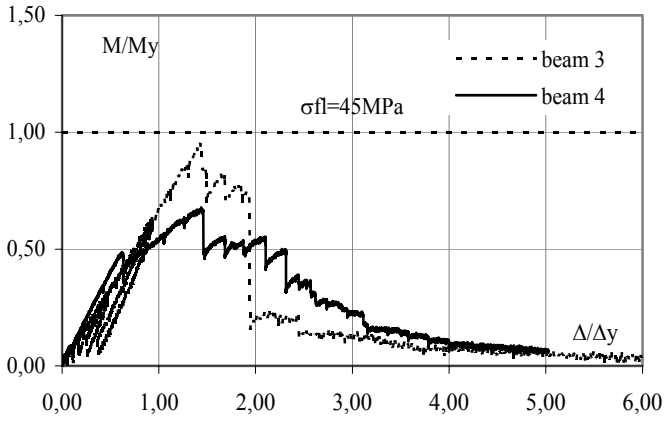

(b)

Figure 25. Normalised M/M_y vs.Δ/Δ_{My} curves for Beams 1 and Beam 2 (a) and for Beams 3 and Beam 4 (b).

3.4. Examination of shear behaviour

In Figure 26, for each tested beam, the tangential stress diagrams throughout the smallest end-beam cross-section are provided. Note that stresses have been calculated according to the classic Jourawski hypothesis. In these diagrams, the continuous curves have been obtained considering the actual section (i.e. with splits and holes), while the dashed ones have been obtained considering the equivalent perfect circular cross-section.

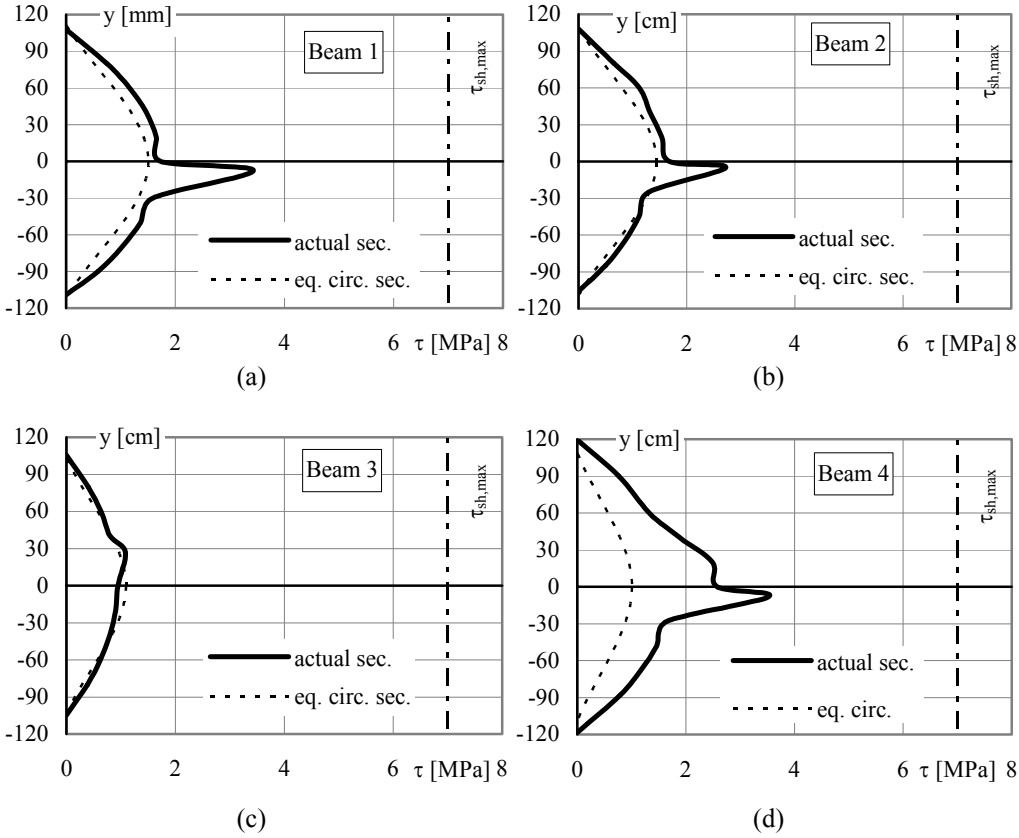

Figure 26. Tangential stress throughout the end-beam cross-section: beam 1 (a), beam 2 (b), beam 3 (c) and beam 4 (d).

The vertical line indicates the average value of the tangential stress obtained by testing small specimens ($\tau_{sh,max}$ = 7 MPa) is well in line with the value given by technical literature for new chestnut wood.

It is worth to observe that the values of the tangential stress for actual cross-section (τ_{ac}) are significantly higher than the ones obtained for the equivalent cross-section (τ_{eq}), with the exception of the Beam 3, which did not present significant defects at its ends. Furthermore, for Beam 3 it can be observed that the maximum value both for actual ($\tau_{ac,max}$) and for equivalent cross-section ($\tau_{eq,max}$) are very far from the experimental limit value ($\tau_{sh,max}$ = 7 MPa), so that the occurrence of a flexural failure mechanism during testing is well justified. The scatters between τ_{ac} and τ_{eq} curves are evident only where significant sub-horizontal fractures are present in the cross-section. For Beam 4, the scatter are notable in the whole diagram because the defects are spread throughout the whole the cross-section.

Table 6. Maximum shear force and corresponding maximum tangential stress in the cross-section for tested beams in actual dimension.

Beam	V_{max} *[kN]*	$\tau_{eq,max}$ *[MPa]*	$\tau_{ac,max}$ *[MPa]*
1	39.02	1.50	3.43
2	39.94	1.44	2.72
3	27.38	1.09	1.08
4	33.29	1.01	3.53
	average values	1.32	3.23

In Table 6, for each beam $\tau_{ac,max}$ and $\tau_{eq,max}$ are reported, together with the corresponding average values obtained from Beams 1,2 and 4, which are equal to $\tau_{ac,av}$= 3.23 MPa and $\tau_{eq,av}$= 1.32 MPa, respectively.

It can be noted that also the average value of τ_{ac} is significantly lower than the one obtained from tests on small samples, with a scatter more than 100%. This differences should be ascribed to the fact that $\tau_{sh,max}$ refers to small specimens without significant defects, while $\tau_{ac,max}$ is obtained directly from ancient wooden beams in full scale, normally characterised by notable starshakes and knots along the whole length, which cannot be accounted for in theoretical evaluation of the maximum tangential stress. The same problem has been evidenced also for flexural behaviour: in that case the ancient beams in actual dimension reached values of M_{max} significantly lower (up to 40%) than the ones obtained from bending tests on small specimens.

The obtained results highlighted that shear verification of ancient beams cannot be performed by evaluating the tangential stress on the equivalent circular perfect cross-section, being necessary at least to consider the visible splits, especially when they are in sub-horizontal direction. Furthermore, the so-evaluated stress has to be compared with a value of the limit tangential stress appropriately reduced on respect to the one given by technical literature for new chestnut. This reduction has to be evaluated on the base of the actual degradation state of the beam.

4. CONCLUSIONS

Full-scale compression and bending tests on ancient wooden beams characterised by significant degradation phenomena have provided interesting and unexpected results especially in terms of experienced collapse mechanism.

Compression tests have highlighted a very similar behaviour for all tested specimens. The F-Δ curves show an initial elastic linear behaviour up to reaching the maximum load, corresponding to the attainment of the collapse mechanism. Later, the load bearing decrease up to a negligible residual load. The maximum compressive stress and longitudinal elastic modulus are equal to 41 MPa and 12500 MPa, respectively. These values are in good agreement with the ones expected from technical literature. They are slightly lower than the ones obtained from the defect-free specimens.

From bending tests the behaviour appears to be elastic linear up to the peak load, with a longitudinal elastic modulus E_{long} equal to about 8000 MPa, significantly lower than the one obtained by compression tests in actual dimension and from bending tests on defect-free specimens in small dimension tested in analogous condition. Also, in the post-elastic range unexpected shear failures have been observed. A flexural collapse mode actually occurred only for Beam 3, with a corresponding maximum flexural stress $\sigma_{fl,max}$ = 43 MPa, which is very close to the peak stress obtained from compression tests in longitudinal direction on defect-free specimens in small dimensions and confirmed by full-scale compression test (about 45 MPa). On the contrary, for the other tested beams, a shear collapse mechanism occurred, with a pronounced slipping in the end-beam cross-section.

It can be observed that structural wooden members in actual dimension subjected to degradation phenomena show a remarkable scatter of tangential stress peak values

with respect to the ones obtained from tests on defect-free specimens in small dimension ($\tau_{sh,max}$). In particular, the ratio between τ_{max} in the actual section of the examined members and $\tau_{sh,max}$ ranges between 0.4 and 0.5. On the other hand, by introducing the hypothesis of equivalent circular cross-section, the ratio between $\tau_{eq,max}$ (value commonly assumed in design) and $\tau_{sh,max}$ is much more pronounced, ranging from 0.15 to 0.2, proving that the shear collapse mode prediction for ancient wooden beams may represent a crucial aspect of the design process.

Therefore, it can be concluded that the simplified methods commonly used to evaluate the bearing capacity of ancient wooden beams should be revised. In fact, degradation phenomena strongly reduce the mechanical properties of wood in comparison to defect-free wooden samples. For these reasons, the design of ancient wooden members can be performed by means of simplified methods based on the equivalent circular cross-section, provided that an adequate reduction factor for the tangential stress with respect to value suggested in current technical literature is considered.

CHAPTER 7:

Experimental analysis on connected ancient timber elements

The mechanical connection between timber elements was commonly used in the Mediterranean Area for ancient floor slabs having long-span beams. Usually, in such a case, load bearing beams are joined together by means of metal fasteners, for instance iron nails, placed along a very large overlapping zone (see Chapter 2).

This connecting system has to provide adequate strength during the whole natural life of the structural element. Nevertheless, the deterioration phenomena occurring in the wood could influence their structural behaviour. Furthermore, the contact between different material could give rise to high tensile stresses in the base material, especially when these stresses are not oriented in direction parallel to the grain.

Then, it should be considered that usually adopted connecting systems for existing wooden structures are not related to specific and scientifically based methods. Therefore, it seems necessary to develop and adopt specific procedures that could be

formally accepted, allowing the correct and reliable prediction of their structural behaviour.

On the basis of the above considerations, an experimental campaign on ancient timber beam-to-beam connection system has been carried out. In particular, it concerns a series of tests on ancient defect-free chestnut beams in small dimension, jointed by means of steel connectors (Calderoni *et al*., 2002).

1. THE EXPERIMENTAL ACTIVITY

The experimental activity has been carried out on specimens extracted from a series of existing ancient timber elements, as in the other experimental campaigns described in this thesis (see Chapter 4). Different typologies of tests have been performed, as reported in Table 1. In particular, the results obtained from embedding tests on wooden samples both in longitudinal and transversal direction and from four-point bending tests on beam connected by means of steel fasteners are shown. The aim of the experimental campaign is to investigate the behaviour of such a connection system, in relation to stiffness and strength capacity, when subjected to stress-strain conditions like the ones of the load-bearing floor-structure. Hence, several specimen configurations have been considered, varying the number and the distance of steel connectors in addition to the width of the connected elements. Finally, some considerations have been discussed on the differences of the overall structural behaviour between the analysed connection system and the corresponding whole beams, having the mechanical properties obtained both from tests on defect-free small specimens (see Chapter 5) and from full-scale bending tests on beams in actual dimension (see Chapter 6).

Table 1. Test typologies and number of specimens for each test

Test typology	*Num. of specimens*
1. Embedding test along longitudinal direction	4
2. Embedding test along transversal direction	2
3. Bending test on connected beam	5

Tests have been experienced according to the Italian UNI-ISO codes. The adopted testing equipments were different for the two test typologies and specifically described in the corresponding paragraphs, while the loading apparatus, already used for tests on defect-free specimens in small dimension (see Chapter 5), was the same. Loads were applied by means of a steel thread bar, restrained by a rigid steel reaction frame. The loading apparatus was also constituted by a cylindrical hinge able to prevent the torsional effects due to the testing equipment, which was placed over a spherical hinge, used to guarantee an uniform distribution of the applied loads. In each test, the displacement increasing rate has been chosen very slow, in order to provide a quasi-static load application.

Displacements has measured by means of LVDTs with accuracy of 1×10^{-3} mm, while the reaction forces given by the loaded specimen has been measured by means of a load cell.

2. EMBEDDING TESTS

Embedding tests have been carried out on a series of ancient wooden specimens in which a steel threat bar is inserted. In particular, tests have been performed considering wooden samples oriented both in the direction parallel (L-test) and perpendicular (T-test) to the grain. Four and two tests have been carried out for L and

T configuration, respectively. According to the relevant part of the European regulation EN 383, the wood specimens had a 20x50 mm^2 cross-section and 100 mm height, while the connecting element was a steel thread bar with a nominal diameter d_n of 5.00 mm and inner core diameter d_c of 3.96 mm (Fig. 1). The samples have been loaded in force control by directly applying a compressive load to the two edges of the bar by means of a specific steel device, as shown in Figures 2, 3a and 3b.

The displacement has been measured by an LVDT placed at the top of the loading device, whose displacement has been considered as representative of the joint displacement (w).

A preliminary test was performed monotonically increasing the load up reaching a joint displacement equal to 5 mm. The corresponding strength of the system has been assumed as the maximum estimated force $F_{,est}$, to be used for the subsequent tests. For all the tests, the adopted loading history is shown in Figure 4. The load has been increased up to 0.4 $F_{,est}$ (point 04 in the diagram) and kept constant for about 30 sec (point 14). Then, the load is reduced up to 0.1 $F_{,est}$ (point 11) and then increased again up to the end of the test, conventionally assumed when the joint displacement becomes equal to 5 mm.

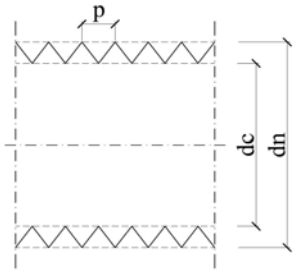

Figure 1. Principal metal fasteners dimensions.

The embedment strength, $\sigma_{emb,\alpha}$ at an angle α to the grain, has been calculated as:

$$\sigma_{emb,\alpha} = \frac{F_{max}}{d \cdot t} \text{ [MPa]} \quad (7.1)$$

where F_{max} is maximum force withdrawn by the specimen in the whole range of joint displacement from 0 to 5 mm, d is the diameter of the metal fastener and t is the thickness of the sample.

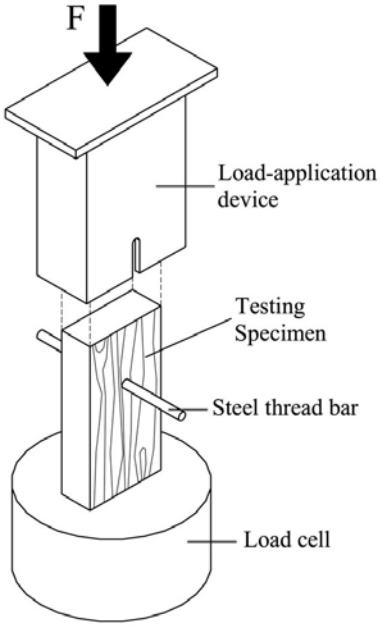

Figure 2. Testing equipment used for embedding tests.

As an example, in Figures 5a and 5b, two specimens, tested one in direction parallel and one in direction perpendicular to the grain, are shown at the end of testing. In Figure 6, the obtained F-w curves are depicted for each test for both L and T configurations. Furthermore, in Figure 7 the σ-w curves are represented grouping the

sample having the same configuration. In this case, the stress σ has been calculated considering an uniform stress distribution along the thickness t of the wooden sample and over the bolt diameter d_c of the steel bar, as in equation (7.1).

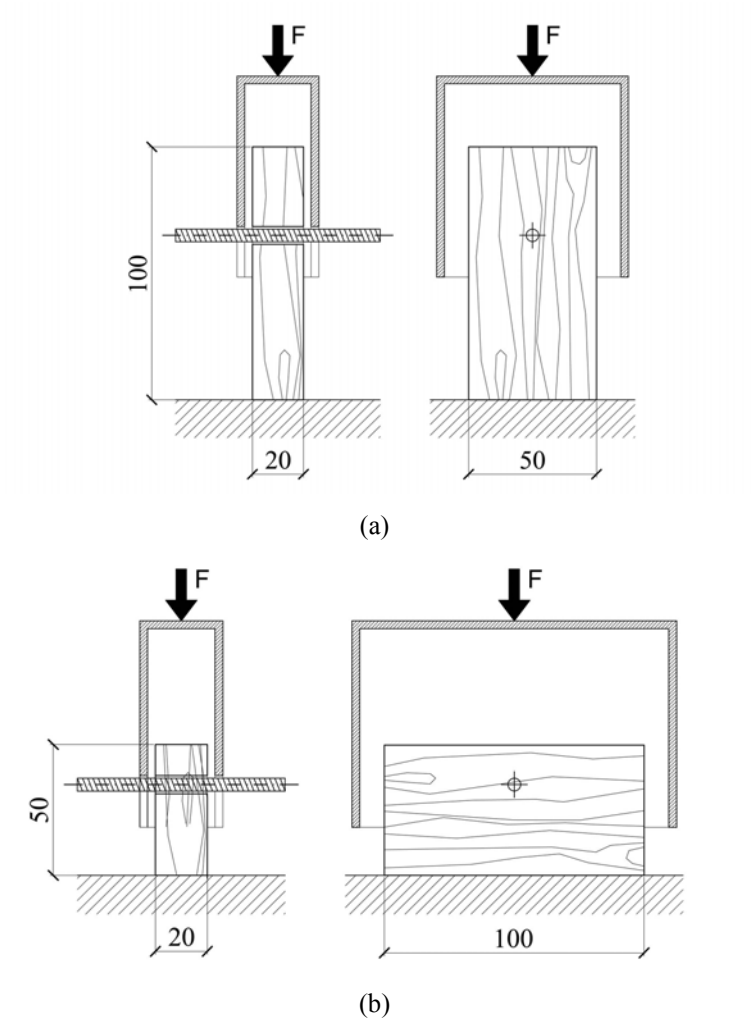

Figure 3. Specimen shape and testing equipment for test in direction parallel (a) and perpendicular (b) to the grain.

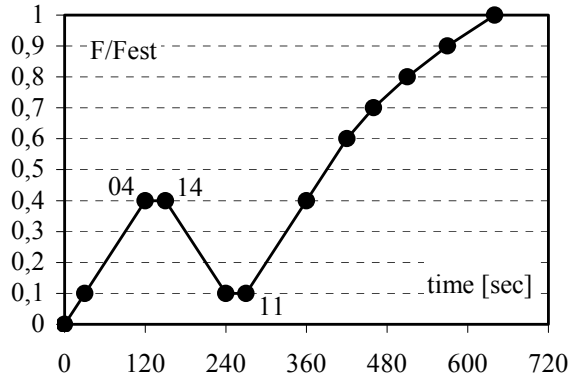

Figure 4. Loading history adopted for embedding test

The curves obtained form both L-test and T-test show a similar shape, with a first practically linear branch characterized by a high value of the initial stiffness k_i, followed by a second nearly linear branch characterized by a reduction of the stiffness k_h, so that the experimental curve can be simulated by a simplified bi-linear relationship.

(a) (b)

Figure 5. The specimen after a L-test (a) and a T-test (b).

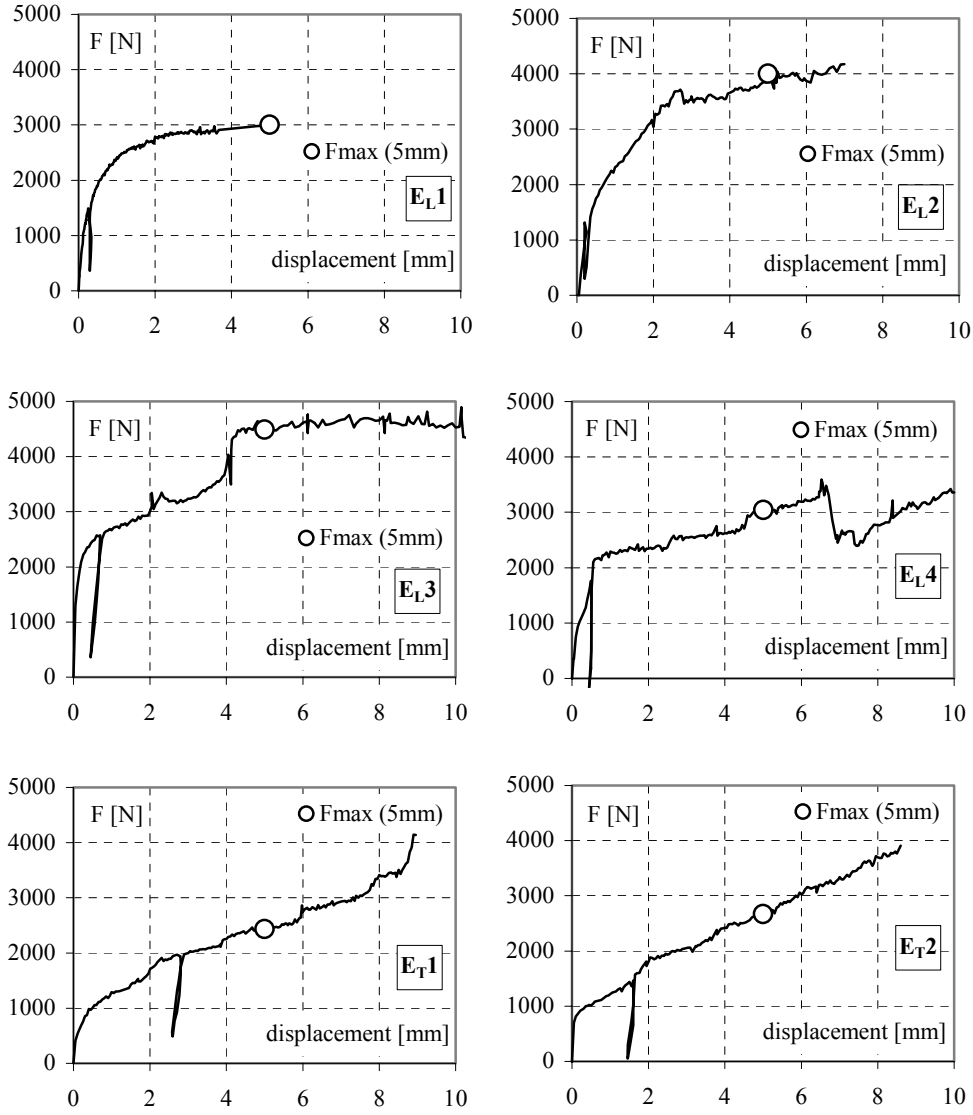

Figure 6. F–w curves of L-test (E_L) and T-test (E_T).

In the case of the L-tests, it can be noted that the experimental curves for sample E_L1, E_L2 and E_L4 are quite similar to each other up to a stress value of about 25 - 30 MPa, all exhibiting similar initial stiffness k_i, ranging from 7200 to 8500 N/mm. On the contrary they become more different throughout the development of the second branch, the corresponding stiffness k_h ranging from 1000 to 1500 N/mm. The sample E_L3 exhibited an initial stiffness k_i significantly higher than the other ones (2700 N/mm), while the stiffness k_h resulted again in accordance with the other samples (about 1000 N/mm).

The experimental curves for sample E_T1 and E_T2 are practically coincident to each other. They present a first nearly linear branch only up to a value of σ of about 10 MPa and a subsequent second linear branch characterized by a stiffness k_h slightly higher than those obtained for L-tests.

Table 2. Main values of embedment strength and local stiffness.

Specimen	F_{max} *(5mm)* *[N]*	$\sigma_{emb,\alpha}$ *(dn)* *[MPa]*	$\sigma_{emb,\alpha}$ *(dc)* *[MPa]*
E_L1	3005	29.1	36.8
E_L2	4002	38.7	48.8
E_L3	4500	43.5	54.9
E_L4	3042	35.1	36.9
E_T1	2436	23.2	29.3
E_T2	2670	25.7	32.4

In Table 2, the experimental embedment strength, calculated for all the samples using both d_n ($\sigma_{emb,\alpha}(d_n)$) and d_c ($\sigma_{emb,\alpha}(d_c)$) values of the bar diameter, are reported. For L-tests, the mean value is equal to 35.1 MPa, considering d_n, and 44.4 MPa, considering d_c. This result is in a good agreement with the outcomes of the executed

compression tests in direction parallel to the grain on defect-free samples in small dimension, previously described in Chapter 5, where a peak stress value of about 45 MPa was obtained.

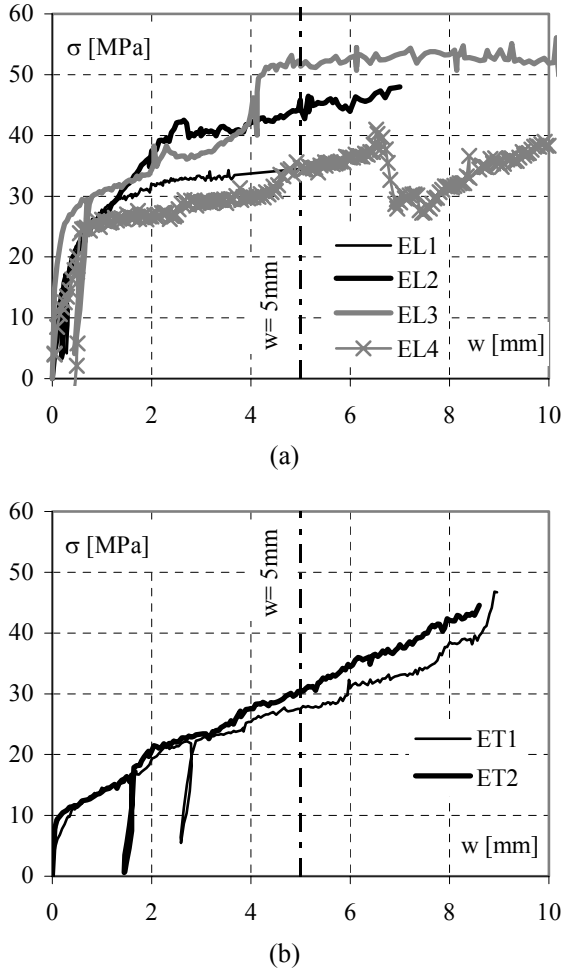

Figure 7. Comparison among σ-w curves: L-test (a) and T-test (b).

The mean values of $\sigma_{emb,a}(d_n)$ and $\sigma_{emb,\alpha}(d_c)$ for T-test specimens are equal to 24.4 MPa and 30.8 MPa, respectively. These values are about 30% lower than the ones of L-tests, while they are much higher than the ones obtained from compression tests executed throughout transversal direction, which resulted in mean of about 5 MPa (see Chapter 5).

According to Eurocode 5, the value of the characteristic embedment strength for new hardwood and bolted connections up to 30 mm bolt-diameter, $f_{h,\alpha,k}$, at an angle α to the grain, can be computed as:

$$f_{h,\alpha,k} = \frac{f_{h,0,k}}{k_{90}\sin^2\alpha + \cos^2\alpha} \tag{7.2}$$

where $f_{h,0,k} = 0{,}082\ (1\text{-}0{,}01d)\rho_k$ is the characteristic embedment strength parallel to the grain, $k_{90} = 0{,}90+0{,}015d$ and ρ_k is the characteristic timber density (kg/m^3).

In our cases, ρ_k was equal to 620 kg/m^3, obtained by an experimental measure of the density on samples extracted from the timber elements (see Chapter 4). Therefore, according to EC5, the characteristic embedment strength parallel to the grain $f_{h,\alpha,k}$ (to be compared with the one obtained from L-tests - α=0°) corresponds to 48.8 MPa and 48.3 MPa, considering d_n and d_c respectively. This is in good accordance with the mean value of $\sigma_{emb,0}(d_c)$ obtained from tests (Table 2).

On the other hand the characteristic embedment strength perpendicular to the grain $f_{h,\alpha,k}$ (to be compared with the one obtained from T-tests - α= 90°) should be equal to 49.5 and 50.9 MPa, considering d_n and d_c respectively. This is significantly over-estimate if compared with the results obtained by tests and on the unsafe side too.

3. BENDING TESTS ON BEAM-TO-BEAM CONNECTION

Bending tests on beam-to-beam connection have been carried out on a series of 5 defect-free ancient chestnut specimens working in the grain direction, connected to each other by steel thread bars, the same used for the embedding tests.

According to the present European provisions for bending tests, a simply supported arrangement of the specimen, loaded by two symmetric concentrated forces (four-points bending test), has been adopted for testing, in order to submit the connecting zone to a constant bending moment (Fig. 8).

Table 3 reports the geometrical characteristics of the specimens, which differ for dimensions of cross section and number of connecting steel thread bars (N_f). In all cases the connectors are distributed along a 12 cm connecting zone. In particular, sample B_C1, B_C4 and B_C5 have different width and equal $N_f = 3$, while sample B_C2 and B_C3 have the same dimension of B_C1 (cross-section 2x5 cm^2) but N_f varying from 3 to 5. The bolt spacing is then variable and equal to 60, 40 and 30 mm for N_f = 3, 4 and 5 respectively.

Table 3. Main dimensions for specimens tested in bending.

Specimen	*Span L [mm]*	*Overlap zone L_o [mm]*	*Cross section*		*Number of connecting bars (N_f)*	*Bolt spacing [mm]*
			width b [mm]	depth h [mm]		
B_C1	580	200	20.5	50.6	3	60
B_C2	580	200	20.7	50.4	4	40
B_C3	580	200	21.0	50.7	5	30
B_C4	580	200	3.04	50.7	3	60
B_C5	580	200	3.95	50.7	3	60

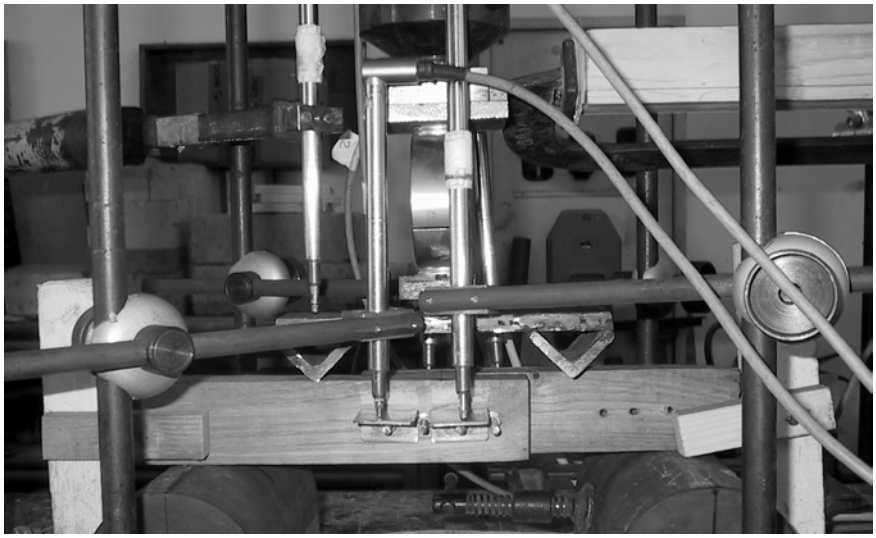

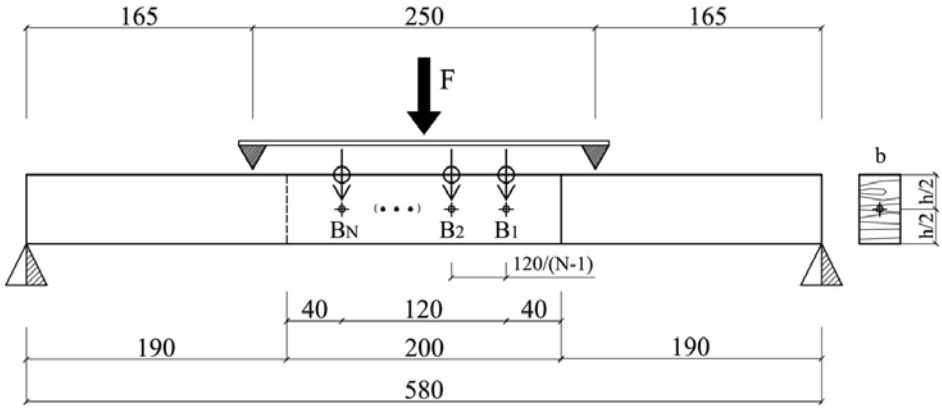

Figure 8. The loading scheme for bending tests.

Tests have been performed under displacement control, by applying a quasi-static loading history. The imposed force has been progressively increased up to the collapse of the specimen. The load has been transferred to the beam by interposing a rigid steel profile between the loading jack and the specimen (Fig. 8). The external

supports were made of two steel half-cylinders. Deflections have been measured by means of displacement transducers (LVDT) placed at the edges of all the connecting elements and at the top of the loading device.

In Figure 9, for all the samples, the experimental curves Acting Force (F) vs. B1-Displacement (Δ) are depicted, where the point B1 corresponds to the location of the first connecting bar, i.e. the one closest to the external support.

Only for comparison, in the same diagrams, the initial linear branch of the F-Δ curve, corresponding to an ideal defect-free ancient chestnut beam having cross-section and length equal to those of the tested sample, are drawn. Such curves have been theoretically defined, adopting a longitudinal elastic modulus E_{long} equal to 13000 MPa, which has been obtained from the experimental campaign performed on defect-free ancient chestnut beams without internal connection, previously described in Chapter 5. Note that from the same tests a conventional elastic maximum stress of the basic material (σ_f) equal to 45 MPa has been also derived, so that the ideal curves have been stopped to the value of the force ($F_{ult,id}$) corresponding to the flexural resistance of the beam evaluated on the base of this stress.

In Figures 10a and 10b, the experimental F-Δ curves are grouped for specimens B_C1, B_C2 and B_C3 (having the same cross-section dimension), and for specimens B_C1, B_C4 and B_C5 (having the same number of fasteners), respectively.

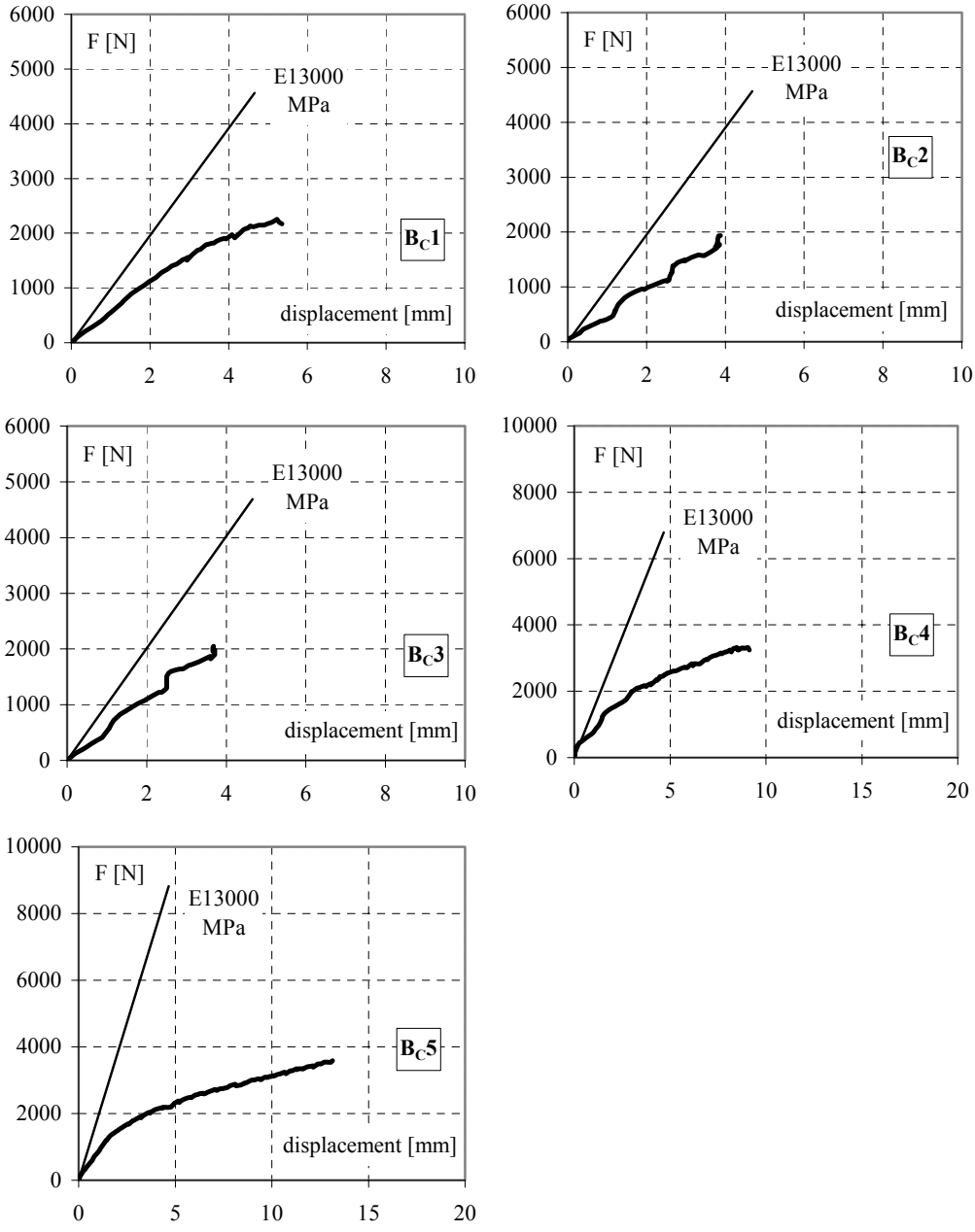

Figure 9. F-Δ curves for all tested specimens.

It can be noted that all samples exhibited an initial flexural stiffness significantly lower (about 40%) than that of the corresponding ideal beam without internal connection. This means that the connection leads to a reduction of stiffness, so that the connected beam is equivalent to an unique beam made of a conventional base material having a longitudinal elastic modulus E^*_{long} of about 8000 MPa.

Specimens B_C1, B_C2 and B_C3, having the same cross-sections, showed experimental curves practically coincident, nearly linear up to the collapse, which occurred for a value of the acting force (F_{ult}) of about 2000 N (Table 4), quite independent of the number of applied fasteners (N_f). On the contrary, the F-Δ curves for specimens B_C1, B_C4 and B_C5 show similar shape, but very different values of collapse load. Such a results is obviously due to the different cross-section of the samples of this group. Note that all the curves present a linear elastic behaviour up to about 1500 N.

As reported in Table 4, the experimental collapse load forces (F_{ult}) for connected beams are significantly lower (up to 55%) than the ultimate load ($F_{ult,id}$) of the corresponding beams without internal connection, evaluated with reference to the conventional maximum elastic stress of the basic material (σ_f).

Table 4. Mean values of ultimate force and displacement for tested beams.

Specimen	F_{ult} *[N]*	Δ_{ult} *[mm]*	$F_{ult,id}$ *[N]*	*S(B1) [N]*	σ_c *(dc) [MPa]*
B_C1	2254	5.3	4560	1550	19.1
B_C2	1936	3.9	4568	1198	14.6
B_C3	2118	4.1	4689	1165	14.0
B_C4	3320	9.0	6788	2282	19.0
B_C5	3588	16.8	8820	2467	15.8

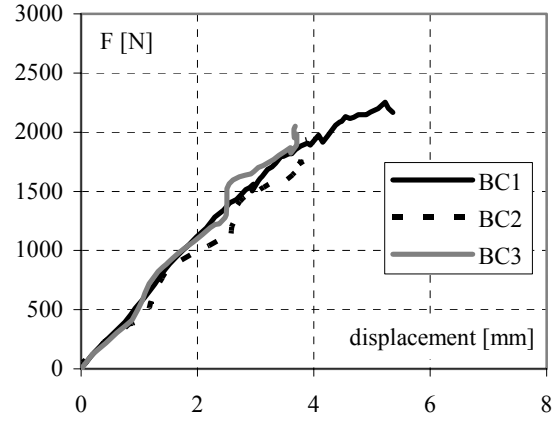

(a)

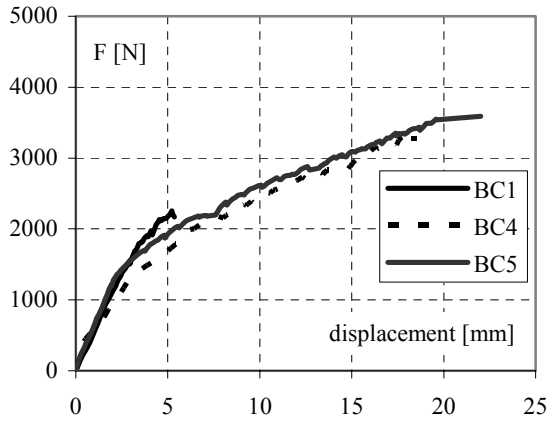

(b)

Figure 10. F-Δ curves for specimens B_C1, B_C2 and B_C3, having same cross-dimension and different N (a), and for specimens B_C1, B_C4 and B_C5, having variable cross-section dimension and N=3 (b).

The typical exhibited collapse mode of the tested beams is shown in Figure 11. For all the tests, the failure occurred in correspondence of the connection. A crack started from the first external bolt B1 and propagated quite horizontally along the line of holes.

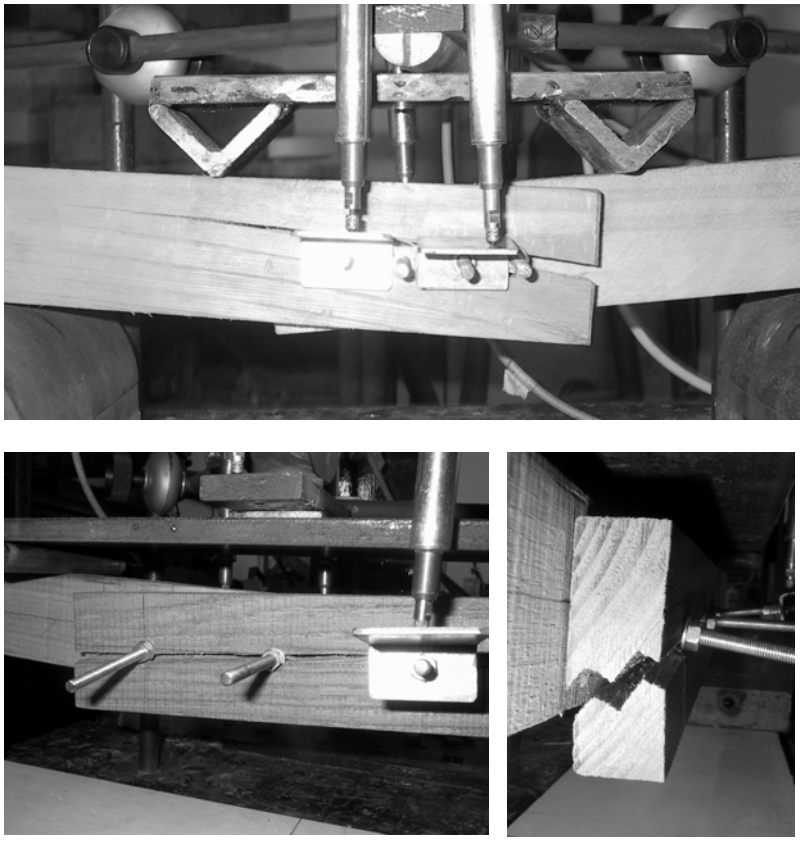

Figure 11. Typical collapse mode.

Evidently the failure was due to an excess of tensile stress ($\sigma_{t,90}$) in direction perpendicular to the grain, before the attainment of the maximum embedment resistance, as determined from the corresponding tests. In fact, if a linear reaction force distribution among the steel bars is assumed, the generic reaction force in a bar $S(B_i)$ can be easily determined by means of the equilibrium equations with reference to the acting bending moment in the connecting zone. The maximum contact stress σ_c in the base material occurred in correspondence of bolt B1. It was calculated

through the application of eq. (1), where F_{max} is assumed equal to S(B1). As shown in Table 4, for all the samples σ_c ranges between 14 and 19 MPa, resulting largely lower than the main value of the embedment stress $\sigma_{emb,90}(d_c)$ in transversal direction. On the other hand, such a contact stress value seems to be realistic in relation to maximum stress value for tensile failure throughout the grain transversal direction. Anyway, such outcomes should be verified on the basis of appropriate tests on beams without internal connections where the failure occurs due to excess of tensile stress throughout such a direction.

4. CONCLUSIONS

The experimental campaign on defect-free ancient chestnut samples in small dimension, connected by means of steel bolts, have provided interesting informations on the local and global behavior of the tested specimens.

In particular, embedment strength measured in direction parallel ($\sigma_{emb,0}$) and perpendicular ($\sigma_{emb,90}$) to the grain have been obtained. A mean value of 44.4 MPa has been calculated for $\sigma_{emb,0}$ considering d_c bolt-diameter, which is in good agreement with both the ultimate compressive stress in the same direction and the characteristic embedment strength computed by EC5 for new hardwood. On the contrary, for $\sigma_{emb,90}$ a mean value of 30.8 MPa has been obtained, it resulting much lower than the one suggested by EC5.

Bending tests on 5 connecting systems have been also performed, varying the number (N_f) and the distance of steel connectors in addition to the thickness of connected elements. In all examined cases, the failure mechanism occurred in the wooden sample, throughout the longitudinal section in correspondence of the steel bars, due to an excess of tensile stress in the transversal direction before the attainment of a remarkable beam embedment. In order to provide a better

understanding of the failure mechanism due to tensile stress in the direction perpendicular to grain, additional tests are necessary. Therefore, further research developments will be addressed to this aspect.

The tests show a remarkable loss of stiffness and bearing capacity in comparison with the whole beams having the same geometry and the mechanical properties obtained from tests on both the defect-free small specimens (see Chapter 5) and beams in actual dimension (see Chapter 6). In fact, the average values of percentage reduction of longitudinal elastic modulus and ultimate strength compared to defect-free beams resulted equal to about 40% and 55%, respectively. On the other side, if compared to ancient timber beams in actual dimension, the reduction in terms of ultimate strength were of about 50%, while the longitudinal elastic modulus appeared practically coincident.

CHAPTER 8:

Non-Destructive Tests on ancient chestnut elements

In this Chapter, the results of an experimental campaign based on Non-Destructive instrumental investigations on ancient chestnut members have been presented. Since the ancient timber structures are usually subjected to defects and degradation phenomena which strongly influenced their structural behaviour, their reinforcing interventions require a preventive reliable acquaintance of the physical and mechanical properties of the timber elements. Such information cannot be obtained by means of destructive tests on sacrificial elements and in-situ Non-Destructive investigations are usually carried out on this structures.

In particular, the so-called "Resistographic" analyses were performed. They allowed providing an in-depth knowledge of deterioration condition and identifying the effective section of degraded structural elements. Furthermore, in order to estimate the load-bearing capacity of such elements, the Resistographic measures (i.e. the drilling resistance) have been correlated to the actual ultimate strengths of material,

which have been already directly obtained from the results of tests on defect-free small specimens (see Chapter 5) and the full-scale tests on beams in actual dimension (see Chapter 6). Interesting correlations values between Destructive and Non-Destructive tests on the same timber members have been obtained. In this way, the effect of the degradation condition, the structural defects and the shape anomalies of the ancient timber elements can be implicitly accounted for a lower value of the resistance to be used for simplified design methods.

1. THE EXPERIMENTAL ACTIVITY

The experimental activity described in this chapter is based on a series of Non-Destructive Tests on ancient chestnut elements. In particular, these elements were obtained by cutting an ancient chestnut beams into three trunks having a length of about 450 mm and cross-section diameters ranging 240 - 260 mm. The trunks were the same subjected to full-scale compressive tests in direction parallel-to-the-grain. They presented the typical defect pattern of ancient timber elements. In Figure 1, the principal dimensions of the tested samples have been reported (see also Chapter 6). Before Destructive tests, a series of Resistographic analyses have been carried out. In particular, NDT investigations have been performed by means of the Resistograph model “Resi F400” produced by IML. As described in detail in Chapter 2, this device measures the resistance of wood to the advancement of a drill having 1.4 mm diameter. The drill advances at a constant speed through the timber. The drilling resistance was recorded at steps of $1x10^{-1}$ mm on a real-time graph. This graph shows the relative amplitude necessary to advancing at a constant speed versus the depth of penetration. Data were also stored on digital support and successively analyzed on PC.

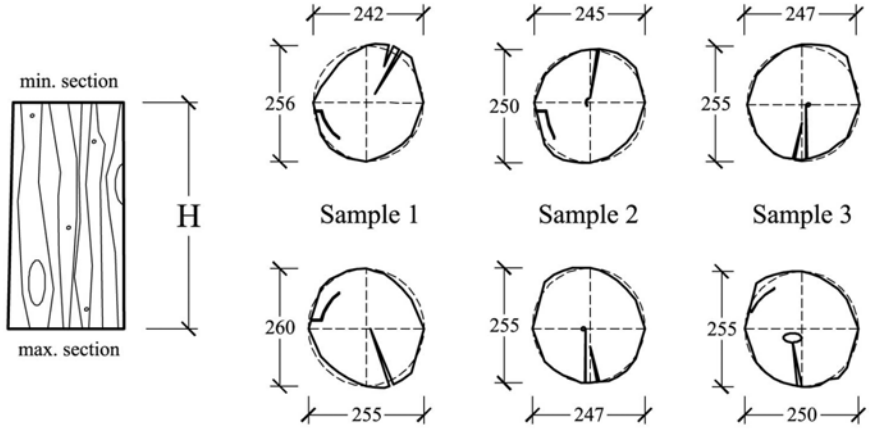

Figure 1. Principal dimensions of the tested samples.

Figure 2. A Resistographic analysis in longitudinal direction.

The experimental campaign consisted of penetrations in parallel-to-the-grain (longitudinal) and transversal direction. Longitudinal resistographic analyses have been carried out on the ends of the samples for a drilling depth of about 200 mm, in

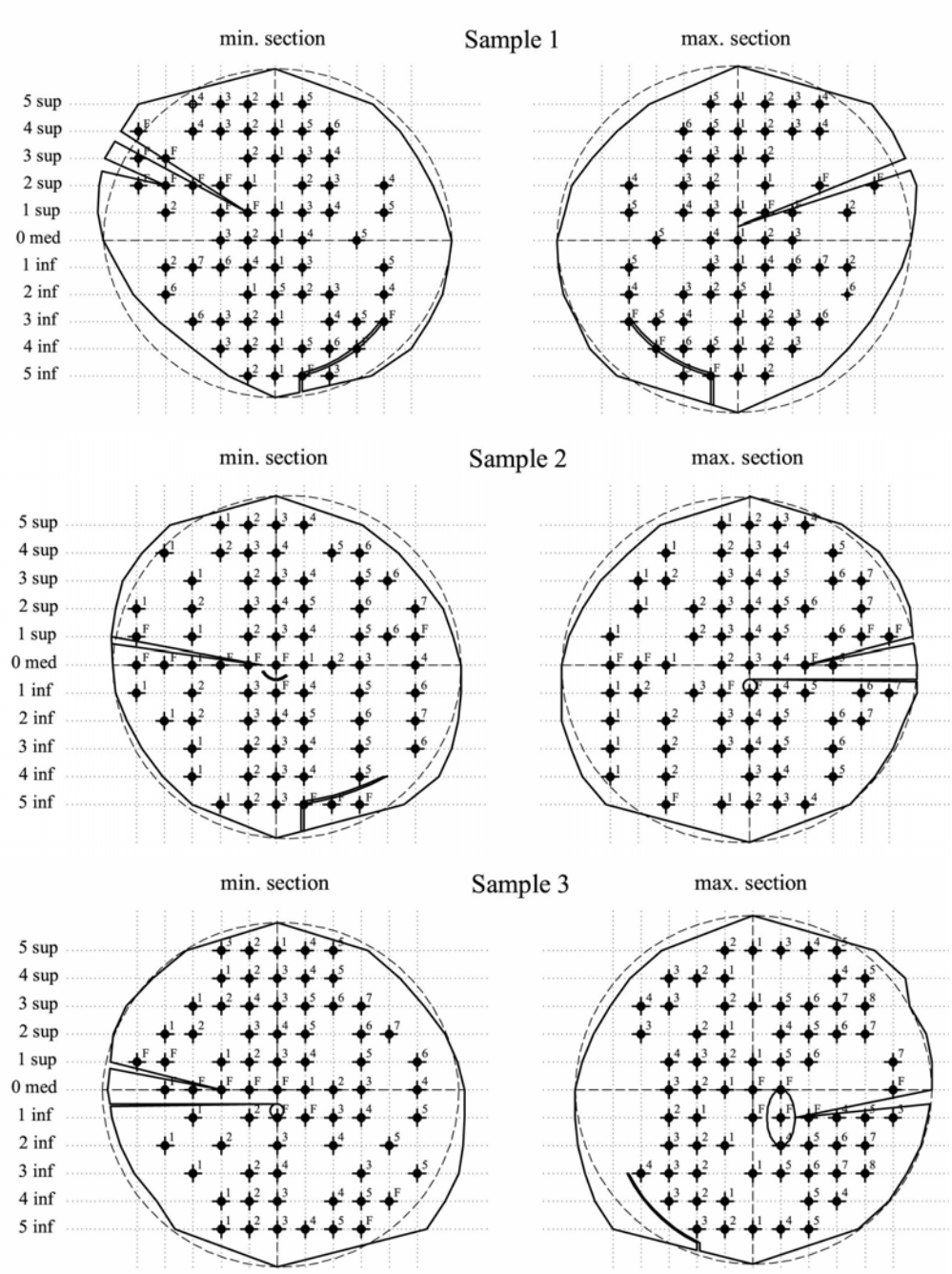

Figure 2. The longitudinal Resistographic measures carried out on Sample 1, 2 and 3.

order to have complete information on the whole length of the sample. On each end-beam, the longitudinal perforations have been undertaken on a square grid having 20 mm side, for a total number of about 80 measures (Fig. 2). In Figures 3a, 3b and 3c the complete relief of the longitudinal Resistographic measurements at the end-beams of each samples is reported.

The transversal Resistographic analyses were performed on the lateral surface of the whole beam, before its cutting (Fig. 3). They were executed along three different lines, obtained by connecting the corresponding three chords of the end-beams grid (3sup, 0bar, 1inf in the Fig. 2). On the median line (0bar) 13 measurements have been carried out, while both on the upper (3sup) and the bottom one (1inf) 8 measurements have been carried out, at a distance on center of about 170 mm, for a total number of 30 measurements. In Figure 4, a complete relief of the transversal penetration disposition on the whole beam is depicted.

Figure 3. The transversal Resistographic analyses carried out on the whole beam.

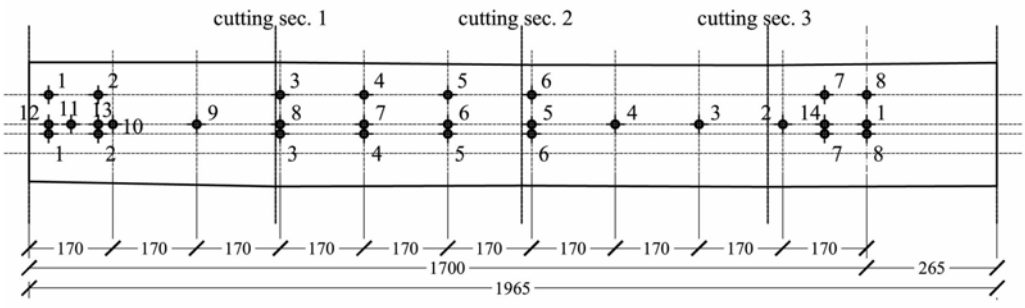

Figure 4. The transversal Resistographic analyses disposition.

2. EXPERIMENTAL ANALYSIS AND REMARKS

2.1. General Informations

The Resistographic measurements have been analysed by means of the relative amplitude (RA) [%] vs. drilling depth (DD) [mm] graphs. By observing the graphs it was possible to detect the presence of defects or degradation state of wood in correspondence of the drilling path. Typical resistographic measures are depicted in Figures 5 and 6 for drilling in longitudinal and transversal direction, respectively. In these figures different condition states of wood appear: wood of good quality, characterised by relative high values of the RA; wood in which defects or degradative state occurs, characterised by very low values of RA; presence of knots on the lateral surface, characterised by strong values of RA. It is worth noting that in the case of ancient timber structures, defects and degradation state largely vary in typologies, location and extension, due to both the environment conditions and the specific features of members. Since this variability occurs randomly, it makes extremely complex its prevision.

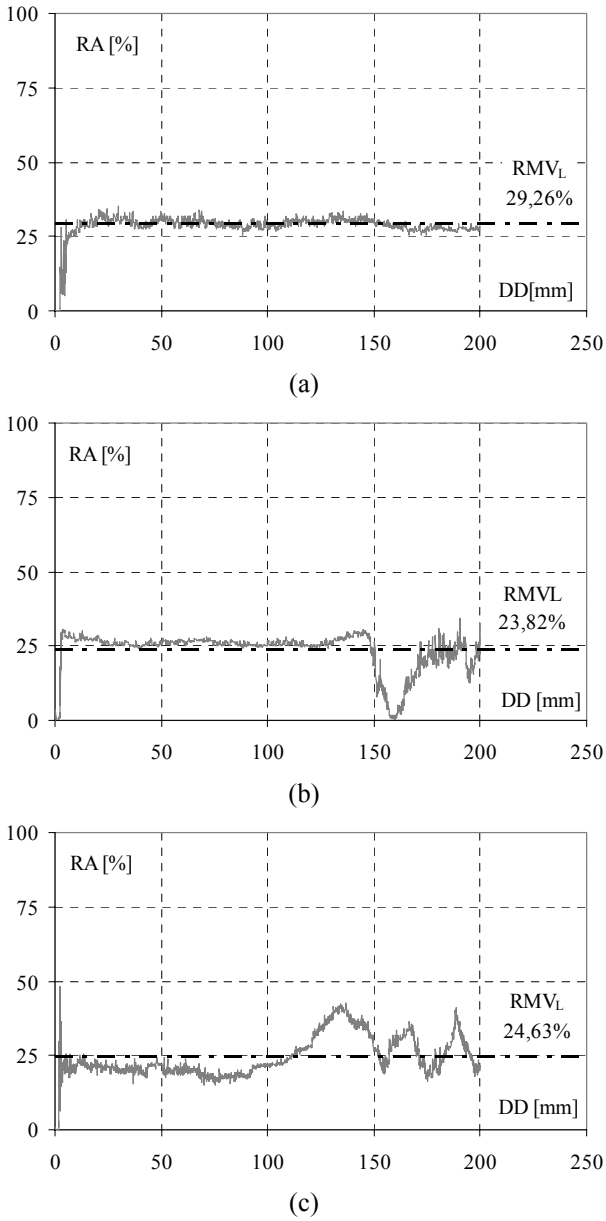

Figure 5. Typical Resistographic measure in longitudinal direction: (a) wood of good quality; (b) presence of a degradative state at a range of 150 - 175 mm of drilling depth; (c) presence of a more resistant part at a range of 120 - 200 mm of drilling depth.

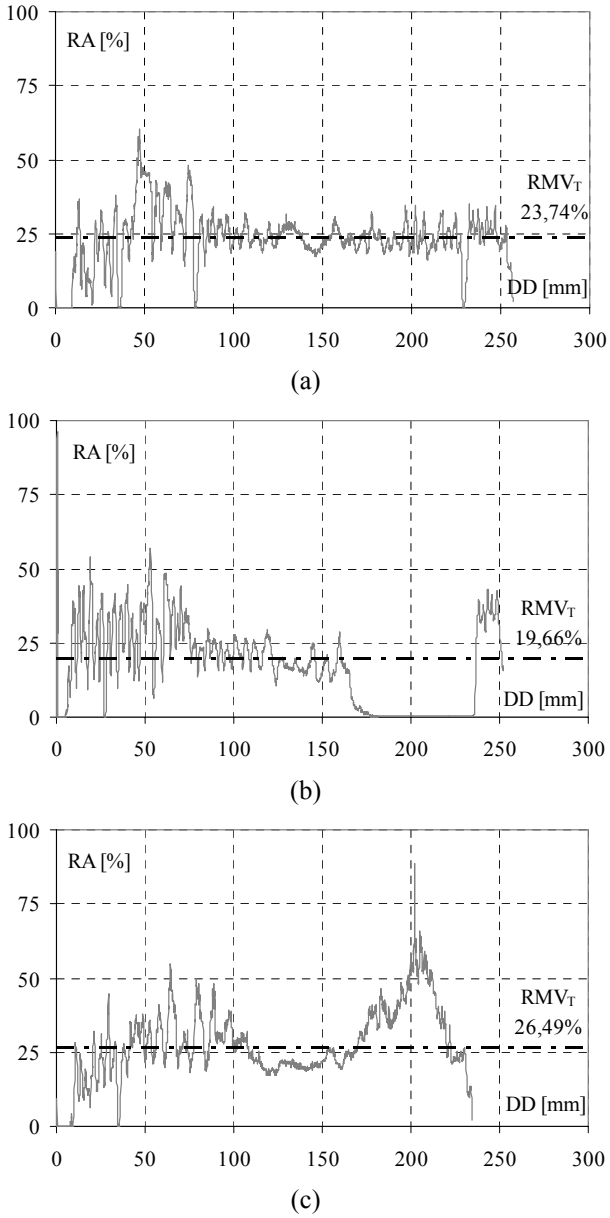

Figure 6. Typical Resistographic measure in transversal direction: (a) wood of good quality; (b) presence of a degradative state at a range of 170 - 230 mm of drilling depth; (c) presence of knots on the lateral surface.

2.2. Longitudinal Resistographic Anlalyses

Longitudinal Resistographic analyses on wooden parts without defects are characterised by RA values quite coincident, as appeared in Figures 5a. In order to realize a correlation between longitudinal drilling measures and the corresponding mechanical properties of wood, a unique parameter RMV_L can be considered. It is defined as:

$$RMV_L = \frac{\int_0^H \text{Area}}{H} \ [\%] \tag{8.1}$$

where: H is the considered drilling depth.

The so-calculated RMV_L is an expression of the mean value of RA in the considered drilling depth (Fig. 7). It results actually representative of wood only if calculated with reference to homogenous parts. Therefore, RMV_L values have been calculated on parts of wood having good quality.

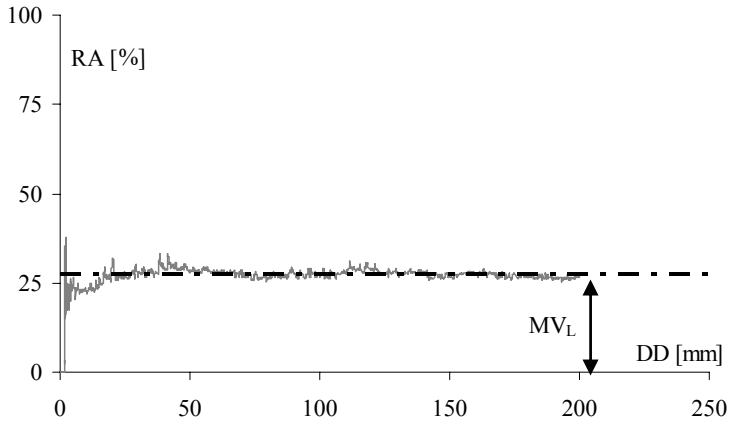

Figure 7. Definition of RMV_L value.

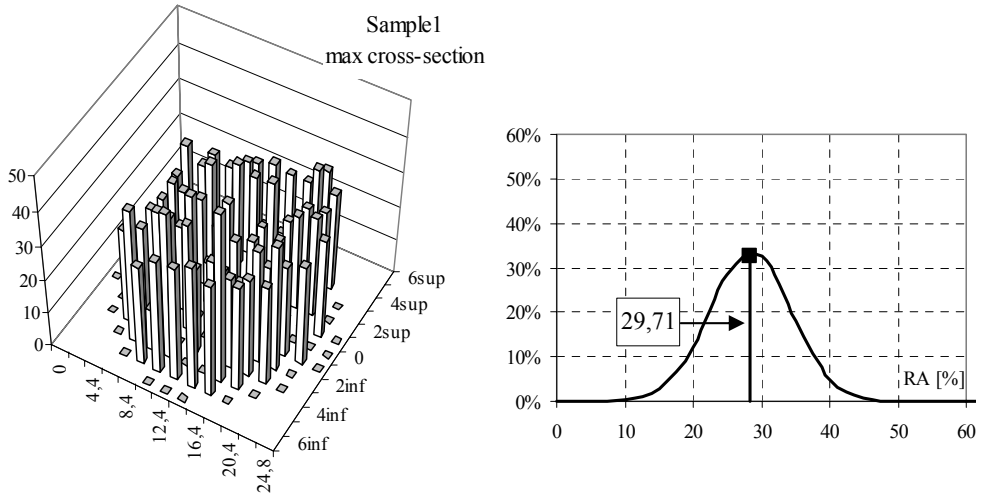

(a)

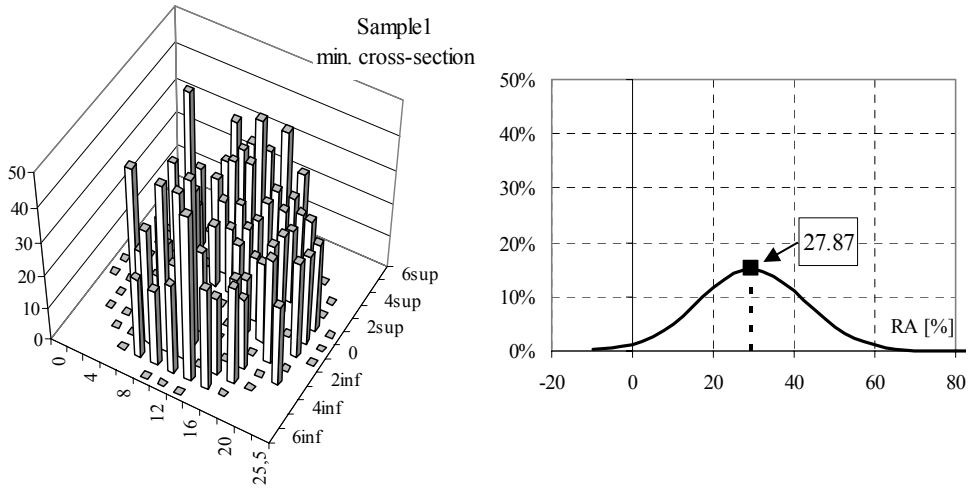

(b)

Figure 8. Tri-dimensional RMV_L distribution and the corresponding Gaussian graph for the max end-beam (a) and the min. end-beam cross-section (b) of Sample 1.

Table 1. Main values of longitudinal Resistographic measures.

Samples	$RMV_{L,SEC0}$ *[%]*	*ST DEV*	$RMV_{L,SEC}$ *[%]*	*ST DEV*	$RMV_{L,Si}$ *[%]*	*ST DEV*
1	26.17	7.82	29.71	7.20	28.79	5.74
	26.06	6.34	27.86	3.95		
2	28.94	7.93	34.01	4.23	32.36	4.32
	28.33	6.28	30.71	3.91		
3	31.84	9.24	38.34	4.56	38.34	4.56
	-	-	-	-		

Starting from this, several information can be obtained by analysing data from a statistical point of view. First of all, complete information on each end-beam were obtained. As an example, in Figures 8a and 8b a tri-dimensional distribution of the RMV_L values on a whole end-beam cross-section and the corresponding Gaussian distribution graph are depicted for the max. and min. cross-section of the Sample 1. Two different values, $RMV_{L,SEC}$ and $RMV_{L,SEC0}$ have been considered. $RMV_{L,SEC}$ represents the mean value of the RMV_L on the cross-section without considering the fault measures, corresponding to low or null values of RMV_L in correspondence of defects of wood, while $RMV_{L,SEC0}$ is the mean value of all the drilling measures. The difference between $RMV_{L,SEC}$ and $RMV_{L,SEC0}$ represents a measure of the defectiveness of wood. In Table 1, $RMV_{L,SEC}$ and $RMV_{L,SEC0}$ are reported for each end-beam, together with the corresponding Standard Deviations (ST DEV). As it can be observed, in the case of $RMV_{L,SEC}$, low values of ST DEV indicates a quite coincident values of the RMV_L measures in the cross-section, so confirming a valid correlation with the properties of wood. Furthermore, $RMV_{L,Si}$ can has been defined as the mean value of the $RMV_{L,SEC}$ corresponding to the end-beams of the i-Sample.

In addition, $RMV_{L,TOT}$ represents the mean value of all the longitudinal Resistographic measures executed on the samples. It results equal to about 33 %. Note that also in this case, the ST DEV calculated considering all the drilling measures is quite low (about 7.4 %). Therefore, $RMV_{L,TOT}$ represents a reliable measure of the timber elements under investigation. It has been compared with the longitudinal ultimate compressive strength σ_0 equal to 48 MPa, obtained by tests on defect-free small specimens extracted from the same members (see Chapter 5). Deepen remarks on this correlation are reported in Chapter 9, where the RMV_L values versus longitudinal compressive strength σ_0 diagram has been showed also for spruce wood.

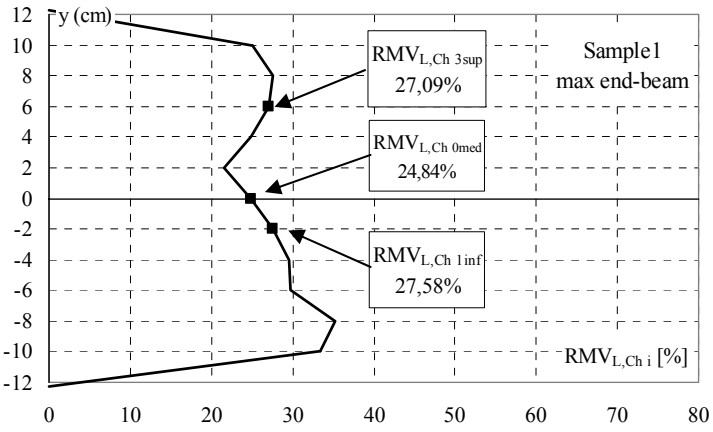

Figure 11. $RMV_{L,Chi}$ values for the max end-beam of Sample 1.

Finally, the mean values of the RMV_L measured on the i-chords of each end-beam cross-section, $RMV_{L,Chi}$, have been determined. As an example, in Figure 11 the $RMV_{L,Chi}$ values are determined for the max end-beam of Sample 1. In Particular, in order to determine a reliable correlation between longitudinal and transversal Resistographic analysis, three different values of $RMV_{L,Chi}$ ($RMV_{L,Ch3sup}$ at 3sup

chord; $RMV_{L,Ch0med}$ at 0med chord; $RMV_{L,Ch1inf}$ at 1inf chord) have been considered and reported in Table 2.

Table 2. $RMV_{L,Chi}$ values for all tested Samples.

	max section			*min section*		
Samples	$RMV_{L,Ch3sup}$	$RMV_{L,Ch0med}$	$RMV_{L,Ch1inf}$	$RMV_{L,Ch3sup}$	$RMV_{L,Ch0med}$	$RMV_{L,Ch1inf}$
1	27.09	24.84	27.58	25.31	23.65	26.48
2	31.89	29.53	31.81	32.46	36.19	30.94
3	33.70	36.89	41.30	/	/	/

2.3. Transversal Resistographic Analyses

Transversal Resistographic analyses are characterised by a not negligible variation of the RA values attained during the drilling penetration, also in the case of wood of good quality (Fig. 6a). Unlike Resistographic measures in direction parallel-to-grain, in this case RA values range around their mean value RMV_T and their variation is due to the crossing of the growth rings during the measure. In such a case, the lowest peaks are far from the base line of RA = 0 %. Otherwise, in presence of defects or deteriorated parts of wood the RA values reach the range 0-5% (Fig. 6b). Furthermore, two different mean values have been determined. They were calculated considering the RA values reaching the range 0-5% (RMV_{T0}) or omitting them (RMV_T) and reported in Figure 12.

For all the transversal Resistographic measurements, the relative difference K_{DEF} [%] between RMV_T and RMV_{T0} has been calculated. It represents the defectiveness of wood obtainable in the transversal Resistograpic analyses.

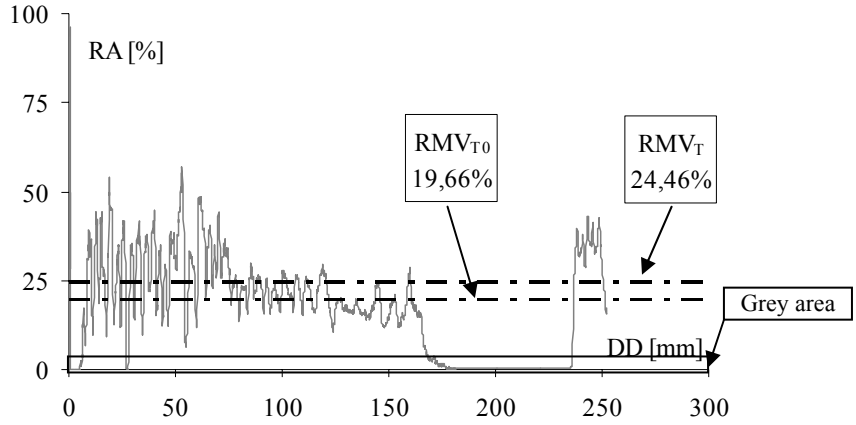

Figure 12. A transversal Resistographic analysis: RMV_T and RMV_{T0} values; the grey area represents the 0-5% range of RA values.

Table 3. $RMV_{T,Chi}$ and the corresponding $K_{DEF,Chi}$ values for all tested Samples.

	Sample 1		*Sample 2*		*Sample 3*	
$RMV_{T,Ch3sup}$ [%]	26.79	6.31%	37.98	2.48%	40.73	1.99%
$RMV_{T0,Ch3sup}$ [%]	28.60		38.95		41.56	
$RMV_{T,Ch0med}$ [%]	24.93	14.21%	21.43	18.51%	28.62	2.39%
$RMV_{T0,Chomed}$ [%]	29.06		26.30		29.32	
$RMV_{T,Ch1inf}$ [%]	28.17	5.51%	34.31	3.96%	25.90	3.45%
$RMV_{T0,Ch1inf}$ [%]	29.81		35.72		26.83	

In addition, the mean values of the RMV_T and RMV_{T0} measured on the i-chords of each sample, $RMV_{T,Chi}$ and $RMV_{T0,Chi}$, respectively, have been determined at 3sup, 0med and 1inf chords. They are reported in Table 3. Furthermore, in the same Table, their relative differences $K_{DEF,Chi}$ have been considered. As it can be noted, in the case of Sample 1 and 2, high values of $K_{DEF,Ch0med}$ have been obtained, due to the presence of a sub-horizontal longitudinal cracking at median chord, while a low value of $K_{DEF,Ch0med}$ for Sample 3 confirmed the absence of notable longitudinal cracking. According to this, a correlation between $K_{DEF,Chi}$ and the ultimate tangential strength can be pointed out, as described in the following.

For each tested sample, a non-dimensional measure (TS) of the tangential stress throughout the end-beam cross-section are provided in Figure 13. TS value represents the ratio between the actual tangential stress and the maximum one attained in the cross-section. Stresses have been calculated according to the classic Jourawski hypothesis. In these diagrams, the continuous curves have been obtained considering the actual section (i.e. with splits and holes), while the dashed curves have been obtained considering the equivalent perfect circular cross-section. It is worth noting that the values of the TS calculated on actual cross-section (TS_{ac}) are significantly higher than the ones obtained on the equivalent cross-section (TS_{eq}), with the exception of the Sample 3, which did not present significant defects at its ends.

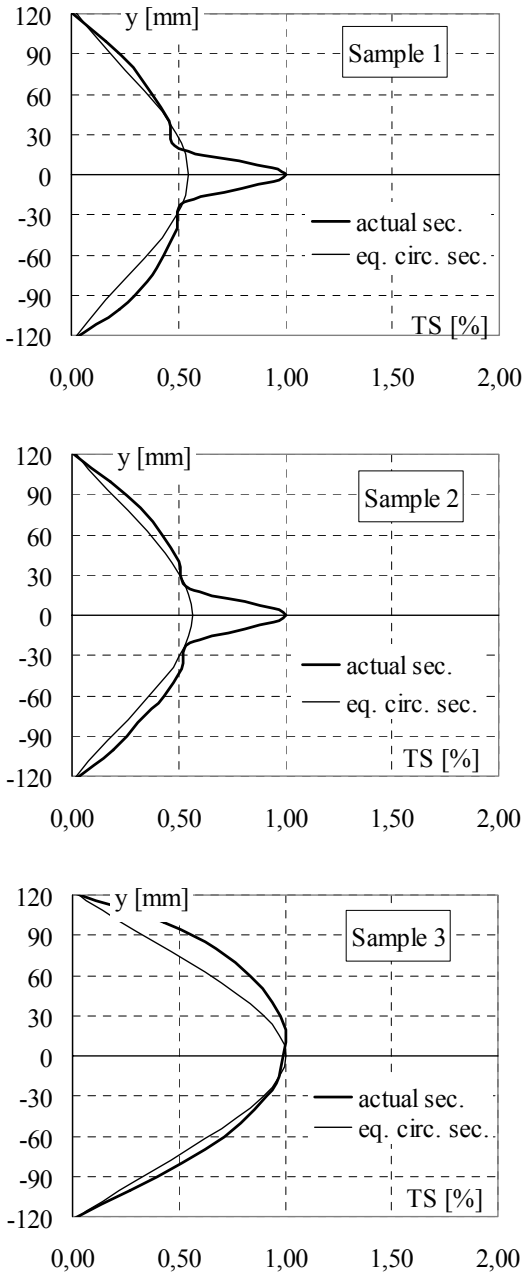

Figure 13. Non-dimensional tangential stress measure TS throughout the end-beam cross-section for Sample 1, 2 and 3.

For each sample the maximum TS value $TS_{eq,max}$ have been calculated and compared to the $TS_{ac,max}$ (equal to 1.00). Their relative difference, K_{TS} [%] appear to be equal to 46 %, 43% and 0 % for Sample 1, 2 and 3, respectively.

Furthermore, the $K_{DEF,Ch0}$ vs. K_{TS} diagram have been depicted in Figure 14. By observing the trend line (the continuous line in the Figure), it appears to be a good correlation between transversal Resistographic analysis and the actual ultimate shear strength of the members. The obtained results highlighted that shear verification of ancient beams can be reliably performed by evaluating the tangential strength by means of Resistographic measurements.

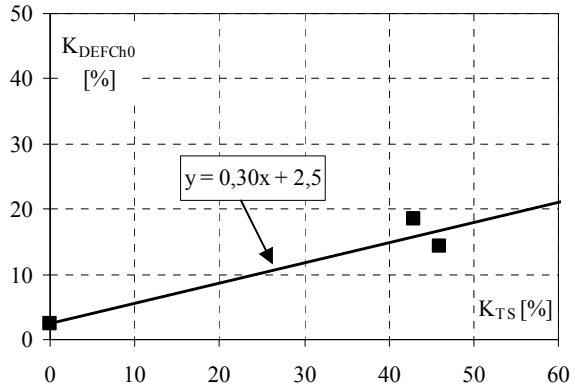

Figure 14. $K_{DEF,Ch0}$ - K_{TS} diagram.

Finally, a correlation between longitudinal and transversal Resistographic analyses has been investigated. Usually, in-situ NDT investigations can be executed only in the transversal direction, due to the impossibility of directly acceded to the end-beam, which are placed in their wall supports. On the other side, as previously shown, longitudinal investigations present resistance drilling measures very close to

their mean values RMV_L, which can be reliably used as expression of the wood properties. Therefore, it appears to be extremely important the acquaintance in the practical applications of such type of correlation.

Particularly, the $RMV_{L,TOT}$, obtained without considering the fault longitudinal Resistographic measures, has been compared with two different values. They represents the main values of the total transversal drilling resistance measured by omitting the 0-5% values of RA, $RMV_{T,TOT}$, and considering them ($RMV_{T0,TOT}$). $RMV_{T,TOT}$ and $RMV_{T0,TOT}$ values resulted equal to 31.79 % and 29.87 %, respectively.

Hence, two different correlation coefficient has been considered. They are obtained as the ratio between $RMV_{T,TOT}$ (or $RMV_{T0,TOT}$) and $RMV_{L,TOT}$ and result equal to 0.96 and 0.90, respectively.

3. CONCLUSIONS

In this Chapter a series of Longitudinal and Transversal Resistographic analyses have been carried out on ancient chestnut elements, before they were subjected to Destructive Tests. They presented the typical defects patterns and degradation phenomena of the ancient timber structures.

In particular, about 80 longitudinal Resistographic measurements have been carried out on each end-beam cross-section of the tested samples, at the points of a square grid of 20 mm side, while the Transversal measurements have been performed on the lateral surface of the samples. The mean value of each analysis has been measured as the average value of the drilling resistance achieved during the test.

In the case of Longitudinal Resistographic analyses, the main value of each drilling measure RMV_L has been calculated on wood having good quality. Furthermore, $RMV_{L,SEC}$ and $RMV_{L,Si}$ have been obtained considering the mean value of the RMV_L on each end-beam and the mean value on the total number of measures on the corresponding i-sample, respectively. All the previously considered measures presented low value of the corresponding Standard deviation coefficient (ST DEV). According to this, also the mean value of the total Longitudinal Resistographic analyses, $RMV_{L,TOT}$ have been considered. It resulted equal to about 33 %. It has been compared to the longitudinal ultimate compressive strength σ_0 obtained by tests on clear specimens extracted from the same elements.

For Transversal Resistographic analyses, two different values were considered, RMV_T and $RMV_{T,0}$. They correspond to the mean value of the drilling resistance obtained by omitting (RMV_T) or considering ($RMV_{T,0}$) the null values reached during the measure. Their relative difference K_{DEF} represents a measure of the defectiveness of wood. This difference was not negligible in the case of transversal measures in presence of sub-horizontal cracking. According to this, a correlation between Resistographic analyses and the corresponding shear strength has been evaluated.

Furthermore, comparisons between the mean values of the total measures in longitudinal and transversal directions have been investigated. In particular, the $RMV_{L,TOT}$ on $RMV_{T,TOT}$ ratio resulted equal to about 0.95.

CHAPTER 9:

Correlation between Destructive and Non-Destructive Tests on spruce defect-free specimens

In this Chapter an experimental activity based on a series of Destructive and Non-Destructive Tests on new spruce small defect-free specimens has been reported. Nowadays, spruce wood is one of the most common woods used in timber structures and the spruce beams are easily available in commerce both as whole and laminated members. The specimens were extracted from a series of classified beams in actual dimension (spruce beam-type "Trieste", according to the Austrian codes), having a square cross-section of 100 mm side and length of about 4 meters. These beams were adjusted in order to obtain a series of square cross-section samples with 50 mm side and length of about 100 mm.

As reported in Table 1, Resistographic analyses in longitudinal and transversal direction have been carried out on 20 samples. Later, compressive tests in parallel-to-

grain direction have been performed on the same samples, in order to obtain a correlation between their drilling resistance and the ultimate longitudinal compressive strength.

Table 1. Test typologies and number of specimens for each test.

Test typology	*Num. of specimens*
1. Resistographic analyses in Longitudinal and transversal direction	20
2. Compression tests along fibre direction	20

1. RESISTOGRAPHIC ANALYSES

Resistographic analyses have been carried out by means of the "Resi F400" produced by IML, which is the same device used for NDT analyses on ancient chestnut elements (see Chapter 8).

Longitudinal Resistographic analyses have been performed at the end of each sample for a drilling depth corresponding to the whole length (about 100 mm). Furthermore, transversal Resistographic measurements have been carried out on the lateral surface of each sample both in direction tangential and radial to the growth rings. In order to have a more complete information, all the spruce samples have been subjected to 3 different measures for each drilling direction. In Figure 1, a sample subjected to longitudinal measurements is depicted. The sample was fixed to the work station by means of rigid clamps and subjected to the Resistographic anlyses.

Figure 1. Spruce samples subjected to Resistographic analysis in longitudinal direction.

As in the case of NDT investigations on ancient chestnut elements. the relative amplitude (RA) [%] vs. drilling depth (DD) [mm] graphs has been obtained. Typical resistographic measures are depicted in Figures 2 and 3 for drilling in longitudinal direction and two transversal directions (tangential and radial to the growth rings), respectively. In these Figures, along the three different directions, it can be noted two different type of drilling resistance. In particular, in longitudinal direction the RA values range between 0–3 % in the first type and 8-10 % in the second one and each measure reveals RA values quite coincident with their main value. Therefore, an unique parameter, RMV_L, can be considered as representative of the Resistographic measure. It has been obtained by dividing the total area under the graph on the total DD, as reported in the equation (8.1).

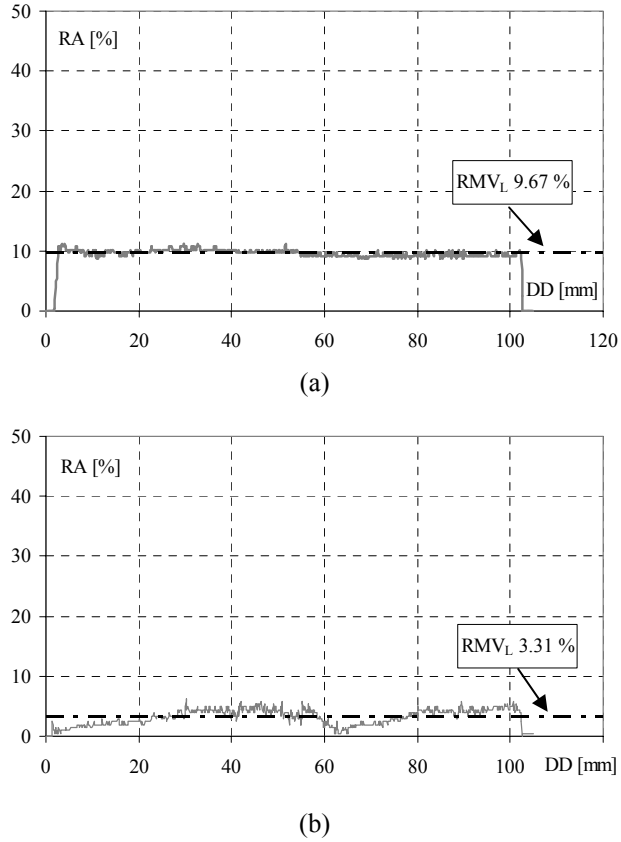

Figure 2. Typical Resistographic measure in longitudinal direction: wood having RA values ranging 8-10 % (a) and wood having RA values ranging 0-3 % (b).

On the other side, the transversal Resistographic analyses presented a strong variation of RA values for each drilling measure. Unlike it occurred for ancient chestnut members, in which RA values ranging 0-5 % corresponded with a presence of defects or degradation phenomena, in this case low values of RA are typical of the wood quality. Therefore, it appears to be important the mean values, RMV_{Tan} and RMV_{Rad}, achieved on the total drilling resistances RA measured for each

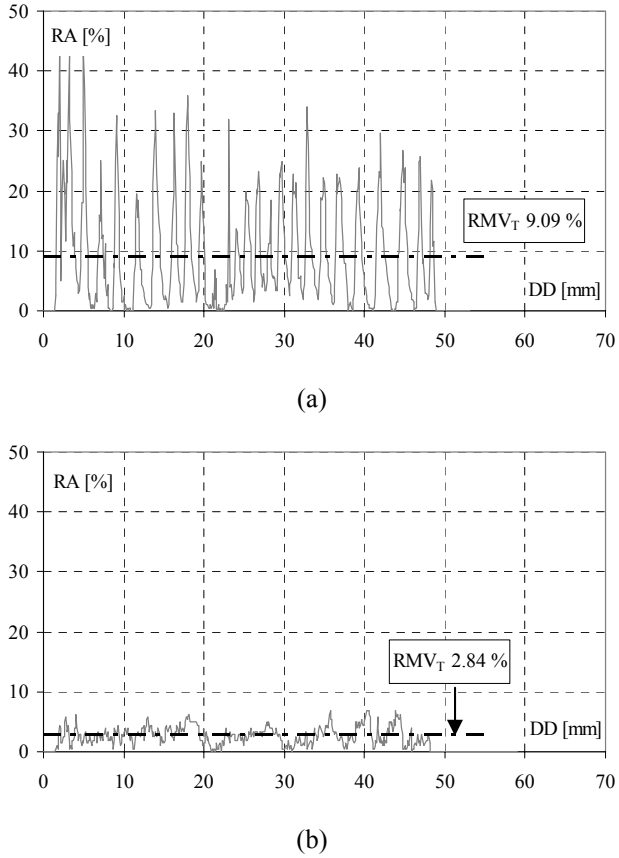

Figure 3. Typical Resistographic measure in transversal direction: wood having RA values ranging 8-10 % (a) and wood having RA values ranging 0-3 % (b).

Resistographic analysis in direction tangential and radial to the annual growth rings, respectively. These values are quite coincident, with a slight prevalence of lower value in the case of tangential measures, probably due to a drilling path into the preferential way between two adjacent growth rings. Therefore, a common value RMV_T can be considered. Also in the case of transversal Resistographic analyses, RA values range between 0–3 % in the first type and 8-10 % in the second one.

These different values obtained in the longitudinal and transversal measurements have been confirmed by compressive tests on the same samples, by which two different ultimate compressive strength ranges have been obtained (see paragraph 3).

Table 2. Mean values of Longitudinal and Transversal Resistographic measures.

Samples	$RMV_{L,Si}$ *[%]*	$RMV_{T,Si}$ *[%]*
1	9,94	6,48
2	12,01	5,98
3	1,41	2,56
4	7,56	6,56
5	1,48	3,45
6	1,31	2,50
7	9,37	5,27
8	5,39	5,12
9	7,30	7,21
10	2,09	2,52
11	7,28	2,99
12	0,38	2,57
13	0,36	2,70
14	9,46	4,01
15	2,25	4,14
16	7,60	3,36
17	9,65	5,90
18	1,37	2,87
19	9,59	4,97
20	2,56	2,57

In conclusion, each i-sample has been completely characterised by two values, $RMV_{L,Si}$, $RMV_{T,Si}$, which represent the mean values of the Resistographic measures obtained for the i-sample in longitudinal and transversal direction, respectively. In Table 2, $RMV_{L,Si}$ and $RMV_{T,Si}$ have been reported for all the tested samples.

Finally, a correlation between longitudinal and transversal Resistographic analyses has been investigated. In fact, as described in Chapter 8, the in-situ NDT investigations on set-up ancient timber structures can be usually carried out only in the transversal direction. In particular, the considered correlation coefficients for each sample, $C_{L/T}$ have been obtained as the ratio between $RMV_{L,Si}$ and $RMV_{T,Si}$. Their mean value results equal to about 0.80.

2. COMPRESSION TESTS IN PARALLEL-TO-GRAIN DIRECTION

Compression tests along the fibre direction have been carried out on all the spruce defect-free samples previously subjected to Resistographic analyses. Tests have been carried out according to the Italian and European regulations UNI-ISO 3787 and UNI-EN 408. Samples have been tested by means of the universal testing machine Mohr Federhaff AG, working in force control. It has a maximum load capacity of 400 kN. The uniform loading distribution at the end of the sample was guarantee by means of a spherical hinge placed between under the loading actuator. In Figure 4 a sample placed under the testing equipment is shown.

Figure 4. The adopting testing equipment.

Loads have been increased up to the sample collapse, corresponding to the maximum compressive strength $\sigma_{0,Sp}$ measured as:

$$\sigma_{0,Sp} = \frac{F_{max}}{A} \text{ [MPa]} \tag{9.1}$$

where: F_{max} [N] is the maximum applied force and A [mm^2] is the whole cross-section area of the sample.

In Figure 5 different failure modes occurred during the tests have been depicted. Like in the case of compressive tests on ancient defect-free chestnut specimens, the principal collapse mechanism is due to a micro-buckling of the fibres, which appear separated from the residuary part because of the attainment of the transversal

ultimate tensile stress. In addition, the attainment of cleavage planes having an angle range 0-30° can be observed.

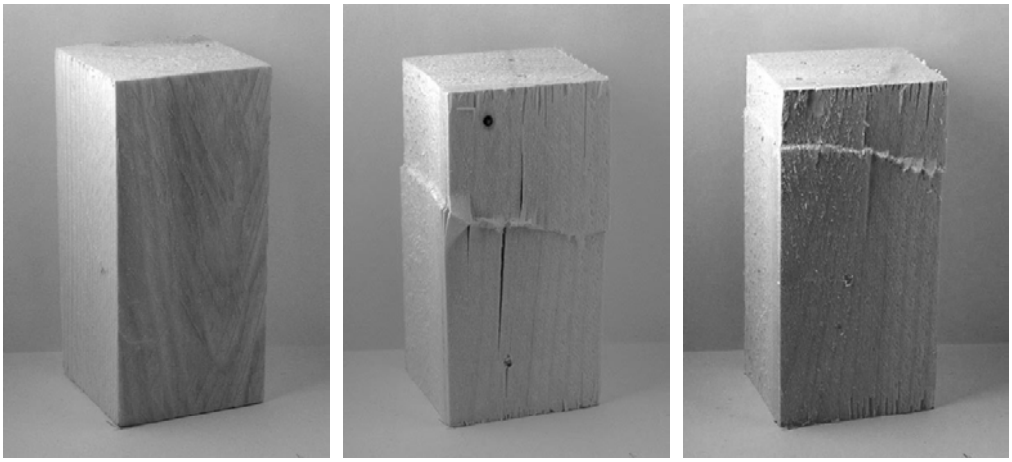

Figure 5. A sample before testing (a) and typical collapse mechanism occurred during the tests (a) and (b).

The ultimate forces F_u and the corresponding longitudinal compressive strengths $\sigma_{0,Sp}$ for all the spruce samples have been reported in Table 3. According to what occurred in the case of Resistographic analyses, it can be noted that the $\sigma_{0,Sp}$ values vary in two different range of about 25 MPa and 30 Mpa.

Finally, the correlation between longitudinal resistographic analyses and ultimate compressive strength in the same direction has been obtained in Figure 6, in terms of σ_0 vs. RMV_L and represented by the triangle dots. In addition, the continuous line in the diagram represents the trend line obtained considering only the spruce samples, while the square dot represents the values obtained for ancient chestnut elements, corresponding to σ_0 and $RMV_{L,TOT}$ equal to about 48 MPa and 33%, respectively. It

is worth noting that this point appears to be quite coincident with the one expected by the trend line. Therefore, its equation (σ_0 = 0.75 RMV_L + 22.50) can be reliably used as a correlation formula available for the two considered wood species. From this, the strength properties of wood seems to be directly dependent only from its resistographic values.

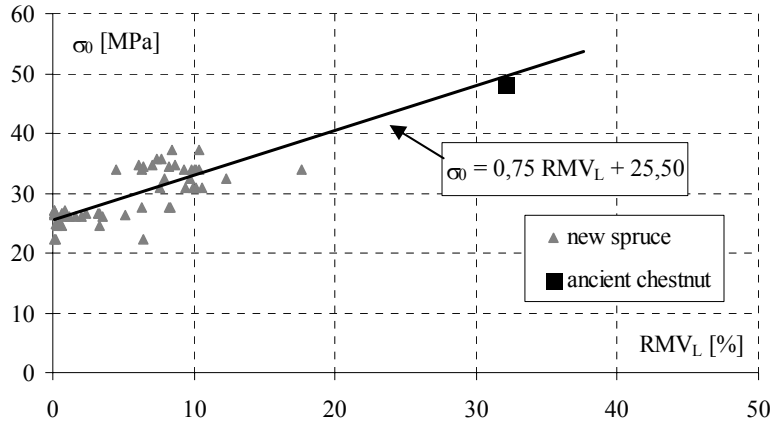

Figure 6. The correlation diagram between longitudinal Resistographic analysis and longitudinal compressive strength.

Table 3. Main values of longitudinal compressive tests.

Samples	F_u *[N]*	$\sigma_{0,Sp}$ *[MPa]*
1	81000	32,40
2	85000	34,00
3	61500	24,60
4	89000	35,60
5	66500	26,60
6	66500	26,60
7	93000	37,20
8	84500	33,80
9	86000	34,40
10	66000	26,40
11	86500	34,60
12	68000	27,20
13	62000	24,80
14	77500	31,00
15	55500	22,20
16	69000	27,60
17	77500	31,00
18	65500	26,20
19	84500	33,80
20	65500	26,20

3. CONCLUSIONS

Destructive and Non-Destructive tests have been carried out on a series of new spruce defect-free small specimens. In particular, Resistographic analyses and compressive tests in parallel-to-grain direction have been performed on 20 samples, in order to obtain a correlation between the longitudinal drilling measures and the corresponding maximum compressive strength. Furthermore, correlation between longitudinal and transversal Resistographic analyses has been investigated.

In particular, a series of 3 measure for each preferential direction (i.e. longitudinal, radial and tangential to the annual growth rings) have been executed for each sample. For longitudinal Resistographic analyses, the mean value of each drilling measure RMV_L has been calculated. In addition, on each i-sample $RMV_{L,Si}$ represents the mean value of the 3 obtained RMV_L. On the other side, radial and tangential drilling measures on each sample present a quite coincident mean value. Therefore, a common parameter $RMV_{T,Si}$ can be considered. As in the previous case, $RMV_{T,Si}$ represents the mean value of all the measures carried out on the same sample. Correlation between longitudinal and transversal Resistographic analyses has been obtained by the $RMV_{T,Si}$ on $RMV_{L,Si}$ ratios for all the samples. The obtained mean value results equal to about 0.80.

Furthermore, longitudinal compressive tests have been carried out on the same samples and the corresponding maximum compressive strengths $\sigma_{0,Sp}$ have been calculated. They range from 22 Mpa to 34 MPa.

Finally, $RMV_{L,Si}$ versus $\sigma_{0,Spi}$ diagram has been considered. On the same diagram also the corresponding values obtained for ancient chestnut elements has been depicted. The trend line obtained by the results for new spruce samples appears to be practically coincident with the point representing ancient chestnut wood. Therefore, the trend-line equation, $\sigma_0 = 0.75\ RMV_L + 22.50$ can be reliably used as a correlation formula available for the two considered wood species. From this, the strength properties of wood seems to be directly dependent only from its resistographic values.

CONCLUSIONS:

In the present thesis the evaluation of the structural behaviour of ancient timber elements has been investigated. In particular, the attention has been focused on the timber members subjected to bending and axial forces, such as the bearing structure of floor and trust structures of buildings of the Italian and Mediterranean historical centres.

A wide experimental campaign has been carried out both in Destructive and Non-Destructive Tests on a series of ancient chestnut beams. In particular, study refers to Destructive Tests on defect-free ancient chestnut samples extracted from the beams, full-scale tests on timber elements in actual dimension, tests on clear specimens connected by means of metal fasteners. In addition, Non-Destructive Resistographic analyses have been executed on the same timber members in order to investigate the in-depth quality of wood.

Experimental activity on defect-free small samples extracted from ancient timber elements have provided complete information on mechanical properties of chestnut

wood. By means of Compression tests along three principal direction and Static Bending tests, the ultimate compressive and tensile strength and the longitudinal elastic modulus were determined, so defining the complete stress-strain relationship. A not negligible ductile capacity of wood in bending can be noted. The obtained results appear to be quite coincident with the one reported in technical literature for new chestnut wood. Interesting considerations have been made by comparing these values with the overall load bearing capacity of ancient timber members deduced by full-scale destructive tests.

Full-scale compression and bending tests have been carried out on a series of ancient timber elements characterised by significant degradation phenomena. In particular, compression tests in longitudinal direction have highlighted a compressive strength and longitudinal elastic modulus slightly lower (about 10 %) than the corresponding values obtained on defect-free samples. On the other side, full-scale bending tests reveal a longitudinal elastic modulus strongly lower than the one expected in compression tests. Also, the flexural collapse mode occurred at the attainment of the maximum compressive stress quite coincident with the one obtained from compressive tests, it revealing a brittle collapse behaviour. Furthermore, unexpected shear failures occurred in some beams before the attainment of the maximum load bearing capacity. This is due to the degradation phenomena, which strongly influence the overall structural behaviour. In particular, it appears appear to be remarkable the scatter between the maximum shear strength evaluated in full-scale tests and the one obtained by defect-free shear tests. It can be concluded that the simplified methods commonly used to evaluate the bearing capacity of ancient timber beams must be revised by introducing adequate reduction factor for the shear strength.

Tests on defect-free chestnut samples connected by means of metal fasteners have provided interesting information. In particular, embedment strength in longitudinal and transversal direction have been obtained. The longitudinal embedment strength appears to be in good accordance with the corresponding values of the EC5, while the transversal one results to be much lower than the corresponding one in EC5. Furthermore, bending tests on connected sample have been performed. Tests were executed according to the same loading conditions used for bending tests on small and actual whole beams. Several differences in the cross-section dimensions and in the number of the metal connectors have been analysed. In all the examined cases, the failure mechanism occurred in the timber sample, in the plane of the steel bars, due to an excess of the tensile stress in longitudinal direction before the attainment of the remarkable embedment in the samples. Tests also show a remarkable loss in stiffness and load-baring capacity (about 40 -50%) respect to the values obtained by defect-free whole beams.

Finally, Non-Destructive Resistographic analyses in longitudinal and transversal direction have been carried out on the same timber elements before their destructive tests. In particular, longitudinal Resistographic measurements have been carried out on each end-beam cross-section of the tested samples, while the Transversal measurements have been performed on the lateral surface of the samples. The average value of the drilling resistance achieved during the test has been considered as representative of the measures. In longitudinal analyses, the so-calculated mean values present low value of the corresponding Standard deviation coefficient (ST DEV). According to this, also the mean value of the total Longitudinal Resistographic analyses have been considered. It resulted equal to about 33 %. It has been compared to the longitudinal ultimate compressive strength σ_0 obtained by tests on clear specimens extracted from the same elements. On the other side, transversal analyses highlighted differences in the mean values of the drilling resistance obtained

by omitting or considering the null values reached during the measure. Their relative difference K_{DEF} represents a measure of the defectiveness of wood. This difference was not negligible in the case of transversal measures in presence of sub-horizontal cracking. According to this, a correlation between Resistographic analyses and the corresponding shear strength has been evaluated.

Finally, Destructive and Non-Destructive tests have been carried out on a series of new spruce defect-free small specimens, in order to obtain a correlation between the longitudinal drilling measures and the corresponding maximum compressive strength. Furthermore, correlation between longitudinal and transversal Resistographic analyses has been investigated. First a correlation between longitudinal and transversal analyses has been obtained. Furthermore, longitudinal compressive tests have been carried out on the same samples and the corresponding maximum compressive strengths have been calculated. From this, a correlation curve between longitudinal Resistographic analyses and the corresponding maximum compressive strength has been obtained. The trend line obtained by the results for new spruce samples appears to be practically coincident with the point representing ancient chestnut wood. Therefore, the trend-line equation can be reliably used as a correlation formula available for the two considered wood species. From this, the strength properties of wood seems to be directly dependent only from its resistographic values.

REFERENCES:

[1] Bale, S. & Browne, C. A. Non-Destructive Identification of Defects in Timber Bridge. Road System & Engineering Technology Forum. 2004

[2] Bertholf, L.D. Use of elementary stress wave theory for prediction of dynamic strain in wood. Bulletin 291. Pullman, WA: Washington State University, College of Engineering. 1965.

[3] Bertolini, C. Problemi di recupero: metodi di indagine, tecnologie di intervento. L'Edilizia, Anno IV, No.12. Milan: De Lettere Editore, 1992.

[4] Bertolini, C., Brunetti, M., Cavallaro, P. & Macchionni, N. A non destructive diagnostic method on ancient timber structures: some practical application examples. Proceedings of 5th World Conference on Timber Engineering. Montreaux. 1998.

[5] Bertolini, C. & Di Lucchio A. Interventions on historical building timber floors: Retractable – visible? Invasive – not visible? A case study. In: Proceedings of the 3th International Seminar "Structural analysis of historical constructions", Guimaraes, Portugal, 2001.

[6] Bonamini, G., Ceccotti, A. & Uzielli, L. Sulla valutazio-ne della resistenza meccanica del legno antico. L'Edilizia, Anno V, No. 12. Milan: De Lettere Editore, 1991

[7] Calderoni B., De Matteis G., Mazzolani F.M. Structural performance of ancient wooden beams: experimental analysis, European timber buildings as an expression of technological and technical cultures, Editions Scientifique et Medicales, Elsevier S.A.S, 2003.

[8] EN 380. Timber structures - Test methods – General principles for static testing, 1994.

[9] EN 383. Timber structures – Test methods – Determination of embedding strength and foundation values for dowel type fasteners, 1994.

[10] EN 408. Timber structures - Test methods – General principles for static testing, 1994.

[11] Feio A.O., Lourenco P.B., Machado J.S. Compressive behaviour and NDT correlations for chestnut wood. In: Proceedings of the 4th International Seminar "Structural analysis of historical constructions", Padova, Italy, 10-13 November 2004.

[12] Giordano G. Tecnica delle Costruzioni in legno (Wooden structure engineering), HOEPLI ed., Milan, Italy, 1989.

[13] ISO 3132. Wood – Testing in compression perpendicular to the grain. 1975.

[14] ISO 3133. Wood – Determination of ultimate strength in static bendiding. 1975.

[15] ISO 3349. Wood – Determination of modulus of elasticity in static bending. 1975.

[16] ISO 3787. Wood – Test methods – Determination of ultimate stress in compression parallel to the grain. 1976.

[17] Jayne, B.A. Jayne, B.A. Vibrational properties of wood as indices of quality. Forest Products Journal. 9(11), 1959.

[18] Jayne, B.A., Bodig, J. Mechanics of Wood and Wood Composites. Van Nostrand Reinhold Co, New York, 1982.

[19] Kasal, B. & Anthony, R. W. Advances in in-situ evaluation of timber structures. Prog. Struct. Engng. Mater. 6. 2004

[20] Lanius, Tichy, Bullet. Strength of old joists. Journal of Structural Division ASCE, No. 107, ST12, 1981.

[21] Madsen, B. Length effects in timber. In: Proceedings of "1991 International Timber Engineering Conference", London, UK, 1991.

[22] Mazzolani F. M., Calderoni B., De Matteis G., Giubileo C. Experimental analysis of ancient chestnut beams by small specimens. In: Proceedings of the 4th International Seminar "Structural analysis of historical constructions", Padova, Italy, 10-13 November 2004 (a).

[23] Mazzolani F. M., Calderoni B., De Matteis G., Giubileo C. Experimental analysis of ancient wooden beams for flexural and shear failure: In: Proceedings of the 4th International Seminar "Structural analysis of historical constructions", Padova, Italy, 10-13 November. 2004 (b).

[24] Rinn, F. Resistographic inspection of construction timber, poles and trees. Proceedings of Pacific Timber Engineering Conference. Gold Coast, Australia. 1994.

[25] Ross, R. J. & Pellerin, R. F. Nondestructive testing for assessing wood members in structures: a review. United States Department of Agriculture - General Technical Report FPL-GTR 70. 1994.

[26] Tampone, G. Il Restauro delle Strutture di Legno, U. Hoepli Editore, Milan. 1996.

[27] Tampone, G. Acquaintance of the ancient timber structures. In: Lourenco, P.B. & Roca, P. (ed.) "Historical Constructions. Possibilities of numerical and experimental tecniques", 2001.

[28] Turrini, G. & Piazza, M. Una Tecnica di Recupero Statico dei Solai in Legno. Recuperare, Anno II, No. 5, 1983.

[29] Uzielli, L. Valutazione della Capacità Portante di Elementi strutturali Lignei. L'Edilizia, Anno IV, No. 12. Milan: De Lettere Editore, 1992

[30] United States Department of Agriculture (U.S.D.A) – Forest Service. Wood Handbook – Wood as an Engineering Material. General Technical Report FPL-GTR 113 (a).

[31] United States Department of Agriculture (U.S.D.A.) – Forest Service. Stress wave timing nondestructive evaluation tools fir inspecting historic structures – A guide for use and interpretation. General Technical Report FPL-GTR 119 (b).